ESPOO 2007 VTT PUBLICATIONS 637

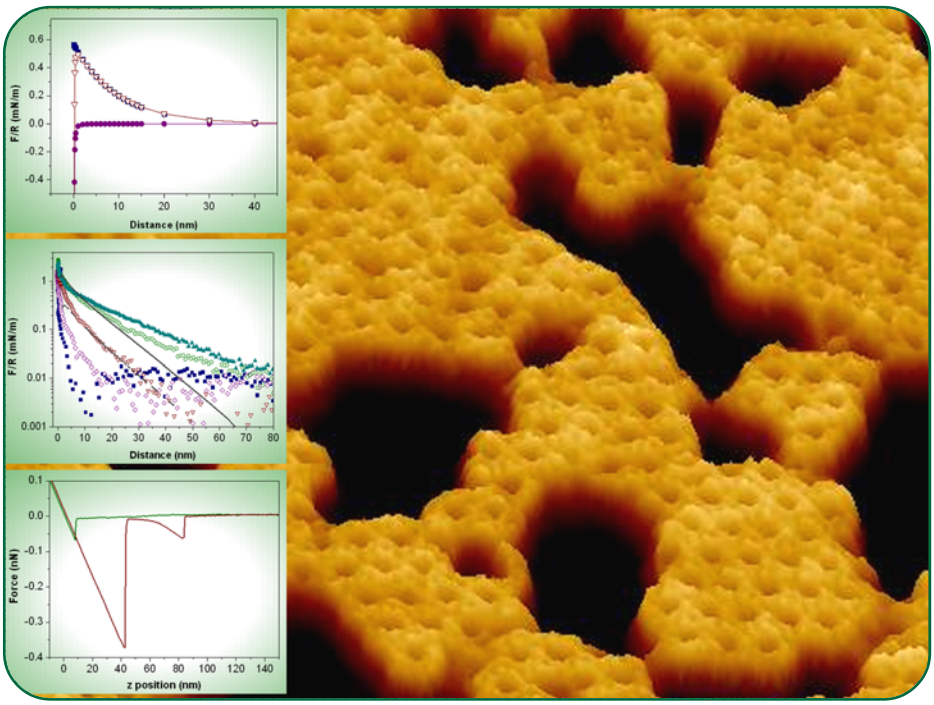

Arja Paananen

On the interactions and interfacial behaviour of biopolymers

An AFM study

ÅBO AKADEMI

VTT

VTT PUBLICATIONS 637

On the interactions and interfacial behaviour of biopolymers

An AFM study

Arja Paananen
VTT

ACADEMIC DISSERTATION

Department of Physical Chemistry
Faculty of Mathematics and Natural Sciences
Åbo Akademi University
Turku, Finland

ISBN 978-951-38-7012-6 (soft back ed.)
ISSN 1235-0621 (soft back ed.)

ISBN 978-951-38-7013-3 (URL: http://www.vtt.fi/publications/index.jsp)
ISSN 1455-0849 (URL: http://www.vtt.fi/publications/index.jsp)

JULKAISIJA – UTGIVARE – PUBLISHER

VTT, Vuorimiehentie 3, PL 1000, 02044 VTT
puh. vaihde 020 722 111, faksi 020 722 4374

VTT, Bergsmansvägen 3, PB 1000, 02044 VTT
tel. växel 020 722 111, fax 020 722 4374

VTT Technical Research Centre of Finland, Vuorimiehentie 3, P.O. Box 1000, FI-02044 VTT, Finland
phone internat. +358 20 722 111, fax + 358 20 722 4374

VTT, Tietotie 2, PL 1000, 02044 VTT
puh. vaihde 020 722 111, faksi 020 722 7071

VTT, Datavägen 2, PB 1000, 02044 VTT
tel. växel 020 722 111, fax 020 722 7071

VTT Technical Research Centre of Finland, Tietotie 2, P.O. Box 1000, FI-02044 VTT, Finland
phone internat. +358 20 722 111, fax +358 20 722 7071

Technical editing Maini Manninen

Edita Prima Oy, Helsinki 2007

Paananen, Arja. On the interactions and interfacial behaviour of biopolymers. An AFM study. Espoo 2007. VTT Publications 637. 106 p. + app. 66 p.

Keywords interactions, surface forces, atomic force microscopy, biopolymers, cellulose, hemicellulose, xylan, gluten proteins, gliadin, surface active protein, hydrophobin, HFBI, HFBII

Abstract

Surface forces and interactions are a key issue in colloid and surface science, including biopolymer systems. Covalent and ionic bonds determine the structure and composition of materials, but the weaker non-covalent interactions define their functions. This thesis deals with the surface forces and interactions occurring between biopolymer surfaces and affecting the self-assembly and interfacial behaviour of biopolymers. The research was aimed at deepening the understanding of molecular interactions and the nature and strength of surface forces in the studied biopolymer systems. The main research tool was atomic force microscopy (AFM). This technique allows imaging of the sample topography in either gas or liquid environments at high resolution. Data on intra- and intermolecular interactions can also be obtained. Interesting phenomena revealed by AFM were supported and confirmed by other relevant surface analytical techniques.

The nanomechanical force measurements focused on interactions relevant in papermaking, i.e. between cellulose and xylan, and food technology, i.e. between gliadins (wheat gluten proteins). In the cellulose-xylan interaction work the colloidal probe technique was exploited by attaching cellulose beads to the tip and to the sample surface. The interaction between these beads was measured in different xylan solutions. The main result of the cellulosic systems provided a new perspective on the role of xylan in papermaking. It has been reported previously that the adsorption of xylan increases paper strength and that this is due to formation of hydrogen bonds. Our results indicate that the increase in paper strength cannot originate from such bonds in wet paper, but must be due to effects of xylan on fibre bonds during drying of paper.

The viscous and elastic properties of gliadins and glutenins facilitate the production of bread, pasta and many other food products from wheat flour. Gliadin proteins (α- and ω-gliadins) were attached to both the tip and the sample surfaces, and the interaction forces between monomeric gliadins (α-α, ω-ω, and α-ω) were measured. On the basis of the nanomechanical force measurements, different roles of different types of gliadins were proposed: whereas ω-gliadins still have a compact structure and are responsible for the viscous flow, α-gliadins have already started to participate in forming the network in dough. This may provide a new viewpoint in understanding the interfacial properties of gliadins in relation to baking.

The studies of interfacial behaviour of biopolymers focused on hydrophobins, which are very surface active proteins. Hydrophobins are amphiphilic proteins which self-assemble due to the interplay of various surface forces and interactions in solution and at interfaces. Films of Class II hydrophobins, HFBI and HFBII, at the air-water interface were transferred to solid supports and imaged by AFM. The interfacial films of hydrophobins were imaged at nanometer resolution. The results showed that both HFBI and HFBII form organised structures at the air-water interface. Moreover, the nanostructured films formed spontaneously. The HFBI films were imaged and the organised pattern was seen both on the hydrophobic and the hydrophilic side. The dimensions were similar to those of hydrophobin tetramers in solution obtained by small angle X-ray scattering. Protein engineering enabled assignment of a specific functionality to HFBI. The results confirmed the expected orientation of hydrophobins at the air-water interface, and indicated that the hydrophobin retained its capability to form organised films and the covalently attached molecule its functionality.

Preface

This work was carried out at VTT Technical Research Centre of Finland, at the Helsinki University of Technology, and at the H.H. Wills Physics laboratory, University of Bristol. I thank Professor Juha Ahvenainen, Professor Hans Söderlund and Research Manager Richard Fagerström for providing excellent working facilities at VTT. I am very grateful to professor Per Stenius for the inspiring atmosphere at the Laboratory of Forest Products Chemistry, HUT. Professor Mervyn Miles is warmly thanked for letting me be part of his dynamic SPM group at the University of Bristol. I also thank professor Jarl Rosenholm, Åbo Akademi University for his help during the studies. Docent Tommy Nylander and Dr. Tapani Viitala are thanked for reviewing this thesis. Financial support from EU (FAIR-CT96-1624), the Finnish Funding Agency for Technology and Innovation (Tekes), the Academy of Finland and VTT is gratefully acknowledged.

I am very grateful to all my supervisors. Docent Kirsi Tappura guided me throughout the work at VTT, and I express my deepest gratitude to her. She is warmly thanked for helping me with the issues related to physics, for her endless encouragement, her friendship and for many, many discussions on many subjects. I am also very grateful to docent Markus Linder for helping me with the biological issues, for teaching me many biochemical techniques (and the whole story behind one milligram of pure protein), and especially for making me part of the hydrophobin research team at VTT. Thanks to him my PhD became a goal rather than just a dream. Professor Jouko Peltonen from Åbo Akademi University is warmly thanked for sharing his knowledge in surface science and AFM, and especially for his encouragement during the writing of this thesis. I am very grateful to Professor Per Stenius for many fruitful and inspiring discussions related to colloids and cellulose work, and for his utmost willingness to help, even in a very tight schedule. Docent Monika Österberg is warmly thanked for her friendship, for sharing her knowledge about surface forces and cellulose interactions, and for making the slow cellulose experiments more bearable and more fun. During my two-month visit to the University of Bristol I was very fortunate to have Dr. Terry McMaster as my supervisor. I am very grateful to him for sharing his knowledge about force measurements and sample

preparation tricks related to AFM, and especially for his cheerful and encouraging way of teaching (the best scanner is a happy scanner!).

I also thank all my co-authors. Within the cellulose-xylan work I thank docent Monika Österberg, professors Per Stenius and Mark Rutland, as well as Dr. Tekla Tammelin and Terhi Saarinen. Professor Maija Tenkanen and Jaakko Pere are thanked for their discussions and thoughts, and Dr. Andrepeter Heiner and Lauri Kuutti for explaining to me the fine details of cellulose structure. I thank docent Kirsi Tappura and Dr. Terry McMaster, especially, for the happy end to the gliadin work. I am also grateful to professor Mervyn Miles and the whole Bristol SPM group for making my stay in Bristol so enjoyable – special thanks to Dr. Andy Baker for his help. I also thank Gillian Tallents, my lovely house mate, for her kindness and many (not so work-related) discussions. The hydrophobin work presented in this thesis is only a small part of the ongoing research with several collaborators. I thank Dr. Elina Vuorimaa-Laukkanen at Tampere University of Technology, professor Ritva Serimaa and Dr. Mika Torkkeli from the University of Helsinki, professor Olli Ikkala from Helsinki University of Technology, and professor Juha Rouvinen and Dr. Johanna Hakanpää from the University of Joensuu. My warmest thanks within the hydrophobin work goes to my VTT colleagues, especially to Markus Linder, Géza Szilvay, Riitta Suihkonen and Katri Kurppa. I am very grateful to them for sharing their knowledge of hydrophobins with the utmost willingness and for showing me many helpful tricks in the laboratory, and for the joyful times spent together outside the laboratory.

All past and former members of the Molecular modeling group, the Computational biophysics and bioinformatics group, the Protein engineering group, the Protein Technology group and the Nanobiomaterials group are thanked for creating a pleasant working atmosphere. Nana Munck is warmly thanked for her friendship and for sharing all the ups and downs in research as a room mate. Drs. Tarja Nevanen, Anu Koivula and Harry Boer are thanked for many helpful discussions. Oili Lappalainen is thanked for helping me with finding many important articles. I am grateful to Michael Bailey for revising the language of this thesis.

My grandmother, parents, other family members, family-in-law and friends are warmly thanked for their support, encouragement and love during this long

journey. I am especially grateful to Anne, Annika, Anniina, Anumaija, Viki and Elsu for the vivid sister connection and for many, many discussions more or less distant from science. Above all, I thank my husband Pekka and my son Juho for their love, understanding and patience, and for making everything in my life more meaningful.

Arja Paananen

Espoo, April 2007

List of publications

This work is based on the following original publications, which are referred to in the text by their Roman numerals. Some additional complementary data not published in the following publications is included in this thesis.

I Paananen, A., Österberg, M., Rutland, M., Tammelin, T., Saarinen, T., Tappura, K. and Stenius, P. 2003. Interaction between cellulose and xylan: an atomic force microscope and quartz crystal microbalance study. In: Hemicelluloses: Science and Technology. Gatenholm, P. and Tenkanen, M. (Eds). American Chemical Society, Washington, DC. ACS Symp. Ser. 864, pp. 269–290.

II Paananen, A., Tappura, K., Tatham, A.S., Fido, R., Shewry, P.R., Miles, M. and McMaster, T. 2006. Nanomechanical force measurements of gliadin protein interactions. Biopolymers 83, pp. 658–667.

III Paananen, A., Vuorimaa, E., Torkkeli, M., Penttilä, M., Kauranen, M., Ikkala, O., Lemmetyinen, H., Serimaa, R. and Linder, M. 2003. Structural hierarchy in molecular films of two class II hydrophobins. Biochemistry 42, pp. 5253–5258.

IV Hakanpää, J., Paananen, A., Askolin, S., Nakari-Setälä, T., Parkkinen, T., Penttilä, M., Linder, M. and Rouvinen, J. 2004. Atomic resolution structure of the HFBII hydrophobin, a self-assembling amphiphile. J. Biol. Chem. 279, pp. 534–539.

V Szilvay, G., Paananen, A., Laurikainen, K., Vuorimaa, E., Lemmetyinen, H., Peltonen, J. and Linder, M.B. 2007. Self-assembled hydrophobin protein film at the air–water interface: structural analysis and molecular engineering. Biochemistry 46, pp. 2345–2354.

Supporting publication

VI Serimaa, R., Torkkeli, M., Paananen, A., Linder, M., Kisko, K., Knaapila, M., Ikkala, O., Vuorimaa, E., Lemmetyinen, H. and Seeck, O. 2003. Self-assembled structures of hydrophobins HFBI and HFBII. J. Appl. Cryst. 36, pp. 499–502.

Contribution of the author

The author of the present thesis is responsible for the experimental work and contributed to writing in Publications I and II, for the experimental work and writing related to AFM in Publications III and IV, and has partial responsibility for preparing protein films, AFM and writing in Publication V.

Other publications that are not included in this thesis but to which the author has contributed:

VII Alakomi, H., Paananen, A., Suihko, M.-L., Helander, I. and Saarela, M. 2006. Weakening effect of cell permeabilizers on gram-negative bacteria causing biodeterioration. Appl. Environ. Microbiol. 72, pp. 4695–4703.

VIII Kruus, K., Kiiskinen, L.-L., Saloheimo, M., Hakulinen, N., Rouvinen, J., Paananen, A., Linder, M. and Viikari, L. 2003. A novel laccase from the ascomycete *Melanocarpus albomyces*. In: Applications of Enzymes to Lignocellulosics. Mansfield, S. D. and Saddler, J. N. (Eds). American Chemical Society, Washington, DC. ACS Symp. Ser. 855. Pp. 315–331.

IX Hakulinen, N., Kiiskinen, L.-L. Kruus, K., Saloheimo, M., Paananen, A., Koivula, A. and Rouvinen, J. 2002. Crystal structure of a laccase from Melanocarpus albomyces with an intact trinuclear copper site. Nat. Struct. Biol. 9, pp. 601–605.

X Tenkanen, M., Paananen, A. and Kroon-Batenburg, L. 2000. Wood fibre strength at the molecular level. Carbohydr. Eur. 28, pp. 34–37.

XI Paananen, A. 2000. Atomintarkat mikroskoopit. Tietoyhteys 4, pp. 21–22. (In Finnish)

Contents

Appendices

Appendices I–V of this publication are not included in the electronic version. Please order the printed version to get the complete publication (http://www.vtt.fi/inf/pdf/)

List of abbreviations

AFM	Atomic force microscopy
CD	Circular dichroism
DLVO	Derjaguin, Landau, Verwey and Overbeek
DP	Degree of polymerisation
EM	Electron microscopy
GIXD	Grazing incidence X-ray diffraction
HOPG	Highly oriented pyrolytic graphite
LB	Langmuir-Blodgett
LS	Langmuir-Shaefer
M_w	Molecular weight
PB	Poisson-Boltzmann
QCM-D	Quartz crystal microbalance with dissipation monitoring
SAXS	Small-angle X-ray scattering
SEM	Scanning electron microscopy
SFA	Surface force apparatus
TEM	Transmission electron microscopy

1. Introduction

1.1 Atomic force microscopy in biophysical sciences

The invention of the atomic force microscope (AFM) in 1986 (Binnig *et al*., 1986) opened a new perspective in the investigation of samples of biological origin. Compared to its predecessor, the scanning tunneling microscope (STM) (Binnig *et al*., 1982), AFM enabled measurements of non-conductive materials. A special feature and one of the major advantages of AFM compared to other microscopic techniques such as scanning electron microscopy (SEM) or transmission electron microscopy (TEM) is that it allows measurements in a liquid environment. From a biophysical point of view this is particularly important because biological samples can be observed in a near-physiological environment. The power and versatility of AFM in biophysical research is overwhelming (Table 1). In addition to the basic function of imaging sample topography at high resolution, AFM can be used to map chemical and mechanical surface properties, to track dynamic biochemical processes on surfaces and to directly measure intra- and intermolecular interactions.

DNA has been the most studied biological sample from the very beginning (Lindsay *et al*., 1989; Weisenhorn *et al*., 1990), and the review articles by Hansma (2001) and Lyubchenko (2004) outline AFM studies of DNA ranging from imaging of DNA conformations in air and in liquid to measuring single-molecule mechanics and thermodynamics. Recent DNA studies using AFM have shown the bioeffects of therapeutic ultrasound in the *in vitro* gene-delivery process (Duvshani-Eshet *et al*., 2006), and revealed structural properties of the complex formed when the SfiI restriction enzyme binds to DNA (Lushnikov *et al*., 2006). AFM has also been exploited in chromosomal research (Tamayo and Miles, 2002).

Another group of biomolecules widely studied with AFM is lipids, especially in the form of supported lipid films. Dufrêne and Lee (2000) reviewed AFM research on structural and physical properties of lipid films (mono/bi/multilayers). Their review covered studies of lipid films as homogeneous mono- and bilayers (Zasadzinski *et al*., 1991; Vikholm *et al*., 1995; Györvary *et al*., 1999) and as mixtures with other lipids (Solletti *et al*., 1996; Dufrêne *et al*., 1997) or other biomolecules (Egger *et al*., 1990; Vikholm

and Peltonen, 1996). Research using lipid films as a support for attaching individual biomolecules (DNA, Weisenhorn *et al*., 1991; acetyl choline esterase, Ohlsson *et al*. 1995; single-chain antibody, Vikholm *et al.*, 1996) or crystalline protein arrays (OmpF porin, Schabert *et al.*, 1995; s-layer, Wetzer *et al*., 1997; annexin V, Reviakine *et al*., 1998; streptavidin, Scheuring *et al*., 1999) has also been reported. The more recent studies of lipids using AFM continue characterisation of one- and two-component lipid films (Kaasgaard *et al*., 2003; Burns *et al*., 2005; Park and Lee, 2006; Steltenkamp *et al*., 2006), as well as biofunctionalization of solids and biosensor applications (Viitala *et al*., 2000; Ye *et al*., 2003; Ihalainen, 2004; Urisu *et al*., 2005).

The power of AFM is demonstrated in studies of membrane proteins, not only in imaging the structural properties (OmpF porin, Schabert *et al.*, 1995; purple membrane, Müller *et al*., 1995; aquaporin Z, Scheuring *et al*., 1999; ATP synthase, Seelert *et al*., 2000; Scheuring, 2000), but also in gaining functional (HPI, Müller *et al.*, 1996; OmpF porin, Müller and Engel, 1999; ATP synthase, Müller *et al*., 2003) and mechanical information (HPI, Müller *et al*., 1999; bacteriorhodopsin, Müller *et al.*, 2002). In addition to reconstituted membranes, the AFM studies of native membranes have also shown organised patterns of membrane proteins in high resolution (photosynthetic core complex, Scheuring *et al*., 2003; Scheuring *et al*., 2005). The organised structures of s-layer proteins have also been investigated by AFM (Wetzer *et al*., 1997; Moll *et al*., 2002; Györvary *et al*., 2003; Ebner *et al*., 2006). Averaging structural information from arrays of proteins may reveal details of single proteins, but shapes of individual proteins have also been imaged directly by conventional AFM setup in aqueous solution (GroES oligomer, Mou *et al*., 1996) and by enhancing imaging resolution using carbon nanotube tips (IgM, Hafner *et al*., 1999; GroES, Cheung *et al*., 2000; Guo *et al*., 2005) or cryogenic temperatures (IgG, IgM, Han *et al*., 1995; Sheng and Shao, 2002).

As in the case of DNA research (Lee *et al*., 1994a; Clausen-Schaumann *et al*., 2000), an important part of studying proteins with AFM has been force measurements (Butt *et al.*, 2005), which allow even individual molecular pairs or single molecules to be investigated (force spectroscopy, Zlatanova *et al.*, 2000; Hugel and Seitz, 2001). As examples of intermolecular force measurements between receptor and ligand across a surrounding medium, the strength of the biotin-(strept)avidin interaction has been determined (Lee *et al*.,

1994b; Florin *et al.*, 1994; Moy *et al*., 1994), and antibody-antigen interactions have been measured directly (Hinterdorfer *et al*. 1996; Dammer *et al*., 1996; Allen *et al*., 1997). Moreover, Schwesinger *et al*. (2000) and Kienberger *et al.* (2005) studied the relationship between the unbinding forces of antibody-antigen complexes obtained by AFM and the dissociation constants. AFM has also been shown to be very useful in studying intramolecular interactions, which are in general weaker forces than those related to breaking bonds. For example, an intramolecular unfolding force has been measured for titin, a protein that is involved in the contraction of muscle tissues (Rief *et al*., 1997a), the extracellular matrix protein tenascin (Oberhauser *et al*., 1998), the cytoskeletal protein spectrin (Rief *et al*., 1999) and Ig domains of a cell adhesion molecule (Carl *et al*., 2001). The unfolding pathway for bacteriorhodopsin has also been determined (Oesterhelt *et al*., 2000; Müller *et al*., 2002). Recently, protein engineering techniques have been exploited in combination with AFM force measurements to study the effect of point mutations on mechanical properties of proteins (Li et al., 2000) and on the stability of individual transmembrane domains (Müller *et al*., 2002). The sensitivity of AFM allows measurement of forces of interaction below 10 pN (10^{-11} N) (Butt *et al*., 2005), which has also been utilized in the development of cantilever-based biosensors (Fritz *et al*., 2000; Raiteri *et al*., 2001; Carrascosa *et al*., 2006).

Table 1. Overview of biophysical research using AFM. More detailed general reviews of AFM in biophysacial applications are listed at the end of section 1.1. The published AFM research related to biopolymers studied in this thesis is described in Results and Discussion.

Research interest	Examples	Selected references
Imaging of		
biomolecules	Antibodies	Cheung *et al*., 2000; Sheng and Shao, 2002
	DNA, RNA	Hansma, 2001; Lyubchenko, 2004
	Heat shock proteins	Cheung *et al*., 2000
biomolecular assemblies	Cellulose microfibrils	Kuutti *et al*., 1995; Baker *et al*., 1997
	Lipid layers	Dufrêne and Lee, 2000; Steltenkamp *et al.*, 2006
	Membrane proteins	Scheuring, 2000; Scheuring *et al*., 2005
	S-layer proteins	Györvary *et al*., 2003; Ebner *et al*., 2006
cells	Bacterial cells	Dufrêne, 2004
	Living cells in general	Henderson, 1994
	Wood fibre	Niemi *et al*., 2002; Gustafsson, 2004
Measuring interactions		
intramolecular	Proteins	Rief *et al*., 1997a; Oesterhelt *et al*., 2000
	Polysaccharides	Rief *et al*., 1997b
intermolecular	DNA strands	Lee *et al*., 1994a
	Biotin-(Strept)avidin	Florin *et al*., 1994; Moy *et al*., 1994
	Antibody-Antigen	Hinterdorfer *et al*., 1996; Kienberger *et al*., 2005
cellular	Carbohydrates	Tromas *et al*., 2001
	Integrins	Lehenkari and Horton, 1999
	Lectin-Ligand	Fritz *et al*., 1998; Lekka *et al*., 2006
Obtaining with topography		
chemical	Lipids	Berger *et al*., 1995
functional	Antibody-antigen	Hinterdorfer *et al*., 1996
	Receptors on cell membrane	Grandbois *et al*., 2000; Horton *et al*., 2002
mechanical information	Friction on lipid monolayers	Dufrêne and Lee, 2000
Monitoring processes *in situ*		
function observed by conformational change	Lysozyme	Radmacher *et al*., 1994b
	Membrane proteins	Müller and Engel, 1999
growth and disassembly	Protein crystals	Reviakine *et al*., 1998
	Structural proteins	Cisneros *et al*., 2006; Gosal *et al*., 2006
cellular processes	Motility of cells	Oberleithner *et al*., 1993
	Platelet activation	Fritz *et al*., 1994
others	RNA polymerase	Kasas *et al*., 1997
	Starch degradation	Thomson *et al*., 1994

There is a growing interest in obtaining functional, chemical or mechanical information simultaneously with topographical information in biological systems. Dufrêne and Lee (2000) reported studies of measuring mechanical properties of lipid monolayers, and Radmacher *et al*. (1994a) mapped interaction forces with AFM. In chemical force microscopy AFM is used to map the spatial arrangement of chemical functional groups and their interactions by chemical derivatization of the tip (Frisbie *et al*., 1994). Chemical differences can be distinguished by measuring frictional or adhesion forces between the functionalised tip and the studied surface. This technique has been applied to the study of lipid monolayers (Berger *et al*., 1995). Closely related to biological issues, McKendry *et al*. (1998) investigated the dependence of chirality on the interaction between molecular pairs. The most widely studied application in mapping surface properties is the localisation of antibody-antigen interactions on surfaces (human serum albumin, Hinterdorfer *et al*., 1996; ferritin, Allen *et al*., 1998; intracellular adhesion molecule-1, Willemsen *et al*., 1998). These have been the basis for the development of molecular recognition imaging, which combines the capability of AFM to image topography in high resolution with force measurement with high sensitivity (lysozyme, Raab *et al*., 1999; skeletal muscle Ca^{2+} release channel, Kada *et al*., 2001; avidin-biotin, Ebner *et al*., 2005). The recent review articles by Kienberger *et al*. (2006) and by Hinterdorfer and Dufrêne (2006) discuss the current status of the technique.

The unique capability of AFM for carrying out measurements in physiological-like environments allows the monitoring of surface processes *in situ* and in real-time. For example, a conformational change of lysozyme during hydrolysis has been observed by monitoring the height of a single molecule (Radmacher *et al*., 1994b). Another good example of recording enzymatic activity in real-time is the transcription of double-stranded DNA templates by RNA polymerase (Kasas *et al*., 1997). Growth of protein crystals has also been observed *in situ* (Reviakine *et al*., 1998), as well as conformational changes related to the functionality of membrane proteins (Müller *et al*., 1996; Müller and Engel, 1999). Growth and disassembly of structural proteins has also been observed in real-time: self-assembly (Cisneros *et al*., 2006) and biodegradation of collagen (Paige *et al*., 2002), disassembly of microtubules (Thomson *et al*., 2003) and growth of amyloid (Goldsbury *et al*., 1999; Gosal *et al*., 2006).

It is not surprising that AFM has been applied in cell biology (Lehenkari *et al*., 2000; Charras *et al.*, 2002). AFM has allowed imaging of cell surfaces (Butt *et al*., 1990; Hoh and Hansma, 1992; Henderson, 1994), measurement of interaction forces of proteins specific to membranes (integrin, Lehenkari and Horton, 1999) and locating of receptors on cell membranes (ABO groups on red blood cells, Grandbois *et al*., 2000; Horton *et al*., 2002; receptor-assisted proteins on fibroblast cells, Osada *et al*., 2003) in almost *in vivo* physiological conditions. Interaction force measurements of carbohydrates related to cell adhesion have also been investigated (P-selectin, Fritz *et al*., 1998; Tromas *et al*., 2001; glucan, Lekka *et al*., 2006). Moreover, dynamic biological cellular phenomena have been monitored by AFM: dynamics of actin filaments (Henderson *et al.*, 1992), surface processes on virus-infected cells (Häberle *et al*., 1992), motility of cells (Oberleithner *et al*., 1993), platelet activation (Fritz *et al*., 1994), motion of particles along cytoskeletal elements (Schoenenberger and Hoh, 1994) and stiffening of the cortex between adherent cells during division of living cells (Matzke *et al*., 2001). Research on microelastic mapping (A-Hassan *et al*., 1998) and nanomechanical intendation of cell surfaces has also been carried out with AFM (Charras and Horton, 2002; Withers and Aston, 2006). Related to cell adhesion there have been studies using AFM in the biomaterials field (Jandt, 2001) and in research focusing on how variables of the mechanical environment affect attachment of cells to surfaces (Thompson *et al*., 2006). Dufrêne (2004) reviewed AFM research focusing on bacterial cell surfaces. For example, changes in surface morphology and composition of bacteria have been detected after applying various treatments (Dufrêne, 2001; publication VII), and enzyme digestion of living cells in real-time has been monitored (Ahimou *et al*., 2003). Adhesion of yeast cells on hydrophobic and protein-coated surfaces has also been measured by means of attaching a single cell to the cantilever and measuring the interaction force between the cell and the substrate surface (Bowen *et al*., 2001).

Plant and algal cell research and food applications using AFM are usually not discussed in the same forum as the general AFM reviews devoted to biological applications, despite the relevance to the subject. Hence, some studies are mentioned here. For example, microcrystalline cellulose, a cell wall component of seaweed, has been imaged at high resolution (Kuutti *et al*., 1995; Baker *et al*., 1997). The AFM images of the crystalline cellulose surface by Baker *et al*. (2000) appear to be of the highest resolution (0.17 nm) hitherto obtained for a sample of biological origin. Continuing with research related to cellulose, a

comprehensive review of studies using AFM in wood, fibre and paper research was presented by Niemi *et al.* (2002), starting from the first publications exploiting AFM in imaging cellulose microfibrils (Hanley *et al*., 1992), wood sections and pulp fibres (Hanley and Gray, 1994). More recent publications report the characterisation of chemical and mechanical pulps (Simola *et al*., 2000; Koljonen *et al*., 2003; Gustafsson *et al*., 2003a; Gustafsson *et al*., 2003b; Gustafsson, 2004), and characterisation of lignin (Simola-Gustafsson *et al*., 2001; Maximova *et al*., 2001) and extractives (Fardim *et al*., 2005; Österberg *et al*., 2006) on fibre surfaces with AFM and other surface analytical techniques. Plant polysaccharides used as food additives, such as pectin and carrageenan, have been visualised (Morris *et al.*, 1997). Gunning *et al.* (2004) studied interactions between surfactants and surface active proteins, β-lactoglobulin and β-casein, at the air-water interface. There are several examples of using AFM in visualising starch samples: degradation of starch granules by α-amylase has been imaged *in situ* in real-time (Thomson *et al*., 1994), ageing of thermoplastic starch film has been followed by means of friction force imaging simultaneously with topography imaging (Kuutti *et al*., 1998), and the ultra structure of starch granules has been imaged (Ridout *et al*., 2002). AFM has also been exploited in investigations of thermally induced aggregates of the soya globulin β-conglycinin (Mills *et al*., 2001), in studies of interfacial behaviour of whey proteins (Woodward *et al*., 2004), in measuring the force required to detach fouling deposits of whey protein concentrate (Liu *et al*., 2006), and in visualising the mesostructure of milk chocolate (Rousseau 2006).

The published AFM research related to the biopolymers studied in this thesis, i.e. cellulose and xylan in pulp and paper research (Publication I), gliadins in food research (Publication II) and hydrophobins (Publications III–V), is discussed in Results and Discussion. The studies referred to above are only a small part of all applications published in the field of AFM and biological materials. For a more thorough discussion of AFM applications in biophysical sciences the reader is referred to review publications by Vansteenkiste *et al*. (1998), Engel and Müller (2000), Fotiadis *et al*. (2002), Hörber and Miles (2003), Santos and Castanho (2004), and Alessandrini and Facci (2005).

1.2 Surface forces and interactions in aqueous medium

Surface forces and interactions determine the behaviour of biopolymers and biopolymer assemblies. The non-covalent surface forces involved in the interactions are weaker than covalent or ionic bonds. The surface forces arise from the surface properties and geometry of the interacting molecules or particles. The properties of the medium are equally important, as well as the distance between the interacting partners. Interactions between biopolymers, like between any macromolecules or colloidal particles, are a combination of different types of forces, where one interaction may dominate over another at certain distances (Israelachvili, 1992).

In this section, the main types of surface forces and interactions are described briefly, concentrating on the interactions relevant to biopolymer systems in an aqueous environment. First the DLVO forces, named according to the DLVO theory (Derjaguin and Landau 1941; Verwey and Overbeek, 1948), are described. These forces include the van der Waals forces and the electrostatic double-layer forces in describing the interaction between surfaces in a liquid medium, and are often a good approximation for the interactions. The DLVO theory contains several assumptions. The ions in the liquid are assumed to be point-like and moving freely. The electrostatic potential at any point in the liquid is assumed to be the time-averaged value of the distribution of potentials at this point resulting from the movements of the ions (the so-called mean field approximation). This is partly the reason why the DLVO theory often fails in describing interactions at very short separations. Another shortcoming is that between the interacting bodies other types of interactions also exist. These often dominate the interactions at short distances in more complex colloidal and biological systems (Israelachvili, 1992). These interactions are referred to here as ‘special interactions’, the terminology and classification of which varies in the literature.

The DLVO theory was applied to the interpretation of the force measurements in cellulosic systems in Publication I, and hence the equations shown here are those used for describing those experiments. The basics of surface forces and interactions are equally relevant for understanding the phenomena taking place in Publications II–V, although theory-based calculations were not applied to the results. There are textbooks (Israelachvili, 1992; Hiemenz and Rajagopalan, 1997) and a recent review article by Butt *et al*. (2005) that discuss the surface

forces in greater detail and these are recommended to the reader for further information.

1.2.1 The DLVO forces

The DLVO forces are the van der Waals forces and the electrostatic double-layer forces. The DLVO theory predicts that the interaction between surfaces with charges of the same sign in a liquid medium is dominated by the repulsion originating from the so-called double-layer of co-ions and counterions at large separations, whereas the van der Waals attraction becomes more significant at shorter distances. For surfaces of opposite sign, the DLVO theory predicts attraction at long distances but repulsion at close to molecular contact. Increasing the electrolyte concentration of the medium will cause shielding of the electrostatic repulsion, and the balance between the DLVO forces can be altered towards van der Waals attraction between the interacting bodies.

van der Waals forces

The van der Waals forces consist of three different types of forces that originate from time-dependent dipoles in atoms or molecules. The Keesom forces are called orientation forces and they occur between two permanent dipoles which change their orientation while interacting. The Debye forces, or induction forces, originate from the permanent dipole – induced dipole interaction, where the dipole moment is induced to the non-polar molecule in the polarizing field coming from the permanent dipole. Temporary induced dipoles exist in all atoms and molecules at any instant because of the varying distribution of electrons around the nuclei; hence all atoms and molecules are polarisable. This is the origin for the third type of van der Waals forces, i.e. London or dispersion forces, which act between two induced dipoles and which are always present between all atoms and molecules, including charged and polar molecules. At short distances the van der Waals forces are all proportional to $1/r^6$, where r is the distance between interacting atoms or molecules. However, the dispersion contribution of the total van der Waals force decays more rapidly at distances beyond 5 nm than at smaller distances. This phenomenon is referred to as the retardation effect. Thus, when a temporary dipole arises and generates an electric field that expands with the speed of light and causes an induced dipole in the

second molecule, the electric field generated by the induced dipole reaches the first dipole at the speed of light in time Δt. If the first dipole is changing faster than Δt, causing less favourable orientation for attraction, the interaction becomes weaker. The retardation effect becomes more important in a liquid medium and between macroscopic bodies.

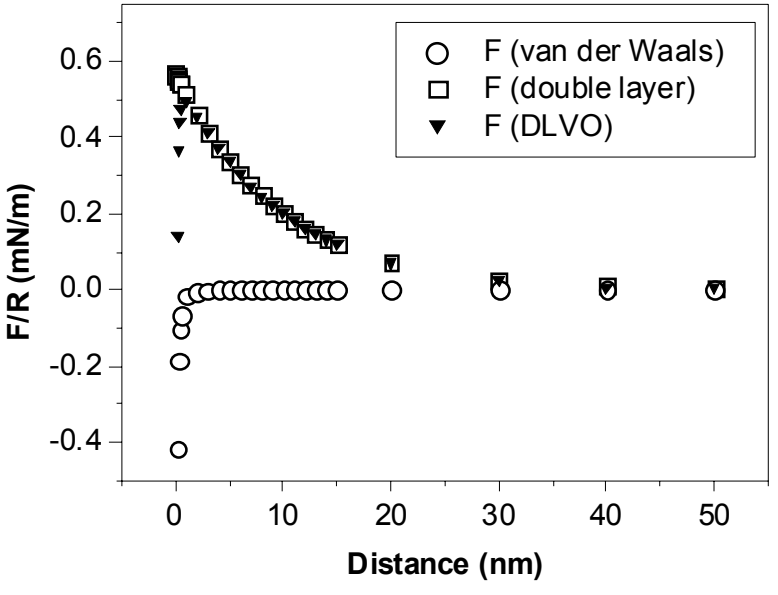

Figure 1. Contribution of the van der Waals (circle) and the electrostatic double-layer forces (square) to the total DLVO interaction (down triangle) between cellulose spheres in 1 mM NaCl (calculated according to equations 1 and 4, assuming constant surface charge).

Between macroscopic bodies the van der Waals forces (Figure 1) are stronger, decay more slowly with distance ($1/D^2$ between planar surfaces) and are more geometry-dependent than between atoms and molecules. According to the method proposed by Hamaker (1937), which assumes additivity of the van der Waals forces, and by using the Derjaguin approximation (Derjaguin, 1934), which relates the energy per unit area between two flat surfaces to the energy between two bodies of arbitrary shape, the expression for the non-retarded van der Waals force ($F_{vdW}(D)$) between two spheres of radius R_1 and R_2 is

$$F_{vdW}(D) = -\frac{A_H}{6D^2} \cdot \frac{R_1 R_2}{R_1 + R_2} \tag{1}$$

where A_H is the Hamaker constant, which depends on molecular polarizability and dipole moments and on the number concentration of molecules, and D is the distance between interacting surfaces. It should be noted here that the Derjaguin approximation is valid only if $D << R$. Assumption of additivity of the van der Waals force neglects the effect of nearby atoms on the couple of interacting atoms, and hence causes large errors in calculating the Hamaker constant. The solution for this problem was the theory proposed by Lifshitz (1956): each body is treated as a continuum with certain dielectric properties, which includes many-body effects automatically. Hence, the Hamaker constant in equation (1) for the interaction between media 1 and 2 across the medium 3 can be calculated using refractive indices (n_i) and dielectric constants (ε_i) of the media:

$$A_H \cong \frac{3}{4} k_B T \left(\frac{\varepsilon_1 - \varepsilon_3}{\varepsilon_1 + \varepsilon_3} \right) \left(\frac{\varepsilon_2 - \varepsilon_3}{\varepsilon_2 + \varepsilon_3} \right) + \frac{3h\nu_e}{8\sqrt{2}} \frac{\left(n_1^2 - n_3^2\right)\left(n_2^2 - n_3^2\right)}{\sqrt{\left|n_1^2 - n_3^2\right|}\sqrt{\left|n_2^2 - n_3^2\right|}\left[\sqrt{\left|n_1^2 - n_3^2\right|} + \sqrt{\left|n_2^2 - n_3^2\right|}\right]} \tag{2}$$

where k_B is the Boltzmann constant, T is the absolute temperature, h is the Planck's constant and ν_e is the mean absorption frequency. According to equations (1) and (2) the van der Waals force between two identical bodies ($\varepsilon_1 = \varepsilon_2$ and $n_1 = n_2$) in a medium (ε_3, n_3) is always attractive, because A_H is positive, whereas the force between two different bodies can be either repulsive or attractive.

Electrostatic double-layer forces

The electrostatic double-layer forces are always present between charged surfaces in liquids containing electrolyte. However, for the double-layer forces to be significant the electrolyte concentration must be rather low, particularly if multivalent counterions are present. The charging of surfaces in liquid can be formed by the ionization of surface groups or by adsorption or binding of ions from solution onto a previously uncharged surface. In the presence of electrolyte in solution the surface charge formed by either of these mechanisms is balanced by an oppositely charged region of counterions, of which some are bound directly to the surface (the so-called Stern layer) and others form a diffuse layer

around the surface. The diffuse layer also contains co-ions that are repelled by the surface and that are balanced by the counterions. The co- and counterions and the charged surface together are called the electric double-layer, where the total charge of co- and counterions is equal but of opposite sign to that of the surface. When two charged surfaces approach each other in electrolyte solution, the double-layers start to overlap at a certain distance, and the resulting force is called the electric double-layer force. If the approaching surfaces have the same charge, the concentration of counterions between surfaces increases and the concentration of co-ions decreases giving rise to repulsion (Figure 1).

The electrostatic double-layer force decays approximately exponentially at large distances. The decay length or the effective range of the double layer force can be described by the Debye length, κ^{-1}, that depends on the dielectric properties (ε) and the ionic strength (I) of the medium (but not on the surface properties):

$$\kappa^{-1} = \sqrt{\frac{\varepsilon\varepsilon_0 k_B T}{e^2 I}}, I = \sum_i c_i Z_i^2 \tag{3}$$

where ε_0 is the permittivity of the vacuum, e is the unit charge, c_i is the bulk concentration and Z_i is the valency of ion *i,* summing over all ions present. As can be seen from equation (3) the Debye length is shorter at higher ionic strengths.

The continuum theory, based on a theory by Gouy (1910), Chapman (1913), and Debye and Hückel (1923), can be used in calculating the electric double-layer force. The theory uses the Poisson-Boltzmann equation (PB) for determining the distribution of charges outside a surface, and requires assumption of boundary conditions for approaching surfaces: either surface charge or surface potential is assumed to remain constant. When the surface charge is assumed to remain constant, adsorption or desorption of ions is presumed not to take place when the distance between interacting surfaces is changing. The opposite situation is assumed with the constant surface potential, where the surface potential remains constant due to free exchange of ions between the media. These boundary conditions greatly affect the electrostatic force at short distances (~below $2\kappa^{-1}$), and the choice of boundary condition for the studied system depends on the material properties of the surfaces. The electrostatic double layer force ($F_{dl}(D)$)

between two spheres of the same material with radius R_1 and R_2 and low surface potentials (about below 25 mV) can be expressed as (Israelachvili, 1992):

$$F_{dl}(D) = 4\pi \frac{R_1 R_2}{R_1 + R_2} \varepsilon \varepsilon_0 \kappa \psi^2 e^{-\kappa D} \tag{4}$$

where ε_0 is the permittivity of the vacuum, ε is dielectric constant of the surface, κ is the reciprocal of the Debye length (equation (3)), and ψ is the surface potential. However, it is more realistic to assume that the real situation at small separations is somewhere in between the boundary conditions of constant surface charge and constant surface potential. One option is to apply the charge regulation model (Ninham and Parsegian 1971), which assumes that the adsorption of ions depends on the distance between the interacting surfaces, and which includes the dissociation constants of adsorbing ions to the calculations. The charge regulation model predicts the dependency of the surface charge on pH and ionic strength, which is relevant but rather too complex to apply to biological systems. Another option is to calculate the two extremes separately and to analyse the result to be somewhere in between the extremes.

1.2.2 Special interactions

In biopolymer systems water is the normal solvent and hence participates in the interactions. The natural mechanism for the involvement of water is through hydrogen bonding (a special case of strong dipole interaction).

Hydration repulsion

Solvation forces between hydrophilic surfaces in aqueous medium are called hydration forces. The hydration forces are short-ranged forces (1–3 nm), and in contrast to the electrostatic double-layer forces, hydration repulsion becomes stronger and longer-ranged with increasing electrolyte concentrations. The hydration repulsion has been thought to arise when water molecules bind to the hydrophilic surfaces by charge-dipole and dipole-dipole (hydrogen bonding) interactions. The strength of repulsion depends on the energy required to remove

the water of hydration, or the surface-adsorbed species containing water molecules, from the surfaces when they approach each other. There are also theories explaining the repulsion by modification of water structure near hydrophilic surfaces (Marčelja and Radić, 1976) or by the osmotic effect of hydrated ions that are trapped between the two approaching surfaces (Marčelja *et al*., 1997). In interactions between biopolymers, the hydration forces are also present but are often very difficult to identify in the experiments due to the softness of biological materials.

Hydrophobic interaction

In general, the hydrophobic interaction is a water-mediated attraction that brings hydrophobic units together in aqueous medium. This type of attraction occurs between molecules containing hydrophobic groups, such as surfactants, proteins and polymers, and between hydrophobic surfaces in aqueous medium. The hydrophobic interaction is stronger than the van der Waals attraction, and it increases in strength with increasing temperature (Israelachvili, 1992). The strong cohesive forces in water play a central role in the hydrophobic interaction, the strength and range of which depend on the size of the hydrophobic partners (molecular units vs large particles) (Chandler, 2005).

Several theories have been proposed on the basis of phenomena observed experimentally to explain the origin of the hydrophobic interaction, but still it is not fully understood (for a review see publications by Christenson and Claesson (2001) and Butt *et al*. (2005)). It has been suggested that hydrophobic forces arise from changes of the water structure, i.e. the rearrangement of the hydrogen bonding network in the vicinity of hydrophobic surfaces when they approach each other (Eriksson *et al*., 1989). This could explain only the short-ranged interaction, but not the long-ranged interaction also observed experimentally, because the reorientation of water molecules near the surface takes place only within a distance of several molecular diameters. Another theory proposes that the attraction is due to induced cavitation, i.e. the spontaneous nucleation of vapour phase between the interacting surfaces after being in contact (Rabinovich *et al*., 1982; Christenson and Claesson, 1988), but the long-ranged interaction observed experimentally (even 100 nm) still remains elusive. A recent hypothesis for explaining the long-range attraction is the pre-existence of so called nanobubbles on the hydrophobic surfaces in aqueous solution and that the

bubbles form bridges between the approaching hydrophobic surfaces, and further on, the formed cavities cause a strong attraction due to meniscus force (Parker *et al*., 1994; Attard, 2000). These hypotheses support the idea expressed by Stillinger (1973), that hydrogen bonding networks cannot be maintained near large hydrophobic surfaces, and this can cause 'drying' of the hydrophobic surface, i.e. the formed interface has similarities to liquid-vapour interface. Based on theoretical calculations Lum *et al*. (1999) further described that fluctuations of such liquid-vapour-like interfaces can cause pressure imbalance between interacting hydrophobic surfaces by destabilizing the remaining liquid between the surfaces, and hence, cause surfaces to attract each other.

In the abovementioned experimental approaches for measuring interaction forces directly, the interacting surfaces are relatively large compared to the molecular scale. In biopolymer systems such large homogeneous hydrophobic regions are not exposed. Hence, the hydrophobic interaction is shorter in range in the molecular scale (Lum *et al*., 1999). Meyer *et al*. (2006) stated that the true hydrophobic interaction, that has an important role for example in determining the structure of proteins and in molecular self-assembly, is only the short-ranged attraction (< 10 nm). Chandler (2005) described the ways in which hydrophobic molecules interact with water based on theoretical work and simulations. In addition to repelling water and acting like cavities where hydrogen bonding is impossible, attractive forces also exist. The van der Waals forces are always present, and have a significant effect on the location of the liquid-vapor-like interface. The strong attraction between water molecules and hydrophilic groups, which is especially important in amphiphilic molecules, affects how hydrophobic assemblies orient themselves in relation to interfaces and other structures, but is not responsible for the formation of hydrophobic assemblies. For the hydrophobic attraction to lead to a stable assembly, the size of the hydrophobic molecule must extend to 1 nm or more. This is due to interplay of interactions favouring association when the critical size of 1 nm is exceeded. When the radius of the volume that excludes water (cavities) is more than 1 nm, the surface can be defined as 'dewetted'. The greater the size the more liquid-vapour-like interface is formed, and more freedom for fluctuations leading to assemblies is introduced (Chandler, 2005). Based on the experimental observations between hydrophobic surfaces, Meyer *et al*. (2006) concluded that only the short-ranged (< 10 nm) attraction is observed in all cases, and hence, contains information about the true hydrophobic interaction.

Polymer-induced interactions

The presence of polymers, including biopolymers, on surfaces creates a thermally mobile layer giving rise to interactions that can be either attractive or repulsive (Figure 2). These interactions depend on the coverage or amount of molecules on the surface, and on how the molecules are attached to the surface (by physisorption or by chemisorption), as well as on the quality of the solvent by affecting for example the shape of molecules protruding from the surface and the thickness of the polymer layer (Israelachvili, 1992; Fleer *et al*., 1993).

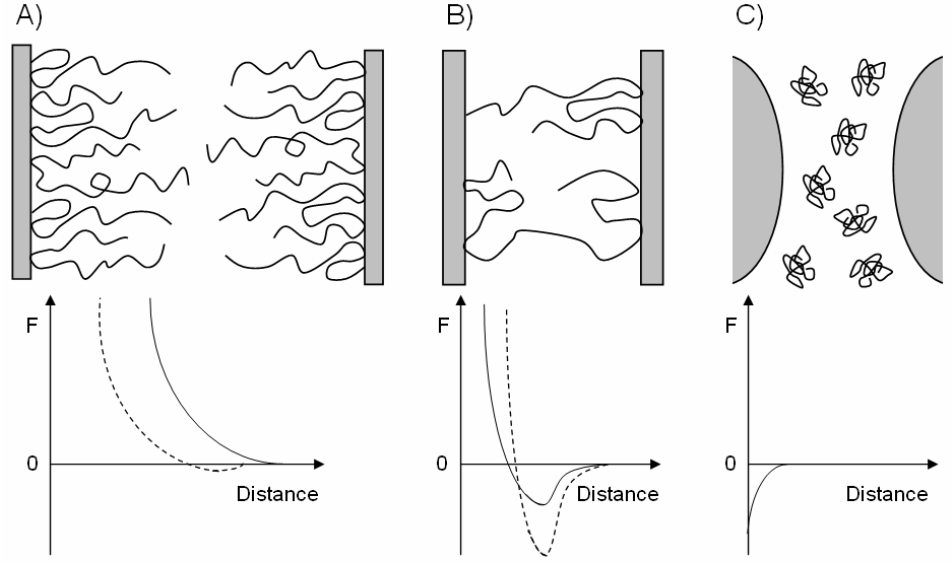

Figure 2. Interaction forces between polymer-coated surfaces (A and B), and between surfaces immersed in a polymer solution (C). Graph A) shows that the interaction between polymer-coated surfaces with high surface coverage (polymer brush) in a good solvent (solid line) is repulsive, but in a poor solvent (dashed line) is first attractive due to intersegment attraction. In graph B) the corresponding situation is shown for polymer-coated surfaces with low surface coverage. In a good solvent (solid line) attraction is due to bridging only, but in a poor solvent (dashed line) attraction also contains contribution to intersegment interaction. Graph C) shows attraction due to depletion. Distances shown in the graphs correspond to the distances between (grey) surfaces in the illustrations. The scales are arbitrary. (According to Israelachvili, 1992; Hiemenz and Rajagopalan, 1997.)

The most important polymer-induced interaction is repulsive. In a good solvent chain molecules that are firmly attached to the surface at some point protrude into the solvent (Figure 2A). When surfaces having a large surface coverage of such chain molecules (polymer-brush) approach each other, the dangling chains start to overlap causing reduced conformational entropy of the polymer chains (Israelachvili, 1992; Hiemenz and Rajagopalan, 1997). The loss of conformational entropy is always repulsive at small separations. On the other hand, upon approach the number of segment-segment contacts on the above-described surfaces increases, replacing the segment-solvent contacts. This may give rise to either repulsion or attraction, depending strongly on the solvent. In a good solvent the long-range interaction is repulsive. In a poor solvent the intersegment interaction is stronger than the segment-solvent interaction, and the most long-ranged interaction can be attractive although the short-range interaction is repulsive. The contribution due to loss of conformational entropy and the intersegment interaction are together called steric interaction between polymer-coated surfaces (Israelachvili, 1992; Hiemenz and Rajagopalan, 1997). If the polymer chains contain charged groups, the interaction may be referred to as 'electrosteric interaction', being a combination of steric and electrostatic double-layer contributions.

If the interacting surfaces are not fully covered by the polymer, and the interaction between surface and polymer is attractive, the polymer may bind to both surfaces. This is called bridging (Figure 2B), which is effective at low surface coverage and results in attraction at large separations. Another type of polymer-induced attraction exists, and is called depletion (Figure 2C). This occurs when polymers are in solution but there is no adsorption to the surfaces. The resulting weak attraction is due to increase in free volume accessible to polymers in solution when interacting surfaces are closer than the average radius of a polymer molecule, and becomes important at high bulk concentrations of polymer molecules. In practice, however, it is difficult to distinguish between bridging and depletion attraction (Israelachvili, 1992; Hiemenz and Rajagopalan, 1997).

Specific interactions

Although specific interactions are not among the key topics of this thesis, they are briefly mentioned here because they are strongly related to proteins, and hence to biopolymers. Specific interactions give rise to (usually) strong adhesion

or binding between interacting molecules or surfaces. Well known examples of specific interactions in molecular recognition are antibody-antigen interaction and enzyme-substrate interaction (ligand-receptor interactions, 'lock and key'). In specific interactions several non-covalent interactions cooperate, i.e. hydrogen bonding, van der Waals, electrostatic and hydrophobic interactions. The specificity is determined by the complementarity of these interactions provided by the local geometry that is precisely complementary to the geometry of the other interacting body and has precise stoichiometry as in covalent bonds (Leckband, 2000)

The specific interaction can also be weak in strength (i.e. comparable to thermal energies), still having the geometrical and chemical complementarity but being difficult to distinguish from non-specific interactions. Non-specific interactions are always present and result from fundamental properties of proteins and interfaces. Experimentally these can in some cases be distinguished by carefully choosing the control experiments, i.e. by replacing either of the interacting partners with an inert protein or by introducing a specific inhibitor that obstructs the interaction (Weisel *et al*., 2003). It has been shown that the strength of non-specific protein-protein adhesion may overlap the forces originating from specific receptor-ligand interactions (Willemsen *et al*., 1998). Litvinov *et al*. (2002) suggested that these weaker non-specific interactions may have physiological significance for example in cell adhesion by cooperating with the specific interactions.

1.3 Self-assembly of amphiphiles at the air-water interface

In general, self-assembly is a reversible process in which components spontaneously organise into structures or patterns without external guidance. This definition is applicable to structural organisation in all scales, from molecules to galaxies, and the concept of self-assembly is used in many disciplines (Whitesides and Grzybowski, 2002). There is some diversity in terminology in the literature (Lehn and Ball, 2000), and hence it should be mentioned here that in this thesis 'self-assembly' also covers the concept of self-organisation.

The emphasis of self-assembly in this thesis is on molecular self-assembly of biopolymers in aqueous solutions, where the assembling components are complementary molecules or segments of macromolecules. The assemblies are held together by the interplay of attractive and repulsive surface forces and interactions that are generally non covalent (van der Waals and electrostatic forces, hydrophobic interactions and hydrogen bonding) and weaker than covalent or ionic bonds. Self-assembly through weak covalent bonds, i.e. metal ion coordination, can also take place. Another important issue in the formation of ordered assemblies is reversibility. The molecules must retain the adjustability of their positions within an aggregate, i.e. the environment must allow motion of the components (Lehn and Ball, 2000; Whitesides and Boncheva, 2002). Whitesides and Boncheva (2002) listed examples of molecular self-assembly and pointed out that whether 'self-assembly', 'molecular recognition' or 'complexation' (or other definition) is used to describe the processes where more ordered is formed from less ordered components, varies along the authors using them. For example, folding of proteins and nucleic acids, receptor-ligand association, phase-separation of polymers, formation of self-assembled monolayers, lipid bilayers, colloids, and molecular crystals are all forms of molecular self-assembly.

Amphiphiles are molecules possessing both hydrophilic and hydrophobic properties, such as surfactants, lipids and proteins. The self-assembly of amphiphiles into different structures in aqueous solutions and their accumulation to interfaces (air-water or oil-water) have been widely studied. The formation and structure of micelles, inverted micelles, bilayers and bilayer vesicles depend on the amphiphile (shape and size of the hydrophilic and hydrophobic parts) and the solution conditions (amphiphile and electrolyte concentration, pH and temperature). The main forces and interactions that act in self-assembly of amphiphiles in solution and in their affinity to interfaces originate from hydrophobic interaction between hydrophobic areas and from repulsion between hydrophilic areas (Israelachvili 1992; Jönsson *et al*., 1998). In this thesis the amphiphiles under study are surface active proteins called hydrophobins that contain regions with distinct hydrophilic and hydrophobic properties. Other examples of surface active biopolymers in nature include the milk protein casein and many salivary proteins. They can be defined as 'surfactants', because they are able to orient themselves so that the hydrophilic regions are towards the polar environment and the hydrophobic regions are exposed to the non-polar phase. Characteristic to polymeric surfactants is that they are effective even at

low concentrations, they have a very strong driving force to interfaces, and they are relatively insensitive to physical variables such as salt concentrations or changes in temperature (Jönsson *et al.*, 1998).

This thesis focuses on studying the behaviour and self-assembly of amphiphilic biopolymers at the air-water interface (Publications III–V), where amphiphiles adsorb with their hydrophilic regions directed towards the aqueous solution and the hydrophobic regions orienting towards air. The surface-activity of amphiphiles disrupts the hydrogen bonding network at the air-water interface and causes lowering of the surface tension of water (72 mJ/m^2). Typical values of surface tension for aqueous solutions of surfactants are in the range of 28–34 mJ/m^2 (Jönsson *et al.*, 1998). At the air-water interface the assembly of amphiphilic molecules is more restricted than in solutions in the sense that the association or organisation of molecules takes place in two dimensions, but on the other hand has more freedom in lateral directions than when adsorbing on a solid surface. This makes the degree of hydrophilicity of the molecular groups also very important in determining the interactions responsible for associations of amphiphilic molecules in lateral directions (Israelachvili, 1992; Chandler, 2005).

1.4 Aims of the present study

This thesis is a combination of three different topics with separate goals. The cellulose-xylan work incorporating AFM was part of an EU project called "The strength of wood fibres: Association between hemicellulose and cellulose at the molecular level" (FAIR-CT96-1624), and aimed at obtaining information about the cellulose-xylan association by AFM interaction force measurements. The gliadin work was carried out during a two-month visit to the group of prof. Mervyn Miles in the H.H. Wills Physics Laboratory, University of Bristol. Their ongoing project on gluten proteins aimed at understanding the nature and strength of the interaction between monomeric gliadin molecules and the possible roles for gliadins in forming the network in dough. The hydrophobin work presented in this thesis was part of ongoing research at VTT related to nanobiomaterials and the AFM work focused on studying self-assembly of hydrophobins at the air-water interface. The combination of these studies demonstrates the versatility of AFM in biophysical research, both as an imaging and as a sensitive force measurement tool.

2. Materials and Methods

2.1 The studied biopolymers

2.1.1 Cellulose and xylan

Cellulose is the most abundant natural polymer, being the main constituent of the cell walls of all plants, many algae and a few bacteria, providing the rigidity of the cell wall, and hence the size and shape of cells. It is the main raw material for the paper, wood and textile industry. Cellulose consists of long unbranched chains of β-(1,4) linked D-glucose molecules, in which every second glucose residue is rotated by 180° with respect to the preceding residue, making cellobiose the smallest repeating unit (Figure 3). The chains form bundels, microfibrils, which are stabilised by inter- and intramolecular hydrogen bonds. The microfibrils associate to form fibrils that finally build up the cellulose fibre wall (Hon, 1994). The naturally occurring form of cellulose is called cellulose I, which comprises two allomorphs, a triclinic (I_α) and monoclinic phase (I_β), that differ in their hydrogen bonding patterns (Atalla and Vanderhart, 1984; Sugiyama *et al*., 1991; Heiner *et al*., 1995). The native cellulose and the other crystalline forms, celluloses II, III and IV, differ in hydrogen bonding networks and unit cell dimensions, and can be identified on the basis of their X-ray diffraction patterns and IR spectra (Blackwell, 1982). Celluloses II, III and IV can be formed by applying certain treatments to cellulose I. For example, cellulose II can be formed by mercerization with subsequent removal of the alkali (Hon, 1994). The native cellulose is an uncharged biopolymer, but carboxylic groups can be introduced by various treatments (Sjöström, 1993).

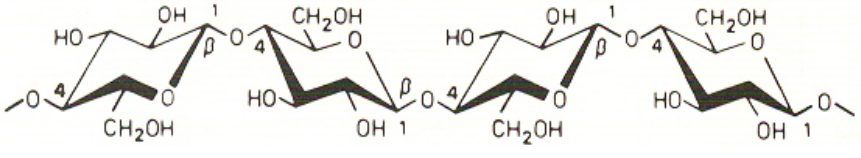

Figure 3. The structure of cellulose (from Sjöström,1993).

The cellulose study presented in this thesis focused on wood processing research. In the wood cell cellulose fibrils are packed together and surrounded by hemicelluloses and lignin. Cellulose, hemicelluloses and lignin are the main

constituents of wood fibres. Hemicelluloses are heteropolymers that function as supporting material in the cell walls. The backbone is composed of β-1,4-linked glucose, mannose, xylose or galactose. The molecular weight of hemicelluloses is usually lower than that of cellulose, and they often have a branched structure (side chains may contain xylose, glucose, arabinose or glucuronic acid) that is relatively easily hydrolyzed by acids to their monomeric components. The xylose-based hemicelluloses in both hardwoods and softwoods are called xylans. 15–30% of the dry weight of hardwood consists of xylan and the corresponding value for softwood is 5–10%, which makes xylan one of the most common hemicelluloses. Lignins are polymers consisting of phenylpropane units, and in wood they exist as an irregular, crosslinked network. Wood cells also contain small amounts fats, resin acids, terpenoids and phenolic substances that are called extractives, as they are soluble in neutral organic solvents or water (Sjöström, 1993).

The cellulose surfaces employed in the cellulose-xylan interaction studies of this thesis were those of crosslinked cellulose beads obtained from Kanebo Co. (Japan). The beads consisted mainly of type II cellulose with a degree of crystallinity of 5–35% (Carambassis and Rutland, 1999). The surface roughness of wet cellulose beads was approximately 30 nm (image size 3 x 3 μm^2, 512 x 512 pixels). Langmuir-Blodgett (LB) films of cellulose (Österberg, 2000a) were used in studying the adsorption kinetics and characteristics of adsorbed xylan on cellulose with a quartz crystal microbalance with dissipation monitoring (QCM-D). The xylan was commercial birch xylan (4-O-methylglucuronoxylan from Roth, M_w 14400 g/mol, DP 100), which contains 7.8% α-D-methylglucuronic acid side groups (Figure 4). The experimental details of the cellulose-xylan interaction work are described in Publication I.

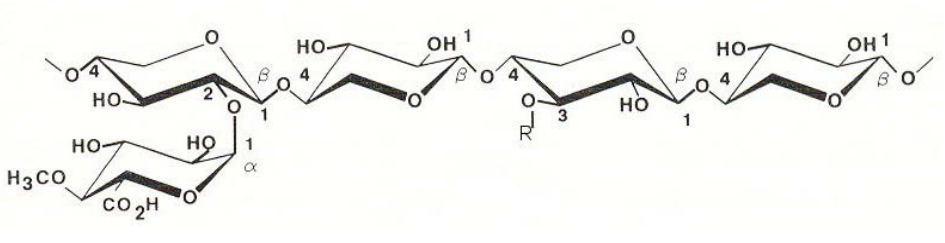

Figure 4. The structure of glucuronoxylan. R is an acetyl group (from Sjöström, 1993).

2.1.2 Gliadins

Gliadins are proteins that together with glutenin proteins form wheat gluten. The gluten proteins are also called prolamins, because proline and glutamine residues predominate in the amino acid composition. About 10% of the grain dry weight consists of proteins, and 80–85% of these are gluten proteins (Shewry *et al.*, 1994; Goesaert *et al*., 2005; Wieser, 2007). The viscous and elastic properties of the gluten proteins facilitate the production of bread, pasta and many other food products. The proteins also show emulsifying activity, foaming and film-forming ability (Örnebro *et al*., 2000). An autoimmune disorder of the small intestine called celiac disease is caused by gluten proteins. In affected individuals gliadins in wheat, hordeins in barley and secalins in rye cause changes in the lining of the intestine which interfere with the absorption of nutrients (Hourigan, 2006).

Gliadins are monomeric, alcohol-soluble proteins and contribute to the viscous nature of gluten (Tatham and Shewry, 1985; Kasarda, 1980). The α-, β-, and γ-gliadins are structurally related, sulphur-rich gliadins. The α-gliadins have a molecular weight around 31 kDa, and consist of two domains (Figure 5A). The N-terminal domain consists of glutamine- and proline-rich repeated sequences, and the secondary structure is rich in a β-reverse turn conformation. The C-terminal domain consists of non-repetitive sequences containing most of the charged amino acid residues and all six α-gliadin cysteinyl residues. The three intramolecular disulphide bonds (Müller and Wieser, 1995; Shewry and Tatham, 1997) result in a compact α-helical structure for the C-terminal domain (Tatham and Shewry, 1985). The α-gliadins adopt a globular conformation (Cole *et al.*, 1984; Shewry *et al*., 1997) and have a diameter of about 4 nm, if considered to be spherical (Richards, 1977). The ω-gliadins are sulphur-poor gliadins and consist of a single repetitive domain, with no cysteinyl residues (Tatham and Shewry, 1995) (Figure 5B). The molecular weight of the ω-gliadins is generally 44–74 kDa (Kasarda *et al.*, 1983). Their secondary structure consists of β-reverse turns (hairpin structure) and a poly-L-proline II-like structure (Tatham *et al.*, 1989), and is influenced by the degree of hydration (Wellner *et al*., 1996). The shape of ω-gliadins is rod-like in solution (Field *et al.*, 1986), and the hydrated solid structure has dimensions of ~ 16 x 3 nm (Shewry *et al.*, 1994). The isoelectric points of the gliadins are in the range of 6.4–8.5 (Søndergaard *et al*., 1994).

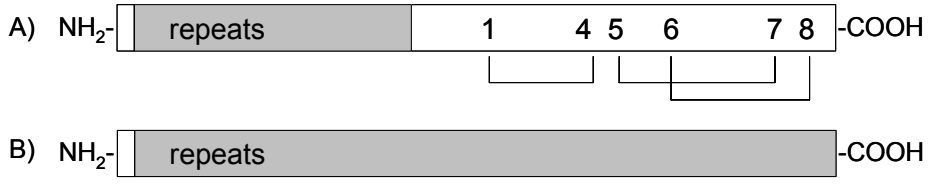

Figure 5. Structures of α-gliadin (A) and ω-gliadin (B). The cysteinyl residues forming disulphide bridges are shown with numbers 1–8 (according to Tatham and Shewry, 1995). The exact three-dimensional structure of gliadins is not known.

The purified gliadins used in the interaction work between gliadin monomers were donated by IACR, Long Ashton, UK. The immobilisation of gliadins to the surfaces and other experimental details are described in Publication II.

2.1.3 Hydrophobins

Hydrophobins are a group of highly surface active proteins that are found in all filamentous fungi (Wösten, 2001; Hektor and Scholtmeijer, 2005; Linder *et al*., 2005). The interfacial activity of these proteins affects the functions of fungi in its growth and development and in the interactions with the environment. Hydrophobins form coatings on spores, hyphae, and fruiting bodies and they participate in the adhesion of fungi onto different surfaces (Whiteford and Spanu, 2002). It has been shown that hydrophobins are involved for example in the infectivity of some pathogenic fungi, which cause Dutch elm disease, rice blast and chestnut blight (Tucker and Talbot, 2001). By lowering the surface tension of water they help fungi to penetrate through the air-water interface and enable the formation of fungal aerial structures (Talbot, 1997; Wösten *et al.*, 1999). Hektor and Scholtmeijer (2005) and Linder *et al*. (2005) listed potential applications based on the surface activity of hydrophobins. For example, hydrophobins can be used as adhesive domains for the immobilisation of proteins onto solid surfaces (Scholtmeijer *et al*., 2002; Linder *et al*., 2002), or as tags in fusion proteins for affinity purification (Collén *et al*., 2002; Linder *et al*., 2004). Highly efficient foam-inducing ability of hydrophobins has also been reported (Sarlin *et al*., 2005).

Hydrophobins are relatively small proteins (about 10 kD), and common to all hydrophobins is that they have eight Cys residues in their primary sequence that form a characteristic pattern (Figure 6A). Hydrophobins are grouped into two classes, I and II (Wessels, 1994), according to sequence alignments and functional characteristics. Hydrophobins of both classes self-assemble into aggregates, but the main difference is in their solubility: the aggregates of class I hydrophobins are higly insoluble (dissolve only in some strong acids, such as trifluoroacetic acid), whereas the aggregates of class II hydrophobins dissolve more readily. Currently about 70 different hydrophobin genes are available in databases (Askolin, 2006).

Probably the most studied example of the class I hydrophobins is the SC3 hydrophobin from *Schizophyllum commune* (Wösten *et al*., 1994; de Vocht *et al*. 2002; Wang *et al*., 2004). The hydrophobins studied in this thesis were Class II hydrophobins HFBI and HFBII from *Trichoderma reesei* (Nakari-Setälä 1995; Linder *et al*., 2001; Askolin, 2006). This filamentous fungi also has a third gene encoding hydrophobins; the produced protein is called HFBIII (Linder *et al*., 2005; Linder and Nakari-Setälä, unpublished). The molecular weights of the proteins are 7.5 kDa and 7.2 kDa for HFBI and HFBII, respectively, and they are very soluble in water. Their amino acid sequences are shown in Figure 6B. The recent high resolution X-ray structures of these hydrophobins were the first three-dimensional structures of hydrophobins at a molecular level (Publication IV, 2004; Hakanpää *et al*., 2006; Hakanpää, 2006). The structures of these hydrophobins show that they are rigid amphiphilic molecules (Figure 6C and 6D), in which the four disulphide bridges interlock to form a unique and compact structure so that a distinct hydrophobic patch is situated on one side of the molecule, thus giving a surfactant-like nature to the proteins. The secondary structure consists of two β-hairpins, the first located near the N-terminus and the second near the C-terminus, and one α-helix located in between the hairpin structures. The relatively flat hydrophobic patch is formed mainly by the residues close to the two β hairpins. The overall shape of these proteins is globular, having a diameter of about 2 nm. The calculated isoelectric point for HFBI is 5.7 and for HFBII 6.7.

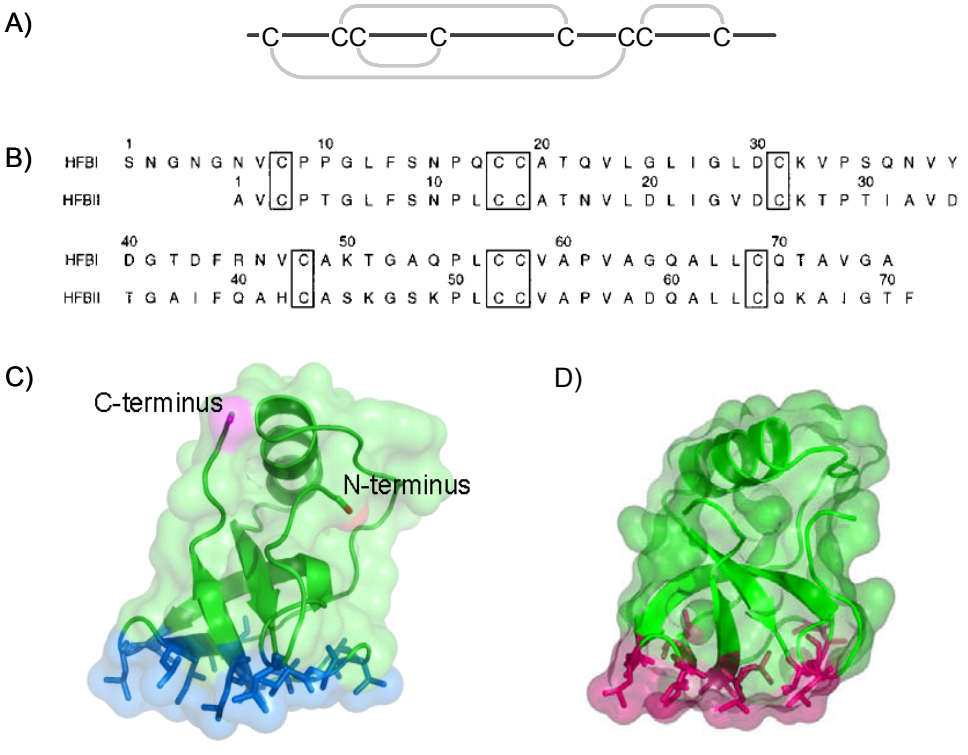

Figure 6. Formation of disulphide bridges in studied Class II hydrophobins. Amino acid sequences (B) and crystal structures of hydrophobins HFBI (C) and HFBII (D). For HFBI (C) the hydrophobic patch is shown in blue and the location of the C- and N-termini in pink. For HFBII (D) the hydrophobic patch is shown in red. Images A, C and D courtesy of Géza Szilvay, and B courtesy of Markus Linder.

The purified HFBI and HFBII hydrophobins were from VTT. The experiments related to the AFM work of hydrophobins are described in detail in the Publications III–V, but the surface film preparation procedures are described briefly below.

2.2 Film preparation

The experiments for studying self-assembly of hydrophobins at the air-water interface with AFM required transfer of the interfacial film onto a solid support (Publications III-IV). Three techniques were used in sample preparation: Langmuir-Blodgett (LB), Langmuir-Schaefer (LS) and the so-called 'drop surface film' -technique (explained below). The LB (Langmuir, 1920; Blodgett, 1935) and LS (Langmuir and Schaefer, 1938) techniques are widely used techniques in interfacial research. The reader is referred to the literature describing the techniques (Gaines, 1966; Roberts, 1990), and hence, only the basic principle for both techniques is shown here (Figure 7). The surface active molecules are spread on an interface (here the air-water interface) present on a LB trough, where the surface pressure is monitored by a Wilhelmy balance and the surface area of the interface, and hence the surface pressure is tunable by movable barriers. The film formation procedure is the same for both LB and LS films, but the transfer of the interfacial film onto a solid support is different. The LB sample (hydrophilic, mica) is lifted vertically while keeping the surface pressure value constant and the hydrophobic side (air-side) of the surface film can be studied. The LS sample (hydrophobic, highly oriented pyrolytic graphite, HOPG) is dipped horizontally to the interfacial film and the hydrophilic side (liquid-side) of the film can be explored. Deposition of both mono- and multilayers onto a solid support is possible.

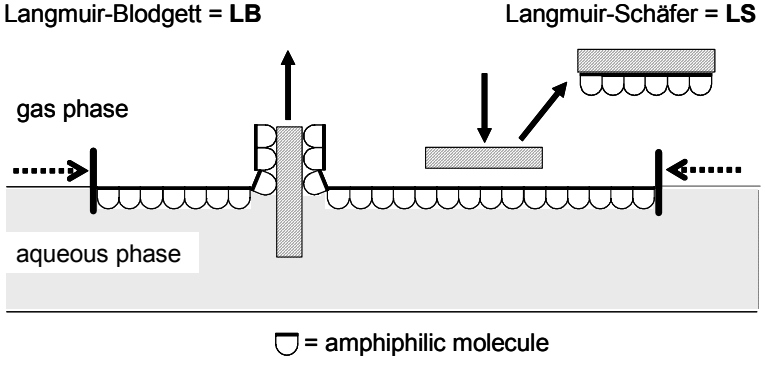

Figure 7. The basic principle of Langmuir-Blodgett and Langmuir-Schaefer techniques. The hydrophobin film was transferred to the hydrophilic sample support (mica) by LB technique, and to the hydrophobic sample support (graphite) by LS technique. Image courtesy of Géza Szilvay.

The experimental details for the LB film preparation used in this thesis are described in publication III and the corresponding details for the LS film in Publication V. However, some details for the LS film formation are highlighted here. A brief sonication of the hydrophobin solution prior to any liquid handling was important in order to avoid possible larger aggregates of hydrophobins in the solution. After spreading the hydrophobin sample at the air-buffer interface, the system was left to equilibriate usually for 30 minutes before starting the compression. During dipping, the HOPG sample was slightly tilted relative to the liquid interface. This was found to be important in order to avoid trapped air bubbles between the hyrophobin film and the solid support. It was also beneficial for further handling of the hydrophobin film, because the transferred film on HOPG needed to be rinsed gently to reduce the amount of possible free proteins in the remaining solution. In order to study the interfacial LS films of hydrophobins in as natural conditions as possible, the films were kept under buffer before AFM measurements and were also imaged in the same buffer.

Preparation of the hydrophobin films from drops of hydrophobin solution (‘drop surface film’ -technique) was performed for demonstration of spontaneous formation of the surface films of hydrophobins without specific laboratory equipment. Two different approaches were used (Figure 8). Drying down a drop of hydrophobin solution (Figure 8A) has similarities to the LB film preparation technique: the hydrophobic side of the film is studied and drying of the drop may act as an external force for compression, similar to barriers in LB. On the other hand, the structure of a film prepared by this approach, referred later as ‘a dried drop surface film’, more often suffered from the free bulk proteins dried under the film. The detailed film preparation procedure for dried drop surface films is described in Publication IV. In the other approach (Figure 8B), the interfacial film on a hydrophobin solution drop was transferred onto HOPG by horizontally dipping HOPG to the drop surface. The hydrophobin film was formed either directly from hydrophobin solution or by injecting an aliquot of more concentrated hydrophobin solution onto a drop of buffer. This hydrophobin film is referred to later as ‘a drop surface film’. This approach contains similarities to the LS film preparation technique in the sense that the hydrophilic side of the film is investigated. The organised hydrophobin films were examined in samples picked up from trapezoidal-like drops as well as in samples picked up from drops kept overnight in a humid environment, still having the same shape as in the beginning of the experiments (although partial drying could still have

taken place). The detailed preparation of the drop surface films is described in Publication V.

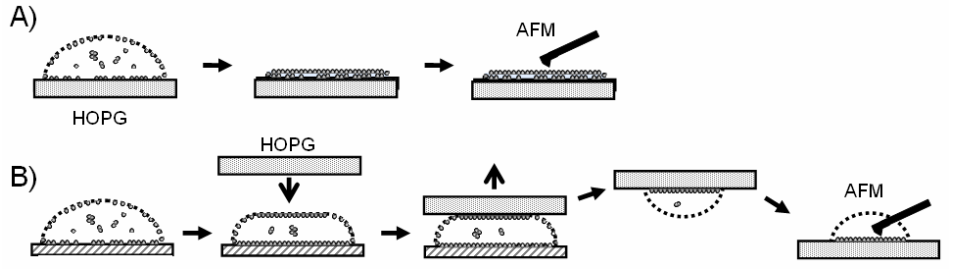

Figure 8. Drop surface film techniques for preparing AFM samples: Imaging the hydrophobic side (A) and hydrophilic side (B) of the interfacial film. Image courtesy of Géza Szilvay.

2.3 Atomic force microscopy

Atomic force microscopy (AFM) (Binnig *et al*., 1986) is one of the scanning probe microscopy techniques (Howland and Benatar, 1993–1996), and has been shown to be a powerful and versatile technique in surface research especially in studying samples of biological origin (see section 1.1). AFM can be operated in ambient air, in different gases or in vacuum, but a unique feature is that AFM allows measurements in liquid environment (Weisenhorn *et al*., 1989; Drake *et al*., 1989). This is particularly important for biological samples, that can hence be observed in near-physiological environments. In sample preparation no staining or surface coating is required, in contrast to many other microscopic techniques, but the studied samples or molecules must be attached firmly enough to the sample support for carrying out successful measurements. There is a wide variety of different methods available for AFM sample preparation (Colton *et al*., 1998; for protein immobilisation, Haugland, 1999). AFM was initially developed for imaging surface topography, but it can also be exploited to map chemical and mechanical surface properties, to track dynamic biochemical processes on surfaces and to directly measure intra- and intermolecular interactions (see section 1.1).

In this thesis a NanoScopeIII Multimode AFM (Digital Instruments/Veeco, CA) was used in imaging surfaces as well as in measuring surface forces in biopolymer systems, and the basic principles of these are described here briefly. More thorough descriptions of AFM and different modes and possibilities can be found in the references Howland and Benatar (1993–1996) and Colton *et al.* (1998), in the review articles referred to in section 1.1, and on the manufacturer's website (www.veeco.com).

2.3.1 Imaging

The basic principle of AFM is shown in Figure 9. The heart of AFM is a tiny tip (or probe; radius of curvature is usually ~10 nm) mounted on the free end of a reflective cantilever. When the tip touches the sample surface, the forces acting between the tip and the sample surface (see section 1.2) cause bending of the cantilever and the deflection is monitored by the laser light reflecting from the cantilever to a photosensitive detector (photodiode). The tip raster-scans the sample surface line by a line in the x and y directions. A feedback loop between the photodetector and the z-scanner provides the height information during xy-scanning: the z-scanner adjusts the sample height position in order to keep the cantilever deflection constant. The accuracy of the piezo movement is in the sub-nanometer range, and sub-Ångström movements of the cantilever can be detected with the optical setup (Colton *et al*., 1998), corresponding to forces of tens of pN with cantilevers usually used with soft samples (typically V-shaped with a spring constant of less than 0.1 N/m).

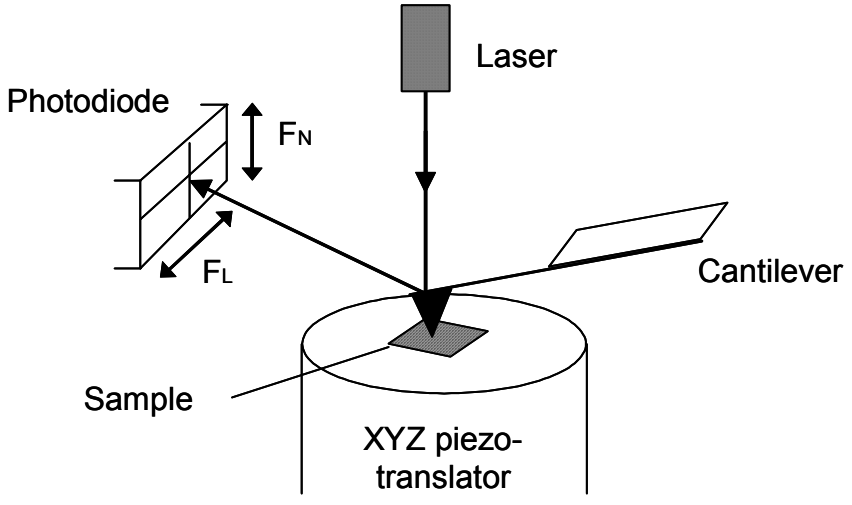

Figure 9. The basic principle of AFM.

Biological samples are very soft and hence easily deformed during contact mode imaging. In order to avoid or at least to minimise the risk of deformation, tapping mode (Zhong *et al*., 1993; or intermittent contact mode) was used in this thesis for imaging sample surfaces in air and in liquid. In tapping mode the cantilever is oscillating near its resonant frequency in the proximity of the surface, touching the sample surface only briefly during each oscillation cycle. This makes the tapping mode a more gentle mode for imaging compared to the contact mode because lateral forces are effectively minimized. During scanning, damping of the predetermined amplitude (free amplitude, A_0) of the cantilever is controlled by changing the setpoint amplitude (A_{sp}), the amplitude of the cantilever when in intermittent contact with the surface. The damping ratio (A_{sp}/A_0) describes the force applied to the sample. The damping allowed in the setpoint amplitude is kept constant during scanning. This is constantly monitored by the feedback system, and changes in the signal observed at the photodiode are corrected back to the predetermined setpoint value by moving the sample by the scanner in z the direction with respect to the cantilever.

The function of AFM is based on detection of surface forces and interactions between the tip and the sample. The forces acting in biopolymer systems in liquid environment are described in section 1.2. When imaging in air capillary forces (or meniscus forces) also contribute to the interaction (Israelachvili, 1992)

and can make imaging of soft surfaces difficult, especially in contact mode. Capillary forces arise from the condensation of water vapour from the atmosphere at surfaces. In tapping mode these forces are lower. The imaging forces between the tip and the sample surface can be further reduced by imaging in liquid environment. Tip-sample forces also have a central role when recording the so-called phase contrast image in tapping mode. The phase contrast image shows the phase difference (phase-shift) between the oscillation of the piezo driving the cantilever and the oscillation of the cantilever detected by the photodiode. It is widely accepted that the phase-shift is related to the energy dissipation during tip-sample interaction (Cleveland *et al*., 1998), and it is proposed to be sensitive to surface properties such as stiffness and viscoelasticity (hard tapping) and chemical composition, i.e. hydrophilicity and hydrophobicity (light tapping), and height differences at edges (Bar *et al*., 1997; Whangbo *et al*., 1998). Chen *et al.* (2002) explained that phase contrast relates to large phase differences between regions of sample where either attraction or repulsion dominates the tip-sample interaction when imaging at the attraction-repulsion transition point.

When analysing and interpreting AFM images it is good to bear in mind the basic types of artefact that are (or can be) involved, especially with soft sample surfaces. Perhaps the most important artefact originates from the tip geometry causing exaggeration of the lateral dimensions of the imaged object (tip convolution), and is most pronounced when the radius of the curvature of the tip and the size of the features to be imaged are comparable in size. The tip shape issues also include the effect caused by tip contamination (double or multiple-tip). The effects due to scanner hysteresis, creep and drift can often be minimised by optimising the scanning parameters. However, this may not be the case with soft sample surfaces because optimisation of the imaging conditions involves minimising the risk of surface deformation. Furthermore, image processing can distort the image data and hence the processing procedures must be chosen carefully (Howland and Benatar, 1993–1996; Colton *et al*., 1998; SPIP, 1998–2006). The processing of the AFM images presented in this thesis included only flattening, which removed the possible tilt in the image data. In Publications III–V the Fourier transfom image processing routine was used only for analysing the surface periodicities, and an averaging routine was used for analysing images further and identifying some periodical details in the images.

2.3.2 Force measurements

A unique property of AFM is the possibility for force measurements. These convey valuable information on the strength and nature of intra- and intermolecular interactions (Cappella and Dietler, 1999; Butt *et al*., 2005) and even allow individual molecular pairs or single molecules to be investigated (force spectroscopy, Hugel and Seitz, 2001). In order to measure biopolymer interactions, the molecules under study must be attached to the tip and/or sample surface by protocols referred to above (Figure 10A). If a defined geometry of the surfaces is needed, the so-called colloidal probe technique by Ducker *et al*. (1991) can be used, where for example spheres or beads with desired diameter are attached to the cantilever (Figure 10B).

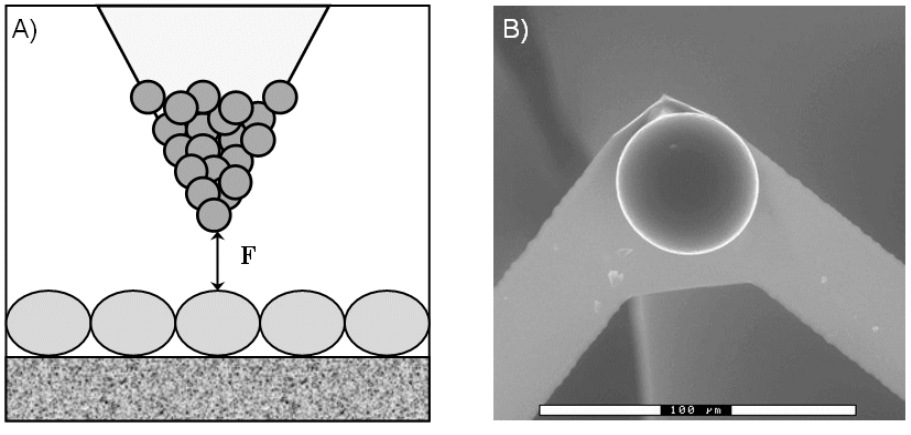

Figure 10. Modification of AFM tips by tethering molecules to the tip surface (A) or by attaching colloidal particles (B) (here a cellulose bead).

The basic procedure of force measurements is shown in Figure 11. In a force measurement the sample is moved towards the tip at a constant velocity until they are in contact. The sample then continues to move upwards, the sample and the cantilever moving together in contact causing the cantilever to bend upwards until a predetermined point of maximum bending force is reached (point C in Figure 11). After this the sample is withdrawn until the cantilever returns to its position of zero deflection. During further withdrawal of the sample the tip remains in contact with the sample, bending downwards until at a certain point it pulls off. The observed tip-sample force just before the pull-off point

corresponds to the maximum adhesive force between the studied surfaces, beyond which the spring force of the cantilever exceeds the tip-sample adhesion causing the release of the cantilever. The approach curve can show the nature of the interaction, i.e. whether repulsion or attraction is involved. If the system is studied in different environments, for example in different electrolyte concentrations, theoretical analysis of the data may yield information about whether the studied system is electrostatically or sterically stabilized (Butt *et al*., 2005). In addition to the adhesion data, the retract curve can also show stretching and unfolding of biopolymers (Figure 11, dashed line), even of single molecules (Butt *et al*., 2005).

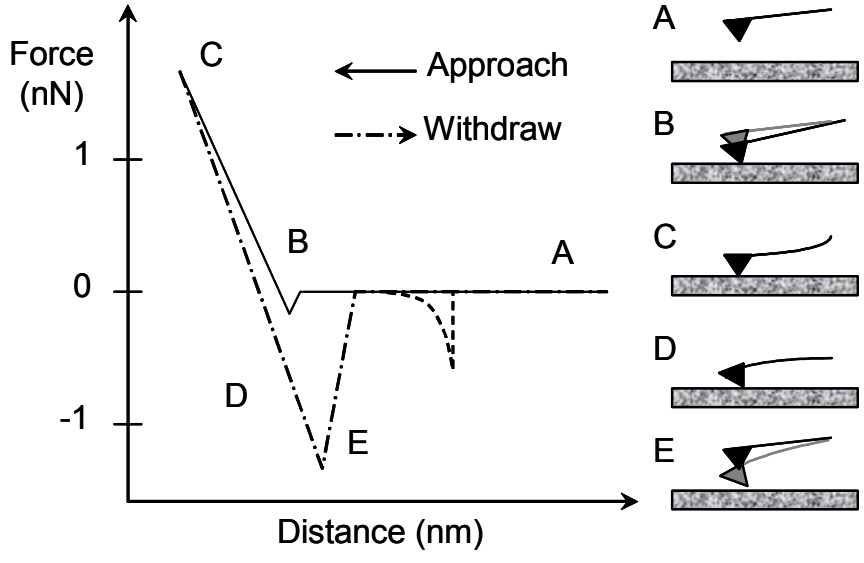

Figure 11. Basic principle of force measurements. A = no interaction, surface approaches the cantilever; B = jump into contact; C = tip and surface are in contact – the constant compliance region – with cantilever bending upwards, and both surfaces moving together; D = tip is withdrawn, a non-specific adhesive force keeps the surfaces together and the cantilever bends downwards; E = release of the cantilever back to its rest position. A post-adhesional stretching event is shown in the withdraw curve (dashed line).

The raw data obtained, i.e. the force curve, is a plot of cantilever deflection (in volts) as a function of the sample position. For presenting the interaction force as a function of tip-sample separation, two parameters need to be known: the zero

distance and the spring constant of the cantilever. The conversion of the cantilever deflection from volts to nanometers can be performed by determining the slope of the constant compliance region (regime C in Figure 11), where the surfaces are in hard-wall contact, i.e. the change in sample position equals the change in cantilever deflection (zero distance). The cantilever acts like a spring so the actual force detected can be calculated according to Hooke's law:

$$F = kx \tag{5}$$

where k is the spring constant (nN/nm) and x the deflection of the cantilever in nanometers. The distance between the tip and the sample cannot be determined directly, but is inferred from the force curve by adding the cantilever deflection to the sample position. For obtaining more quantitative data, the cantilevers must be calibrated. There are several different methods available for determining the spring constant, of which the most widely used methods determine the change in the resonance frequency due to added mass (Cleveland *et al*., 1993), record the thermal noise (Hutter and Bechhoefer, 1993), use an accurately calibrated reference cantilever (Torii *et al*., 1996), or measure the resonance frequency and the quality factor (Sader *et al*., 1999). In this thesis the reference cantilever method and the thermal method were used for their simplicity, applicability to V-shaped cantilevers and non-destructive nature.

2.4 Other methods

Quartz crystal microbalance with dissipation monitoring (QCM-D) (Rodahl *et al*., 1995; Höök, 1997) measures the mass adsorbed on a quartz crystal and provides information about rigidity or softness of the adsorbed layer. QCM-D was used for studying adsorption of xylan on cellulose (Publication I), and adsorption of hydrophobins onto hydrophobic polystyrene surface and binding of avidin to biotinylated hydrophobins attached to polystyrene (Publication V). The QCM-D data comprised valuable information for designing the AFM experiments and interpreting the results by providing insight to the time scale of adsorption. By giving the mass of adsorbed species the QCM-D data verified the exsistence of adsorption, and moreover, proved that only a monolayer of hydrophobins was

adsorbed on polystyrene making the preceeding QCM-D experiments with avidin adsorption comparable with the AFM experiments (Publication V).

Small angle X-ray scattering (SAXS) (Glatter and Kratky, 1982) provides information for example about the size and shape of macromolecules, and was used for studying the solution structure of hydrophobins (Publication III). The structural information from SAXS was combined with the AFM results of hydrophobin films at the air-water interface, because the dimensions obtained by both techniques were very similar. The work presented in publication III gave the most detailed structural information of hydrophobin surface films at the time of publication; no crystallographic data on the structure of any hydrophobin was available at that time.

3. Results and Discussion

3.1 Interactions between cellulose and xylan

Cellulose and hemicellulose are two of the main constituents of wood cells. The importance of understanding the role and behaviour of hemicelluloses in papermaking and particularly the interaction between cellulose and hemicelluloses is evident, since hemicelluloses, for example xylan, affect the properties of the final paper. Early studies of the behaviour of xylan during pulping showed that dissolved xylan is adsorbed onto the cellulose fibres if the pH is lowered at some stage (Yllner and Enström, 1956). In later studies of the readsorption of xylan on cellulose Mora *et al*. (1986) concluded that xylan readsorbs preferentially to xylan rather than to cellulose, and Henriksson and Gatenholm (2001) suggested that besides crystallisation of xylan onto cellulose other types of association also occur. Marchessault *et al*. (1967) showed that the orientation of xylan molecules is parallel to the fibre axis and may hence be important for the mechanical properties of individual pulp fibres. The alignment of xylan molecules on cellulose was later theoretically calculated by Kroon-Batenburg *et al*. (2002). There are also other studies proposing that xylan on the fibre surfaces improves paper strength (Buchert *et al*., 1995; Schönberg *et al*., 2001). Based on FT-IR spectroscopy experiments Åkerholm and Salmén (2001) concluded that xylan is not as closely associated with cellulose as for example mannan (another type of hemicellulose), which had also previously been suggested by Salmén and Olsson (1998). Teleman *et al*. (2001) concluded from CP/MAS ^{13}C NMR results that the supermolecular structure of xylan is highly dependent on the immediate environment.

A wood fibre is a very complex material. In order to study interactions between certain wood components, the use of representative model surfaces is required in the experiments (Österberg, 2000a; Kontturi *et al*., 2006). The first model surface for cellulose (intended for force measurements) was prepared by spin-coating cellulose on mica (Neuman *et al*., 1993). The results of this pioneering work using surface force apparatus (SFA) showed long-ranged repulsion due to swelling of the cellulose surfaces. The roughness and instability issues of spin-coated cellulose were later overcome by SFA studies using LB films of cellulose (Holmberg *et al*., 1997; Österberg and Claesson, 2000). However, the spin-

coating or LB methods cannot be utilised for modifying the AFM tip surface, and in surface force measurements using AFM the colloidal probe technique (Ducker *et al.*, 1991) has been used: between two cellulose beads (Rutland *et al*., 1997; Carambassis and Rutland, 1999; Salmi *et al*., 2006; Salmi *et al*., 2007) or between cellulose beads and spin-coated cellulose surfaces (Zauscher and Klingenberg, 2000; Leporatti *et al*., 2005; Notley *et al*., 2006). In the earlier force measurements between xylan surfaces the xylan model surfaces had been prepared by adsorbing dissolved xylan on mica either overnight (Neuman *et al*., 1993) or during measurements in the measurement chamber directly (Österberg *et al*., 2001). AFM force measurements have also been performed on pulp fibres directly (Furuta and Gray, 1998), but the aim was to study the sensitivity of the fibre surface to the mechanical treatment rather than to measure interactions between fibre components. The AFM colloidal probe technique was used in measuring surface forces between two cellulose beads in the work described in Publication I.

The cellulose-xylan work aimed at eliciting information about the cellulose-xylan association by AFM force measurements. In order to support the interpretation of the actual force measurements, the behaviour of the cellulose beads in aqueous solutions was studied (Publication I). Swelling of the cellulose beads was rather slow, and therefore the beads were incubated in water overnight followed by 3 h incubation in the reference solution (1 mM NaCl, pH 10) before measurements. This was important for observing interaction between fully swollen and stabilised cellulose surfaces rather than measuring interaction during swelling, which may lead to misinterpretation of the results. The radius of the swollen beads was used in the normalisation of forces in order to obtain more realistic values (Derjaguin approximation; Derjaguin, 1934). Swelling makes the surface of the cellulose beads very soft, which causes modifications of the surfaces as a consequence of pushing the surfaces together. This affects the constant compliance region of the force curve: due to indentation of the surfaces the constant compliance may not be fully reached. Hence, in order to obtain more realistic force values, the sensitivity values obtained from the experiments with high loading force were used to analyse the force curves with low loading force for each measurement series separately. The effects of the approach speed, relaxation of the cellulose chains, and the hydrodynamic forces in the studies using cellulose beads were previously described by Carambassis and Rutland (1999) and Zauscher and Klingenberg, (2000). These were taken into account in the force measurements.

3.1.1 Effect of xylan concentration

The effect of xylan concentration on the interaction between cellulose surfaces was investigated in the presence of 1 mM NaCl at pH 10. The results reported in Publication I show that, as expected, adsorption of xylan on cellulose increases with increasing xylan concentration (10, 50 and 100 mg/ml in 1 mM NaCl, pH 10) and adhesion between cellulose surfaces decreases. The results are shown in Figure 12. The effects are observed in the force curves as a stronger and longer-ranged repulsion on approach (Figure 12A) and as a weakening adhesion on separation (changing from 0.1–0.4 mN/m attraction to repulsion; Figure 12B), when the concentration of xylan is increased. Fitting of forces to the DLVO theory was attempted, but only the forces from the measurements with higher concentrations of xylan were large enough for reliable estimations of the surface potential, and only the long-ranged forces in experiments with 50 mg/ml of xylan fitted rather well to the theory (with boundary conditions of constant potential). The fitting results indicate that the long-range forces are mainly electrostatic, whereas steric repulsion becomes dominating at shorter distances (below 6 nm), most probably due to interpenetration of the xylan layers. At the highest xylan concentration, steric forces also appeared to dominate at long distances (the fit to the DLVO theory was poor). After measurements in high xylan concentrations the cellulose surfaces with adsorbed xylan were exposed to reference solution. There were no indications of desorption of xylan, because the repulsion on approach did not change. The QCM-D experiments were performed after AFM experiments. The adsorption of xylan onto cellulose was verified by the QCM-D results, which also showed that the adsorption process is rather slow (several hours) and that the adsorbed xylan layer is rich in water and loosely bound to cellulose.

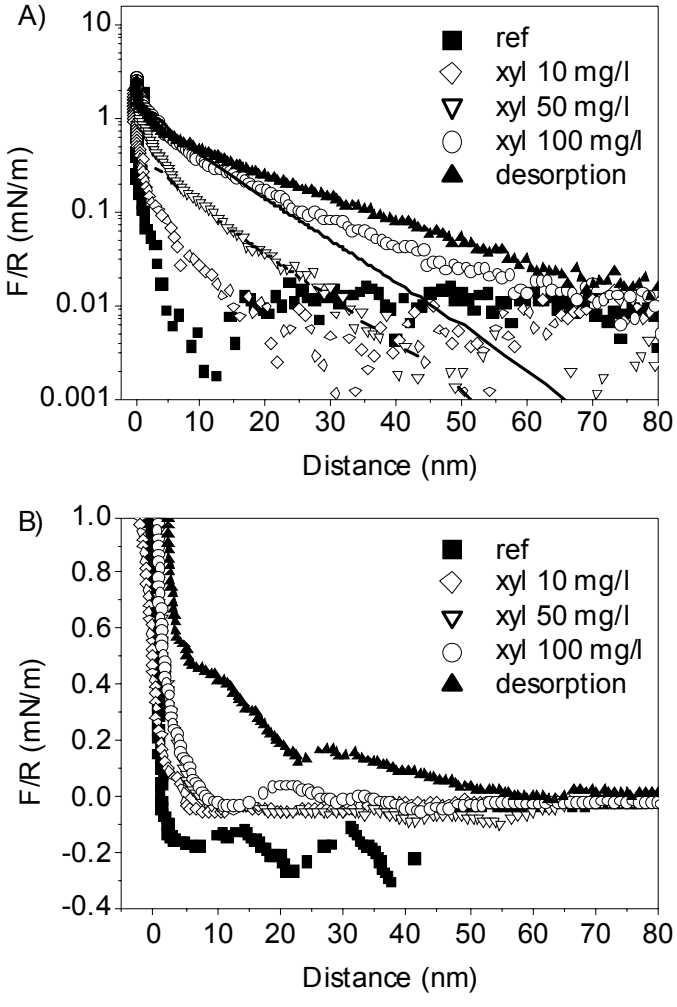

Figure 12. The forces measured on approach (A) and separation (B) between two cellulose beads across xylan solutions at different xylan concentrations (0–100 mg/ml). The forces after changing the solution in the chamber back to the reference solution are also shown (▲). The lines are the best fit to the DLVO theory assuming constant charge. (Modified from Publication I.)

The results show that in weakly alkaline solutions at low ionic strength, xylan adsorbs onto cellulose despite the negative charges on both interacting partners (Publication I). Addition of charges on weakly-charged cellulose surfaces by adsorption of xylan increases electrostatic repulsion. On the other hand, charges also cause swelling of the adsorbed layer and hence, steric repulsion is also

increased. The existence of both types of repulsion is supported by fitting forces to the DLVO theory for the intermediate xylan concentration (50 mg/ml). The domination of steric forces between xylan-coated surfaces has also been reported previously (Österberg *et al*., 2001), as well as the domination of electrostatic repulsion at large distances between xylan-coated mica surfaces (Claesson *et al*., 1995). The results also show that the adhesion between cellulose surfaces is very low whether xylan is adsorbed on cellulose or not. According to the QCM-D results, the cellulose-xylan interaction is weak and the adsorbed xylan layer is soft and most probably contains water. On the other hand, the force measurements show that the cellulose-xylan interaction is strong enough to prevent desorption upon dilution. These findings suggest that the driving force of the cellulose-xylan association is a combination of the inherent entropy increase associated with exchange of polymer-solvent contacts to polymer-polymer contacts and weak van der Waals' attraction, rather than formation of hydrogen bonds as has repeatedly been cited as the driving force of association (Mora *et al*., 1986). Hydrogen bonding may be of great importance in dry systems such as dried fibre networks in paper, and this possibility is not excluded by our results. Hence, the relevance of our results to papermaking is that the role of xylan in increasing the paper strength (interfibre bonding) is probably to increase the contact area between fibres. This would be associated with processes taking place during drying.

3.1.2 Effect of electrolyte concentration

The results of measuring forces between cellulose surfaces with varying xylan concentrations showed that more xylan adsorbed on cellulose with increasing xylan concentration. The natural step forward was to study the effect of electrolyte concentration (NaCl) on the interaction between xylan-coated cellulose surfaces. According to Österberg *et al*. (2001), xylan with a charge density of 9% adsorbs onto negatively charged mica in an extended conformation, giving rise to long-range repulsion, and the repulsion between xylan-coated surfaces decreases with increasing electrolyte concentration, as expected. Similar results were also reported by Claesson *et al*. (1995) for xylan with higher charge density (13.7%), and we also expected to observe this in our experiments (charge density of xylan 7.8%). Details of the experiments are given in Appendix A. Slow adsorption of xylan on cellulose observed in the cellulose-

xylan interaction work with varying xylan concentrations was taken into account in these experiments.

The forces between xylan-coated cellulose surfaces with varying electrolyte concentrations are shown in Figure 13. The cellulose surfaces were first immersed in the reference solution (1 mM NaCl, pH 10) for two hours. Introducing 100 mg/ml xylan (1 mM NaCl, pH 10) to the measurement chamber caused an increase in repulsion on approach and an increase in adhesion on separation (data not shown). This was consistent with results shown in Publication I. Then the electrolyte concentration (with the same xylan concentration and pH) was increased to 10 and 100 mM.

In our experiments the electrolyte did not appear to have a notable effect on the interaction forces on approach. No clear trend in the interaction with increasing electrolyte concentration was observed (Figure 13A). This indicates that the interaction was dominated by steric contributions to the interaction rather than by electrostatic forces, although the presence of electrostatic interaction cannot be excluded. This is contradictory to the results reported previously by Claesson *et al*. (1995) and Österberg *et al*. (2001), which showed that repulsion between xylan-coated surfaces decreased with increasing electrolyte concentration. Moreover, in their experiments xylan was adsorbed on mica, which is much smoother than the surfaces of the cellulose beads used in these experiments (RMS roughness was approximately 30 nm). This could partially explain the observed dominance of steric repulsion. Adsorption of xylan on cellulose most likely differs from that on mica, and material differences between cellulose and mica could also be one reason for the reported differences in the behaviour of xylan. With the model surfaces used in our experiments we aimed at studying conditions that were one step closer to the situation during pulping, where xylan is involved in the cellulose-cellulose interaction by readsorbing onto cellulose fibres (Yllner and Enström, 1956), and therefore interaction between xylan-coated cellulose surfaces was measured. Claesson *et al*. (1995) reported that after prolonged times at elevated pH the adsorbed xylan layers contained long dangling chains. Their explanation of this was a heterogeneous xylan sample and, possibly, multilayer adsorption. Usually increase in electrolyte concentration also decreases the steric interaction by screening out the charge of the polymer molecules protruding from the surface, resulting in a more compact conformation (Österberg *et al*., 2001). Increase in electrolyte concentration also

makes xylan less soluble and hence promotes the adsorption of xylan on cellulose. In our experiments the expected behaviour for xylan in electrolyte solutions was probably buried under a more dominating factor: during a long exposure time more xylan was adsorbing on cellulose either due to very slow adsorption kinetics or enhanced adsorption because of less soluble xylan molecules at higher electrolyte concentrations.

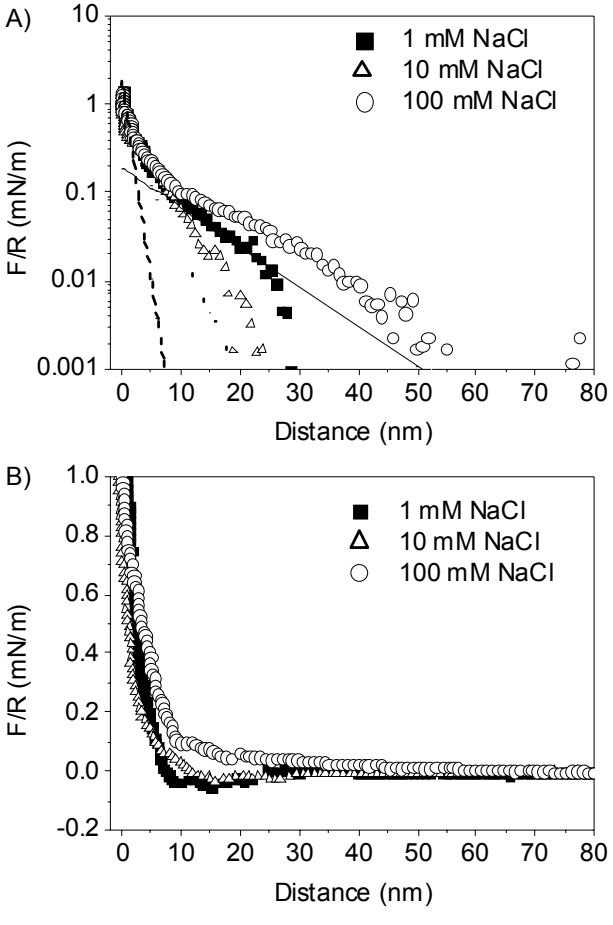

Figure 13. The forces measured on approach (A) and separation (B) between two cellulose beads across 100 mg/ml xylan concentration at different electrolyte concentrations (1–100 mM NaCl). The lines illustrate the expected decay length for a pure double-layer force across electrolyte solutions (NaCl 1 mM, solid; 10 mM dotted; 100 mM dashed; calculated using equation 4).

With increasing electrolyte concentration, the magnitude of the adhesion in the separation curves was low in all cases, and the range of adhesion was similar to that of the results with varying xylan concentrations described in Publication I (Figure 13B). Although adhesion was low and varied between different experiments, some observations were made. When performing measurements at the highest electrolyte concentration with 100 mg/ml xylan, repulsion was seen in the separation curves more often than with the lowest electrolyte concentration. Adhesion may originate from interpenetration of xylan chains from one surface to the other. When the electrolyte concentration is increased, the charges on negatively charged cellulose and xylan are screened out and result in decrease in repulsion between molecules. This in turn causes less protruding chains on the surfaces and less opportunities for interpenetration. In addition to this, when xylan-coated surfaces are pushed together, more segments of xylan are forced to adsorb to the surface (Klein, 1988, resulting in less dangling chains of xylan molecules to interpenetrate between surfaces upon contact. This further diminishes the entanglement of xylan molecules at higher electrolyte concentrations. On the other hand, most probably more xylan adsorbs from solution on the interacting surfaces during the measurements, as discussed above. It would be expected that more adsorbed xylan would result in more dangling chains on the surfaces. Due to the reasons described above the adsorbed xylan at higher concentrations most probably has a rather compact conformation, possessing less dangling chains to interpenetrate and cause adhesion, but still being a source for the steric interaction. Hence, the fact that more xylan appeared to adsorb during measurements hampered closer investigation of the effect of electrolyte concentration.

3.2 Interactions between gliadins

Wheat gluten proteins, glutenins and gliadins (Shewry *et al.*, 1994; Wieser, 2007), are crucial for making bread, pasta and many other food products. Glutenin polymers form a continuous network and are responsible for the strength and elasticity of the dough. These biomechanical properties have been proposed to originate from the β-turn conformation, related to the repetitive amino acid sequences rich in proline, glycine and glutamine (Tatham and Shewry, 2000). The functional role of gliadins is in determining the dough viscosity and they are believed to act as plasticizers of the glutenin polymeric

system. An appropriate balance between dough viscosity and elasticity/strength is required for good flour quality and baking performance (Tatham *et al*., 1990; Goesaert *et al*., 2005). The emulsifying activity, foaming and film-forming ability of gluten proteins have also been reported. For example, gliadins were found to be highly surface active compared to glutenin and were suggested to be of importance in the gas holding capacity of doughs (Örnebro *et al*., 2000; Li *et al*., 2004). In particular α-gliadins have been shown to have a greater affinity to hydrophobic surfaces than ω-gliadins (Örnebro *et al*., 1999), which may partially be due to the level of hydrophobicity of α-gliadins compared to that of ω-gliadins (Fido *et al*., 1997). The differences in the surface hydrophobicity of the α- and ω-gliadins also affect the interactions with other gliadin and glutenin molecules, where other non-covalent interactions are also involved, and lead to macroscopic effects on baking quality (Örnebro *et al*., 2000).

The work presented in Publication II aimed at understanding the nature and strength of the interaction between monomeric gliadin molecules and the possible roles for gliadins in forming the network in dough. The proteins were attached to both the tip and the sample surfaces, and the interaction forces between gliadins (α-α, ω-ω, and α-ω) were measured by AFM. Several kinds of control experiments were carried out for estimating the effect related to the interaction between non-protein-coated surfaces and between protein-glutaraldehyde (α-glut and ω-glut) surfaces in the force curves.

3.2.1 Behaviour in the native environment

The interaction forces between gliadin proteins were measured by AFM in 0.01M acetic acid. The representative force curves for both α-α and ω-ω interaction are shown in Figure 14. The results from the force measurements indicated that the nature of the behaviour at pH 3.5 was similar for both gliadins. The strength and range of the near-surface adhesion was ~0.1–1.5 nN and ~20–50 nm respectively for α-α interaction, and corresponding values for ω-ω interaction were ~0.1–4 nN and ~15–60 nm. The greater variation in the values for ω-ω interaction may be related to the shape differences of the gliadins: ω-gliadins are rod-like in shape compared to globular α-gliadin and may have a greater effect on the penetration of the protein surfaces due to orientation of the molecules on the surfaces. Both gliadins showed a post-adhesion stretching behaviour that was typically weaker

than adhesion: the mean force at maximum extension between α-gliadin surfaces was 0.15 nN and between ω-gliadin surfaces 0.18 nN. The fact that stretching events originated from the proteins was confirmed by the control experiments. The stretching events show partial (or full) unfolding of proteins and were expected to be seen in these experiments. Sometimes stretching had a saw-tooth pattern, which is an indication of more than one unfolding event occurring sequentially. Stretching at greater separations than 100 nm (the length of a fully extended gliadin molecule, see Publication II) also occurred and could be explained by a mutual unfolding of gliadins from the opposing surfaces. On the other hand, the frequency of stretching events in all curves was 5–45% for α-gliadin and 5–60% for ω-gliadin, which indicated low protein coverage on the surfaces and that even interaction between single molecules were observed.

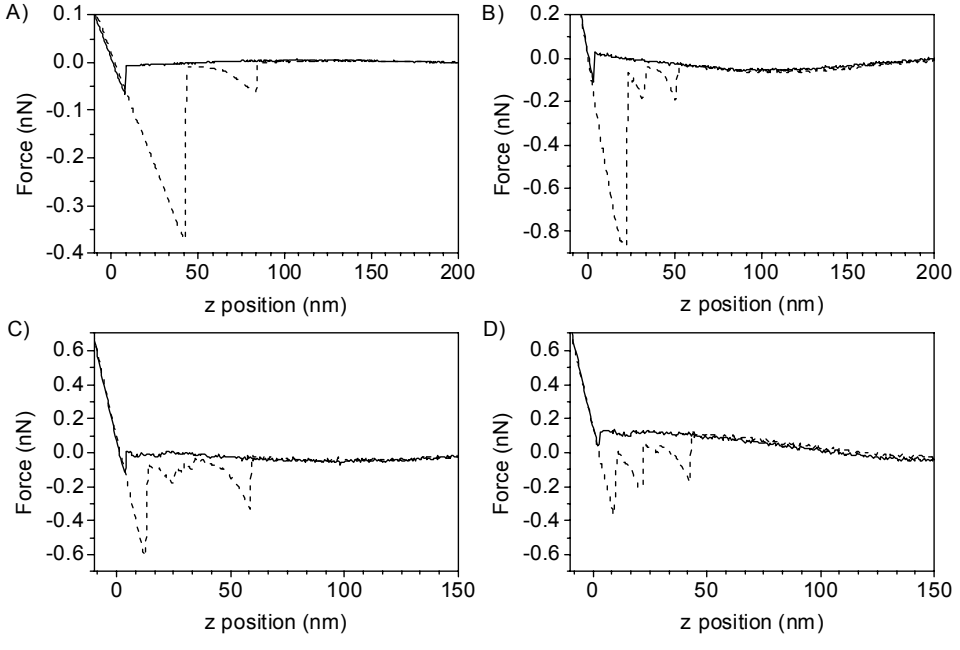

Figure 14. Typical raw data force-sample vertical position curves for α-α interaction (A and B) and ω-ω interaction (C and D) in 0.01 M acetic acid (solid curve for approach and dashed for retract). (Modified from Publication II)

The nature of binding between gliadin proteins is not known. Hydrogen bonding or covalent bonding (formation of disulphide bridges between α-gliadins) are the most likely explanations for the interaction. The lower force magnitudes

indicated the significance of hydrogen bonding in the gliadin-gliadin interaction. However, in our experiments covalent bonds may have formed between a tip- or surface-tethered gliadin molecule and a free glutaraldehyde on the opposing surface. No repulsion was observed between approaching surfaces for either gliadin. It is possible that electrostatic interactions between gliadin proteins may play a minimal role under the experimental conditions of Publication II, although both gliadins have a basic nature at low pH values (Søndergaard *et al*., 1994). This is contradictory to the SFA force measurements by Wannerberger *et al*. (1997), whose results showed domination of electrostatic repulsion between α-gliadin layers. A possible explanation for the contradiction lies in the sample preparation proceedure. Their measurements were performed on surfaces fully covered with α-gliadin, prepared on bare mica either by LB-technique or by adsorbing gliadins from solution. In our experiments the coverage of covalently tethered proteins was rather low and the measured interactions may have involved even single molecules. The relative hydrophobicity of the proteins may be important in explaining how the gliadins behave, because hydrophobicity is involved in determining the loaf volume (van Lonkhuijsen *et al*., 1992; Weegels *et al*., 1994). The α-gliadin is more hydrophobic than ω-gliadin (Fido *et al*., 1997), and it would therefore be expected that interaction between α-gliadins is greater than ω-ω interaction in aqueous solution. In our experiments the strength of interaction for both gliadins was rather similar, and it is suggested that the size and shape of the interacting molecules, and therefore the contact areas between molecules are also important.

3.2.2 Behaviour in a denaturing environment

After studying the behaviour of α- and ω-gliadins in their native environment, the surfaces were immersed in a mixed solution of 0.01M acetic acid and 2M urea and the interaction forces of gliadins were measured in a denaturing environment. The representative force curves for both α-α and ω-ω interaction are shown in Figure 15. The results showed that for α-gliadins (Figure 15A and 15B) the close-to-surface adhesion was on average largely unaffected, but the post-adhesion stretching events occurred at much greater separations, even up to 400 nm. Denaturation by urea involves reducing the level of hydrogen bonding in proteins, although the precise mechanism is not fully understood (Wallqvist *et al*., 1998; Caflisch and Karplus, 1999). The effect of urea on the α-α interaction

is shown in Figure 16, where the coordinates of maximum force and maximum extension in urea are compared with the corresponding values in acetic acid. The compact α-gliadin structure was clearly loosened by the denaturation, but they were still able to form bonds with other molecules and surfaces. The very long-ranged stretching events indicated the presence of proteins bound non-covalently on the surfaces. These were also unfolded in urea and were able to attach to the neighbouring proteins and to open glutaraldehyde ends, causing the long stretching. In the same conditions in which α-gliadins were denatured the interaction between ω-gliadin surfaces did not change (Figure 15C and 15D). Earlier studies on hairpin structures rich in β-turns, as present in the ω-gliadin, have shown that such structures are highly resistant to denaturation (Griffiths-Jones *et al*., 1999). Repeating the measurements in 8M aqueous urea (pH ~7) showed a clear effect on the ω-ω interaction (Figure 15E and 15F). The repulsion in the approach curve ranged up to about 20 nm from the surface, which was greater than the effect seen in the control measurements between glutaraldehyde surfaces in the same conditions. This indicated steric repulsion between surfaces with denatured molecules. Stretching of ω-gliadins did occur in 8M urea, but the effect was not as strong as in the case of α-gliadin in 2 M urea.

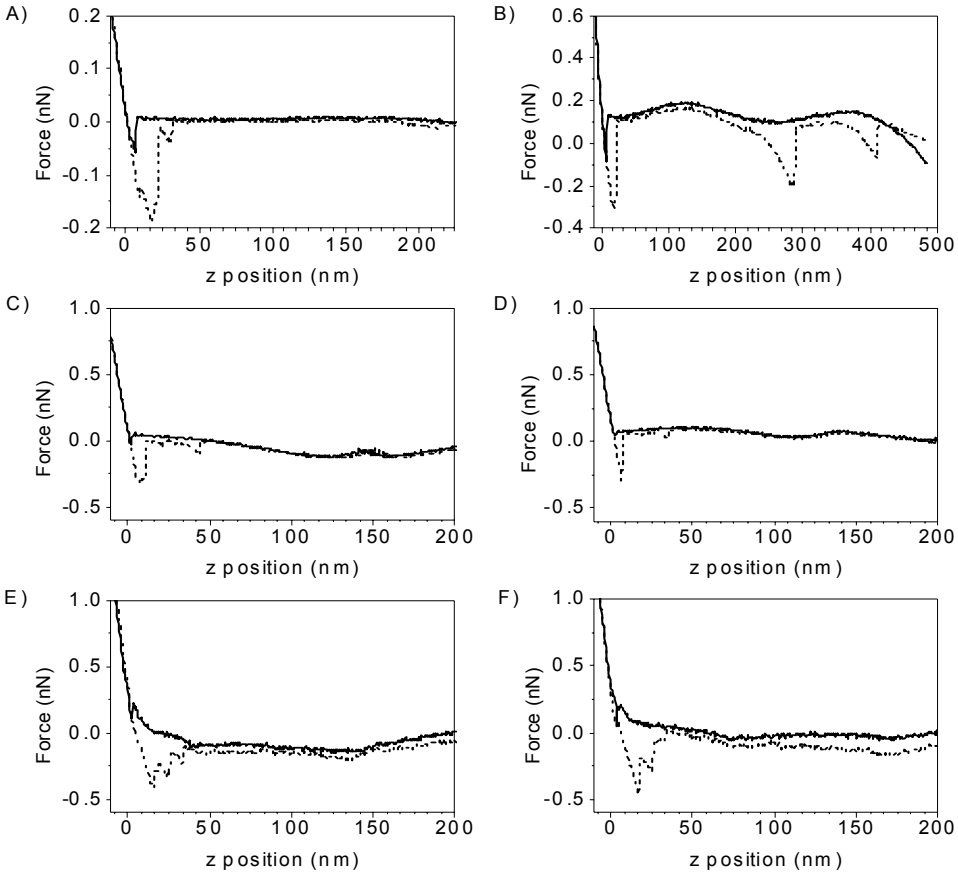

Figure 15. Typical raw data force-sample vertical position curves for α-α interaction (A and B) and ω-ω interaction (C and D) in 0.01 M acetic acid and 2 M urea, and ω-ω interaction (E and F) in 8 M urea (solid curve for approach and dashed for retract). (Modified from Publication II.)

The functional role of gliadins has been reported to be in determining the viscocity/plasticity of dough (Goesaert *et al*., 2005). The differences in behaviour are clearly related to structures and surface interactions of gliadins in the dough systems. Our results showed that the main difference between α-α and ω-ω-interactions was in their response to denaturing environment: whereas the more globular α- gliadins were unfolded in 2M urea, the β-turn-rich ω-gliadins remained rather stable even in 8M urea. Hence it can be suggested that α- and ω-gliadins have different roles during the network-forming process in dough.

Thus, while the ω-gliadins still have a compact structure and are responsible for the viscous flow, the α-gliadins have already started to participate in forming the network. It would have been interesting to study the effect of temperature on the gliadin-gliadin interaction, but this was not investigated in this work. The expected results of the effect of temperature would have been similar to those presented here, because β-turn-rich structures also present in ω-gliadins have been shown to exhibit unusual thermal stability (Tatham *et al*., 1985) and exposure of thiol groups upon heating favours aggregation of molecules containing disulphide bridges, such as α-gliadins (Tatham and Shewry, 1985; Singh and MacRitchie, 2004).

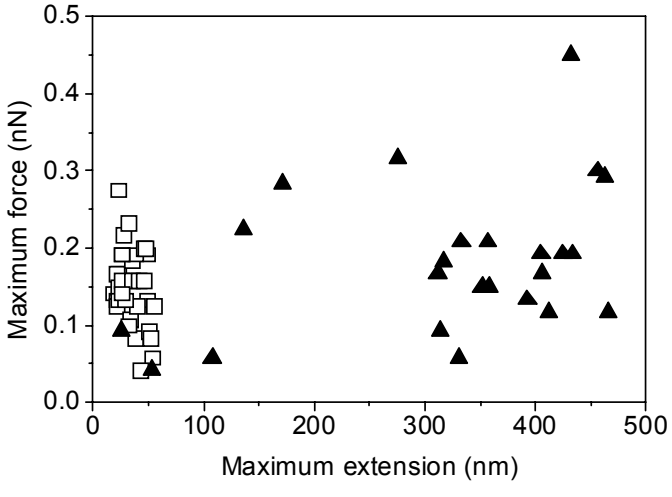

Figure 16. Comparison of maximum extension-maximum force coordinates for α-gliadin in acetic acid (square symbols) and in urea (triangles). (Modified from Publication II.)

3.3 Class II hydrophobins at the air-water interface

The knowledge of hydrophobins, their structure, functions and behaviour, has increased greatly during recent years. At the time when the AFM studies on the interfacial films of Class II hydrophobins HFBI and HFBII were initiated (Publication III), no high-resolution crystal structure of any hydrophobin was available. The structural information at that time was the sequence data (HFBI and HFBII, Nakari-Setälä *et al*. 1997; Class I and Class II hydrophobins,

Wösten, 2001) showing for example that a characteristic of all hydrophobins was eight cysteinyl residues that must be of importance for their function, and circular dichroism (CD) data providing information of secondary structures for some Class I and Class II hydrophobins (Wösten and de Vocht, 2000).

The studies on interfacial self-assembly of hydrophobins on solid surfaces indicated the amphiphilic nature of hydrophobins and that self-assembly plays a major role in their function (Wösten *et al*., 1993; Wösten *et al*., 1994; Wessels, 1996). Accumulation of 10 nm thick rodlets at the air-water interface had been reported when drying down drops of the class I hydrophobin SC3 and observing the residue under an electron microscope (Wösten *et al*., 1993). The interfacial and self-assembly studies of HFBI and HFBII showed efficient interactions with non-ionic surfactants (Linder *et al*., 2001), adhesion to hydrophobic surfaces (Linder *et al.*, 2002) and demonstrated that they form crystalline assemblies in solution (Torkkeli *et al*., 2002). It was also reported that at higher concentrations HFBII tends to form tetramers, but occurs as dimers and monomers at lower concentrations (Torkkeli *et al*., 2002). The capability of hydrophobins to lower the surface tension of water and their involvement in formation of aerial structures was suggested to be one of the biological roles of hydrophobins (Wessels *et al*., 1991; Talbot, 1999). Wösten *et al*. (1999) reported that SC3 hydrophobin was able to reduce the surface tension of water (72 mJ/m^2) down to 24 mJ/m^2.

Because of the interesting interfacial phenomena reported for Class I hydrophobins and the difference observed in solution structures for Class II hydrophobins, the interfacial behaviour and structures of the surface films formed by HFBI and HFBII were investigated. The hydrophobic side of the hydrophobin films (HFBI and HFBII) at the air-water interface was imaged by AFM and compared to structural information obtained by SAXS (publication III) and by X-ray crystallography (Publication IV). In Publication V the hydrophilic side of never-dried HFBI film was imaged by AFM, and the possibility of functionalisation of the ordered structures of HFBI hydrophobins was studied by AFM and QCM-D.

3.3.1 Hydrophobic side of the HFBI and HFBII films

In Publication III molecular films of HFBI and HFBII were prepared by LB technique on mica and analysed in ambient conditions by AFM. The results showed highly ordered two-dimensional crystalline structures for both hydrophobins (Figure 17), which was the most detailed structural study of hydrophobin films at that time. At best even 1 nm resolution was achieved. The Fourier transformations of the image data gave lattice constants a = 5.92 nm, b = 4.99 nm and with the angle in between $\gamma = 118.9°$ for HFBI and a = 5.87 nm, b = 4.41 nm and $\gamma = 122.6°$ for HFBII (also in Table 2). The obtained lattice parameters for HFBI and HFBII are qualitatively very similar, but the AFM images revealed structural differences at the molecular level. It is important to note here that the dimensions are affected by a slight distortion observed in the AFM images due to scanner hysteresis, creep and drift in the microscope. This was because of capturing the images with relatively slow scan speeds in order to avoid causing deformation of the soft sample surface by the tip as well as to avoid contamination of the tip. The average thickness of the HFBI film on mica was 1.3 ± 0.2 nm, which was obtained from measuring the height difference between the top surface layer and lower flat surface. The flat regions were plain mica surface and were located between crystalline domains of proteins. They were large enough for reliable measurements of layer thicknesses. Similar regions were not found for HFBII, where areas in between crystalline domains were covered by amorphous protein structures and the thickness of the protein layers could not be measured.

The AFM results were compared with SAXS data (Torkkeli *et al*., 2002), which gave a dimension of 6.5 nm for the largest diameter of the molecular entities in the solution and when combined with size exclusion chromatography results showed that these hydrophobin entities are tetramers with a thickness of 1.5 nm. The dimensions obtained from AFM and SAXS were rather similar, which indicated a hierarchial assembly: hydrophobins first assemble as tetrameric supramolecules in solution and then pack into crystalline arrays at the interface. Moreover, the thickness measurements indicated that the hydrophobin layer at the air-water interface was a monolayer. The further analysis of averaged hydrophobin domains in the AFM images and SAXS solution structures arranged to provide the best geometrical packing did show details for HFBII structures that helped to explain features and packing of hydrophobins in the

AFM images. The corresponding analysis for HFBI explained the overall dimensions, but did not provide more detailed information. Structures of HFBI and HFBII films at air-water interface on a water droplet were studied directly by grazing incidence X-ray diffraction (GIXD) (supporting Publication VI), which provides information on structures both parallel and perpendicular to the film surface (Als-Nielsen *et al*., 1994). The results for HFBII showed higher crystallinity than for HFBI: the lattice parameters for HFBII crystallites were a = 3.81 nm, b = 4.61 nm, c = 5.46 nm and γ = 122.3° (c-axis along the interface). These figures were again rather similar to the AFM results.

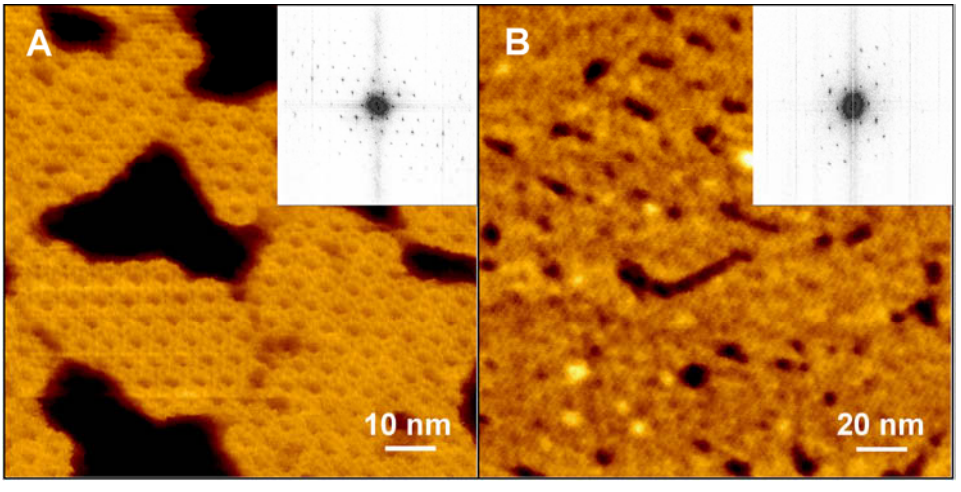

Figure 17. AFM topography images of hydrophobin LB films on mica. A) HFBI, image size 100 x 100 nm^2 and height scale 2 nm. B) HFBII, image size 200 x 200 nm^2 and height scale 2 nm. The power spectra for both hydrophobins are shown in insets. The corresponding crystalline oblique unit cells in real space are a = 5.92 nm, b= 4.99 nm and γ = 118.9° for HFBI, and a = 5.87 nm, b= 4.41 nm and γ = 122.6° HFBII. (Modified from Publication III.)

A rather different sample preparation procedure was then used for studying the structure of hydrophobin films. The previous data (Publication III) showed that higly ordered films of HFBI and HFBII could be formed by the LB technique. This data (Publication IV) showed that such ordered interfacial films are formed spontaneously at the surface of water droplets. The water droplet was dried down and the hydrophobic side of the hydrophobin film was imaged by AFM. The crystalline structures were again seen in the surface layers of HFBII, and the

lattice parameters determined by Fourier transformation from the AFM images were a = 6.71 nm, b = 4.48 nm, γ = 139.2°, agreeing with corresponding values found in LB films for HFBII (see Table 2). In Publication IV the first crystal structure of hydrophobin (HFBII) was reported and revealed a rigid structure interlocked by four disulphide bridges giving amphiphilic characteristics. This valuable information provided a new viewpoint for understanding the assembly and functions of hydrophobins: the surface activity of the HFBII most probably originates from the amphiphilicity, and the size and rigid structure of the hydrophobin must play a role in the self-assembly process. The crystal structure of an HFBII dimer was discussed as a high-energy stated structure that would favour location of hydrophobin at the air-water interface for lowering the energy-state by exposure of hydrophobic patches towards air. The ordered structure shown in the AFM images indicated the importance of lateral intermolecular contacts. Similar dimensions have also been observed in multilayer LB films measured by GIXD, where results showed hexagonal packing of hydrophobins with lattice constants a = b = 5.4 nm for HFBI and a = b = 5.5 nm for HFBII (Kisko *et al*., 2005). Hexagonal packing with the same lattice constants has also been observed directly at the air-water interface (Kisko *et al*., 2007).

Table 2. Lattice parameters of organised structures of hydrophobins. Constants are obtained from Fourier transforms of AFM topography images. SAXS solution structures for hydrophobins had the largest dimension of 6.5 nm, and the shapes were torus-like for HFBI and four-armed structures for HFBII. GIXD data for HFBII at the air-water interface has given lattice parameters a = 3.81 nm, b = 4.61 nm, c = 5.46 nm and γ = 122.3°

Protein	**Publication**	**Side of the film**	**a (nm)**	**b (nm)**	**γ (deg)**
HFBI	III	hydrophobic[a]	5.92	4.99	118.9
HFBI	V	hydrophobic[a]	6.07	5.05	119.5
HFBI	V	hydrophilic[b]	6.11	6.61	125.6
HFBI	V	hydrophobic[c]	5.92	4.31	116.8
Biotin-NCys-HFBI	V	hydrophilic[d]	5.50	5.65	119.0
HFBI-CysC-Biotin	V	hydrophilic[b]	6.43	5.81	126.1
HFBII	III	hydrophobic[a]	5.87	4.41	122.6
HFBII	IV	hydrophilic[e]	6.71	4.48	139.2
Hexagonal lattice	-	-	a = b	b = a	120.0

a = LB film, b = LS film, c = drop surface film, d = dried LS film, e = dried drop surface film

3.3.2 Hydrophilic side of the HFBI film

The interfacial films of HFBI were transferred onto HOPG by the LS and drop surface film techniques and the hydrophilic side of the films was imaged in liquid by AFM (Publication V). The never-dried films were studied in liquid in order to exclude the possible artefacts due to drying and to image the film structure in conditions closer to the native environment. The interaction between hydrophobic HOPG surface and HFBI appeared to be strong enough to allow rinsing cycles of the surface, indicating hydrophobic interaction between them and the expected orientation for hydrophobins. The AFM images shown in Figure 18 revealed ordered structure of proteins with dimensions comparable to previous results (Publication III) for both film preparation techniques (see Table 2). The measured thicknesses for LS and drop surface films were 2.8 ± 0.2 nm and 2.0 ± 0.2 nm, respectively. The value for LS film is more realistic, because that film contained large enough surface defects for reliable measurements. The thickness values were greater than that of the LB-film imaged in air (1.3 ± 0.2 nm), indicating possible drying effects in the LB film. The value for the LS film was very close to the dimensions obtained from HFBI crystal structure (2–3 nm, Hakanpää *et al*., 2006), verifying the exsistence of a monomolecular layer of hydrophobin. The results showed that the ordered strucutures observed in the LB and LS films of hydrophobins formed by compression also form spontaneously.

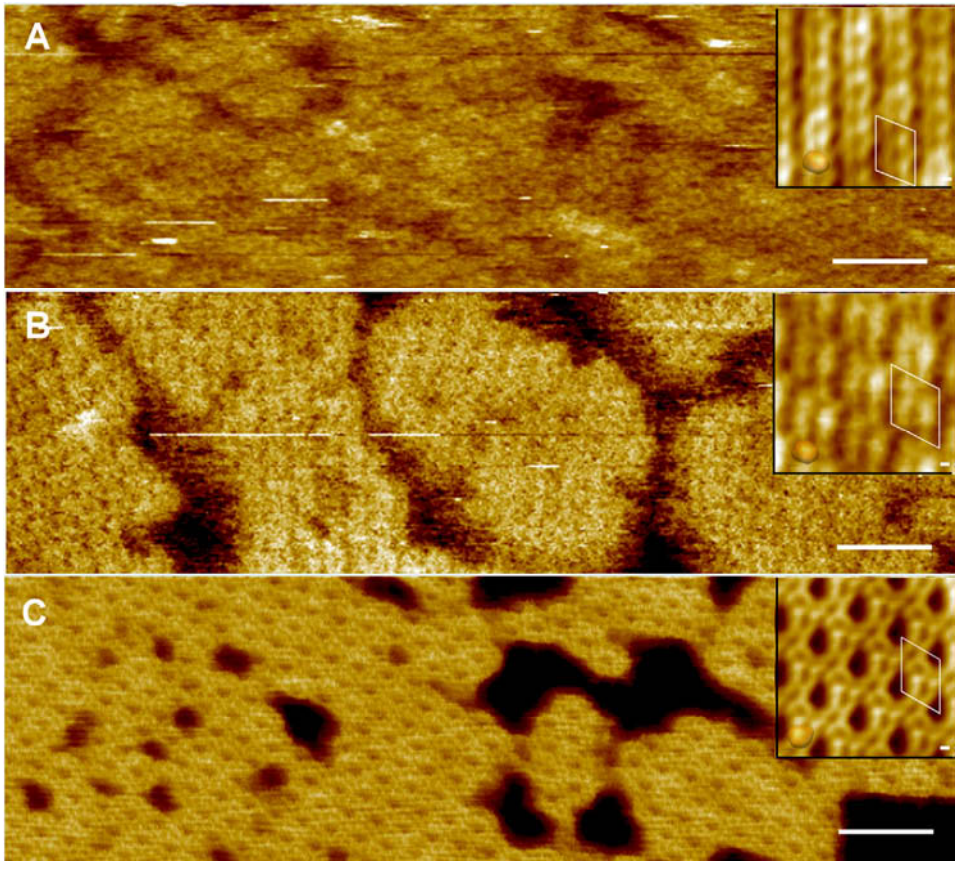

Figure 18. AFM topography images of HFBI films: drop surface film (A, hydrophilic side, imaged in buffer), LS film (B, hydrophilic side, imaged in buffer) and LB film (C, hydrophobic side, imaged in air). Scale bars are 20 nm. The correlation averages of ordered structures are shown in insets, scale bar 1 nm. (Modified from Publication V.)

3.3.3 Films of functionalised HFBI

Amphiphilic molecules tend to orient themselves at air-water interfaces by facing hydrophobic parts of the molecules towards the air. For confirming the orientation of hydrophobins in the interfacial film, structural variants of HFBI were prepared by protein engineering (see Publication V for details). A single cysteinyl residue was first added to the N-terminal of the hydrophobin and labelled specifically with biotin (Biotin-NCys-HFBI). The functionality of the

Biotin-NCys-HFBI layer formed from solution on a solid hydrophobic surface was studied by QCM-D. Addition of avidin clearly verified the functionality, as avidin was bound to biotinylated hydrophobin surfaces but not to HFBI control surfaces. Although high-resolution AFM images of Biotin-NCys-HFBI were not achieved in liquid, probably due to disturbance of the flexible linker with biotin, attachment of avidin was clearly seen and confirmed by roughness analysis (roughness analysis according to Peltonen *et al*., 2004). However, the periodical structure characteristic of hydrophobins was seen in the dried sample.

Another variant with additional cysteinyl residue in the C terminal and labelled with biotin (HFBI-CysC-Biotin) was studied. The size of the linker with biotin was shorter and it was located closer to the core of the protein (Figure 6). The functionality was also demonstrated with QCM-D and similar behaviour was observed for both variants. The high resolution images of HFBI-CysC-Biotin films were reproducibly achieved in liquid environment (Figure 19A), and the results showed ordered structures with dimensions similar to those of native HFBI. This indicated that functionalisation did not restrict the self-assembling properties of HFBI molecules. Binding of avidin to the surface was again clearly seen in the AFM images (Figure 19C) and confirmed by roughness analysis. One of the aims was also to image ordered functionalised hydrophobin surfaces so that individual avidin molecules bound to biotinylated hydrophobins could be seen and located on the surface. The best result of this is shown in Figure 19B. Probably the linker allowed some degree of freedom to bound avidin molecules hampering the AFM imaging. Altogether these results proved the expected orientation for hydrophobins in the interfacial films. Because hydrophobins clearly orient themselves at the air-water interface by facing the hydrophobic patch towards the air, it would be expected that the smallest repeating unit in the lattice would be of the size of a single hydrophobin molecule. However this appeared not to be the case. The dimensions in the lattice were reproducibly close to those of tetramers, which indicated the importance of the lateral interactions between hydrophobins. Maybe the presence of gaps or holes in the protein network is crucial for the strength and elasticity of the hydrophobin film at the air-water interface, and formation of more closely packed film is necessary in some other conditions.

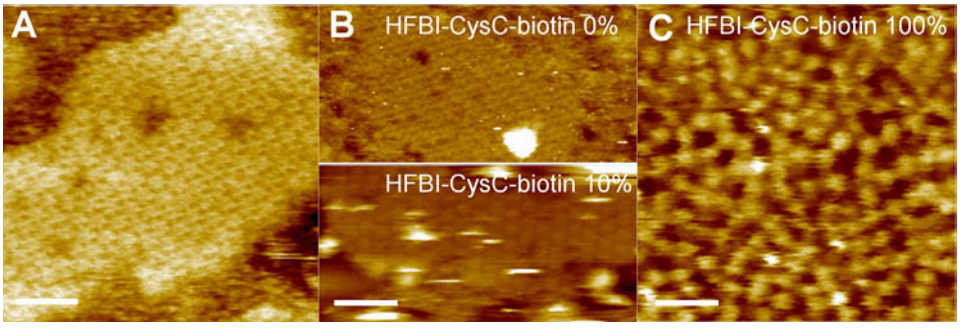

Figure 19. AFM topography images of HFBI-CysC-Biotin (A) and with avidin when biotinylated HFBI variant is involved in the film formation 0% or 10% (B) or 100% (C). Scale bars are 20 nm. (Modified from Publication V.)

Some very recent studies on HFBI and HFBII have further broadened our understanding of the behaviour of hydrophobins. The research by Szilvay *et al*. (2006) supported the model of multimerisation of hydrophobins in solution. Askolin *et al*. (2006) reported stability and interfacial behaviour of SC3, HFBI and HFBII. The results showed that the Class II hydrophobins do not form rodlet layers and there were no changes in the secondary structure upon adsorption at interfaces like those observed (Wösten *et al*., 1993; de Vocht *et al*., 2002) and simulated (Fan *et al*., 2006) for SC3. They also reported that the surface tension of aqueous solutions of HFBI and HFBII were as low as 37 and 28 mJ/m^2, respectively, and that both hydrophobins are stable at temperatures from 25 to 90 ºC. Kostiainen *et al*. (2006) reported successful conjugation of DNA-binding dendrimers to HFBI, in which the functionality of both components was retained, including the capability of HFBI molecules to form ordered structures (unpublished data).

As reported in many publications, the capability to decrease surface tension of water and formation of coatings are believed to be the major biological roles of hydrophobins (Linder et al., 2005). At the air-water interface the studied Class II hydrophobins form a visible film that is very elastic (see Figure 2 in Publication V). The unusual interfacial properties of hydrophobins as surfactants originate from the molecular interactions determined by their rigid structure, shape and relatively large size. In aqueous solutions of HFBI or HFBII these interactions lead to an organised network of proteins at the air-water interface. The interactions are rather strong – they are able to deform the shape of a water

droplet into a trapezoidal appearance. This again brings out the importance of lateral interactions. The difference in tetramer structure and crystallinity between HFBI and HFBII may be related to their different roles in fungal growth. Based on the results obtained by means of molecular engineering Askolin *et al.* (2005) and Askolin (2006) have suggested that the biological functions of HFBI are related to formation of aerial hyphae and hydrophobicity of hyphae, whereas HFBII is mainly involved in sporulation and hydrophobicity of spores and hyphae. The results of Linder *et al.* (2002) and Askolin *et al.* (2006) indicated that interaction between HFBI and a hydrophobic solid is stronger than that of HFBII, which may be of importance when a fungus adheres to solid surfaces.

4. Conclusions

This thesis deals with surface forces and interactions involved between biopolymer surfaces as well as in self-assembly and interfacial behaviour of biopolymers. The research aimed at deepening the understanding of molecular interactions and the nature and strength of surface forces in the studied biopolymer systems. The main research technique, AFM, revealed interesting phenomena that were supported and confirmed by other relevant surface analytical techniques. The nanomechanical force measurements focused on interactions relevant in papermaking, i.e. between cellulose and xylan, and food technology, i.e. between gliadins (wheat gluten proteins). The studies of interfacial behaviour of biopolymers were focused on hydrophobins, which are very surface active proteins.

The main result of the studied cellulosic systems provided a new perspective to the role of xylan in papermaking. It has been reported previously that the adsorption of xylan increases paper strength and that this is due to formation of hydrogen bonds. Our results indicated that the increase in paper strength cannot originate from such bonds in wet paper, but must be due to effects of xylan on fibre bonds during drying of paper. Possibly dehydration of the cellulose-xylan complex enables xylan to orient on cellulose fibrils and adsorb more efficiently (by forming hydrogen bonds), and simultaneously to adsorb on two parallel cellulose chains thus enhancing the paper strength. The results also showed that xylan did not desorb from the cellulose surfaces. This could be exploited in sample preparation of further studies using model surfaces, in order to eliminate the phenomenon that hampered these measurements – the continuous readsorption of xylan from solution. Measuring forces between xylan-coated cellulose surfaces and between xylan-coated cellulose and cellulose surfaces without free xylan molecules in the solution might provide new insight into the interaction at the molecular level. Closer to the idea of xylan enhancing the paper strength would be to measure the force required to separate dried cellulose surfaces with varying amounts of adsorbed xylan on the cellulose. Although such measurements of paper strength at the nanoscale would be interesting, AFM might not be the easiest technique for carrying out such experiments.

The force measurement approach was also applied to a food technology related subject, where a group of cereal plant proteins, wheat gliadin proteins, were investigated. The gluten proteins, gliadins and glutenins, facilitate the production of bread, pasta and noodles and many other food products from wheat flour. Hence, the study of the mechanical properties of gliadins was important from both a scientific and a practical point of view. On the basis of the nanomechanical force measurements the roles of different types of gliadins could be proposed: whereas ω-gliadins still have a compact structure and are responsible for the viscous flow in dough, α-gliadins have already started to participate in forming the dough network. This may provide a new viewpoint in understanding the interfacial properties of gliadins in relation to baking. It would have been interesting to study the effect of temperature on gliadin-gliadin interaction, but this was not investigated in this work.

In addition to measuring surface forces directly, AFM imaging was used in studying hydrophobins that self-assemble due to interplay of various surface forces and interactions in solution and at interfaces. The research presented in this thesis focused on the behaviour of Class II hydrophobins, HFBI and HFBII at the air-water interface. The organised structures of hydrophobins were imaged at nanometer resolution. The results showed that both HFBI and HFBII form organized structures at the air-water interface, and that the dimensions corresponded with those of the solution structures obtained by SAXS. Moreover, the results also showed that the nanostructured films form spontaneously. The HFBI films were imaged by AFM both from the hydrophobic and hydrophilic side. The organisation at the air-water interface has also been observed by GIXD. Surface activity and capability to self-assemble in solution and at interfaces are fascinating properties of hydrophobins. As presented in the literature, these properties most probably originate from the unique structure of hydrophobins. These amphiphilic, rigid molecules have on their surface a relatively large hydrophobic patch that is involved in the self-assembly process of hydrophobins at least through hydrophobic interaction. It would be interesting to use AFM to measure interaction forces between hydrophobins and between hydrophobins and surfaces. The force measurements of these naturally existing hydrophobic surfaces might provide more information to augment the current view of hydrophobic interaction. Another interesting, more theoretical study would be to simulate the formation of ordered structures and to determine the elasticity of the film and how conditions affect the organisation of hydrophobins

at the air-water interface. Possibly simulations would provide insight into the presence of gaps or holes in the protein network. Molecular biology tools made it possible to assign a specific functionality to HFBI. The results clearly indicated that hydrophobin oriented at the air-water interface in the way expected for an amphiphilic molecule. The results also indicated that hydrophobin retained the capability to form organised films, and the covalently attached molecule its functionality. By this self-assembling characteristic, hydrophobins could offer new options for surface modifications and nanostructured functional surfaces that could have potential applications in nanotechnology in the future. Other potential end-users could be within food research (stabilization of the air-water interface in foams), as well as within diagnostics and biosensor research (functionality with defined orientation).

Interactions between biopolymers are vital in life sciences. The strong covalent and ionic bonds define the structure and composition of materials, but the weaker non-covalent interactions play a crucial role in determining their functions. As expressed by Lehn and Ball (2000), the non-covalent interactions are the way in which biomolecules communicate. This level of communication is measurable with AFM, either directly by force measurements or by imaging the surface structures formed as a consequence of the interplay of non-covalent interactions. The AFM approach in aiming at understanding the biophysical interactions can be very challenging, but it can also be very rewarding because of its unique advantages. Despite some drawbacks, AFM has rapidly become a very popular technique in surface science. However, at least within biophysical sciences, AFM still cannot be described as a technique for routine analysis. Possibly one day it will be – there are many laboratories that are further developing the AFM technique, and even more groups around the world applying AFM to various biological samples.

References

A-Hassan, E., Heinz, W.F., Antonik, M.D., D'Costa, N.P., Nageswaran, S., Schoenenberger, C.-A. and Hoh, J.H. 1998. Relative microelastic mapping of living cells by atomic force microscopy. Biophys. J. 74, pp. 1564–1578.

Ahimou, F., Touhami, A. and Dufrêne, Y.F. 2003. Real-time imaging of the surface topography of living yeast cells by atomic force microscopy. Yeast 20, pp. 25–30.

Alessandrini, A. and Facci, P. 2005. AFM: a versatile tool in biophysics. Meas. Sci. Technol. 16, pp. R65–R92.

Allen, S., Chen, X., Davies, J., Davies, M.C., Dawkes, A.C., Edwards, J.C., Roberts, C.J., Sefton, J., Tendler, S.J.B. and Williams, P.M. 1997. Detection of antigen-antibody binding events with the atomic force microscope. Biochemistry 36, pp. 7457–7463.

Allen, S., Chen, X., Davies, J., Davies, M.C., Dawkes, A.C., Edwards, J.C., Roberts, C.J., Tendler, S.J.B. and Williams, P.M. 1998. The application of force microscopy to immunodiagnostic systems: imaging and biomolecular adhesion measurements. Appl. Phys. A 66, pp. S255–S261.

Als-Nielsen, J., Jacquemain, D., Kjaer, K., Leveiller, F., Lahav, M. and Leiserowitz, L. 1994. Principles and applications of grazing incidence X-ray and neutron scattering from ordered molecular monolayers at the air-water interface. Phys. Rep. 246, pp. 251–313.

Askolin, S. 2006. Characterization of the *Trichoderma reesei* hydrophobins HFBI and HFBII. Ph.D. Thesis. VTT, Espoo: VTT Publications 601. 99 p. ISBN 951-38-6836-2. http://www.vtt.fi/inf/pdf/publications/2006/P601.pdf.

Askolin, S., Linder, M., Scholtmeijer, K., Tenkanen, M., Penttilä, M., de Vocht, M.L. and Wösten, H.A. 2006. Interaction and comparison of a class I hydrophobin from *Schizophyllum commune* and class II hydrophobins from *Trichoderma reesei*. Biomacromolecules 7, pp. 1295–1301.

Askolin, S., Penttilä, M, Wösten, H.A. and Nakari-Setälä, T. 2005. The *Trichoderma reesei* hydrophobin genes *hfb1* and *hfb2* have diverse functions in fungal development. FEMS Microbiol. Lett. 253, pp. 281–288.

Atalla, R. and Vanderhart, D. 1984. Native cellulose: a composite of two distinct crystalline forms. Science 223, pp. 283–285.

Attard, P. 2000. Thermodynamic analysis of bridging bubbles and a quantitative comparison with the measured hydrophobic attraction. Langmuir 16, pp. 4455–4466.

Baker, A.A., Helbert, W., Sugiyama, J. and Miles, M.J. 1997. High-resolution atomic force microscopy of native *Valonia* cellulose I microcrystals. J. Struct. Biol. 119, pp. 129–138.

Baker, A.A., Helbert, W., Sugiyama, J. and Miles, M.J. 2000. New insight into cellulose structure by atomic force microscopy shows the I_α crystal phase at near-atomic resolution. Biophys. J. 79, 1139–1145.

Bar, G., Thomann, Y., Brandsch, R., Cantow, H.-J. and Whangbo, M.-H. 1997. Factors affecting the height and phase images in tapping mode atomic force microscopy. Study of phase-separated polymer blends of poly(ethene-co-styrene) and poly(2,6-dimethyl-1,4-phenylene oxide). Langmuir 13, pp. 3807–3812.

Berger, C.E.H., van der Werf, K.O., Kooyman, R.P.H., De Grooth, B.G. and Greve, J. 1995. Functional group imaging by adhesion AFM applied to lipid monolayers. Langmuir 11, pp. 4188–4192.

Binnig, G., Quate, C.F. and Gerber, C. 1986. Atomic force microscope. Phys. Rev. Lett. 56, pp. 930–933.

Binnig, G., Rohrer, H., Gerber, C. and Weibel, E. 1982. Surface studies by scanning tunnelling microscopy. Phys. Rev. Lett. 49, pp. 57–61.

Blackwell, J. 1982. The macromolecular organization of cellulose and chitin. In: Cellulose and other natural polymer systems. Brown, R.M. Jr. (Ed.). Plenum Press, New York. Pp. 403–428.

Blodgett, KB. 1935. Films built by depositing successive monomolecular layers on a solid surface. J. Am. Chem. Soc. 57, pp. 1007–1022.

Bowen, W.R., Lovitt, R.W. and Wright, C.J. 2001. Atomic force microscopy study of the adhesion of *Saccharomyces cerevisiae*. J. Colloid Interface Sci. 237, pp. 54–61.

Buchert, J., Teleman, A., Harjunpää, V., Tenkanen, M., Viikari, L. and Vuorinen, T. 1995. Effect of cooking and bleaching on the structure of xylan in conventional pine kraft pulp. Tappi J. 78, pp. 125–130.

Burns, A.R., Frankel, D.J. and Buranda, T. 2005. Local mobility in lipid domains of supported bilayers characterized by atomic force microscopy and fluorescence correlation spectroscopy. Biophys. J. 89, pp. 1081–1093.

Butt, H.-J., Cappella, B. and Kappl, M. 2005. Force measurements with the atomic force microscope: Technique, interpretation and applications. Surf. Sci. Rep. 59, pp. 1–152.

Butt, H.-J., Wolff, E.K., Gould, S.A.C., Dixon Northern, B., Peterson, C.M. and Hansma, P.K. 1990. Imaging cells with the atomic force microscope. J. Struct. Biol. 105, pp. 54–61.

Caflisch, A. and Karplus, M. 1999. Structural details of urea binding to barnase: a molecular dynamics analysis. Structure 7, pp. 477–488.

Cappella, B. and Dietler, G. 1999. Force-distance curves by atomic force microscopy. Surf. Sci. Rep. 34, pp. 1–104.

Carambassis, A. and Rutland, M.W. 1999. Interactions of cellulose surfaces: Effect of electrolyte. Langmuir 15, pp. 5584–5590.

Carl, P., Kwok, C.H., Manderson, G., Speicher, D.W. and Discher, D.E. 2001. Forced unfolding modulated by disulfide bonds in the Ig domains of a cell adhesion molecule. Proc. Natl. Acad. Sci. USA 98, pp. 1565–1570.

Carrascosa, L.G., Moreno, M., Álvarez, M. and Lechuga, L.M. 2006. Nano-mechanical biosensors: a new sensing tool. Trends Anal. Chem. 25, pp. 196–206.

Chandler, D. 2005. Interfaces and the driving force of hydrophobic assembly. Nature 47, pp. 640–647.

Chapman, D.L. 1913. A contribution to the theory of electrocapillarity. Phil. Mag. 25, pp. 475–481.

Charras, G.T. and Horton, M.A. 2002. Single cell mechanotransduction and its modulation analyzed by atomic force microscope indentation. Biophys. J. 82, pp. 2970–2981.

Charras, G.T., Lehenkari, P. and Horton, M. 2002. Biotechnological applications of atomic force microscopy. Methods Cell Biol. 68, pp. 171–191.

Chen, X., Roberts, C.J., Zhang, J., Davies, M.C. and Tendler, S.J.B. 2002. Phase contrast and attraction–repulsion transition in tapping mode atomic force microscopy. Surf. Sci. 519, pp. L593–L598.

Cheung, C.L., Hafner, J.H. and Lieber, C.M. 2000. Carbon nanotube atomic force microscopy tips: Direct growth by chemical vapor deposition and application to high-resolution imaging. Proc. Natl. Acad. Sci. USA 97, pp. 3809–3813.

Christenson, H.K. and Claesson, P.M. 1988. Cavitation and the interaction between macroscopic hydrophobic surfaces. Science 239, pp. 390–392.

Christenson, H.K. and Claesson, P.M. 2001. Direct measurements of the force between hydrophobic surfaces in water. Adv. Colloid Interface Sci. 91, pp. 391–436.

Cisneros, D.A., Hung, C., Franz, C.M. and Müller, D.J. 2006. Observing growth steps of collagen self-assembly by time-lapse high-resolution atomic force microscopy. J. Struct. Biol. 154, pp. 232–245.

Claesson, P.M., Christenson, H.K., Berg, J.M. and Neuman, R.D. 1995. Interactions between mica surfaces in the presence of carbohydrates. Colloid Interface Sci. 172, pp. 415–424.

Clausen-Schaumann, H., Rief, M., Tolksdorf, C. and Gaub, H.E. 2000. Mechanical stability of single DNA molecules. Biophys. J. 78, pp. 1997–2007.

Cleveland, J.P., Anczykowski, B., Schmid, A.E. and Elings, V.B. 1998. Energy dissipation in tapping-mode atomic force microscopy. Appl. Phys. Lett. 72, pp. 2613–2615.

Cleveland, J.P., Manne, S., Bocek, D. and Hansma, P.K. 1993. A nondestructive method for determining the spring constant of cantilevers for scanning force microscopy. Rev. Sci. Instrum. 64, pp. 403–405.

Cole, E.W., Kasarda, D.D. and Lafiandra, D. 1984. The conformational structure of A-gliadin. Intrinsic viscosities under conditions approaching the native state and under denaturing conditions. Biochim. Biophys. Acta 787, pp. 244–251.

Collén, A, Persson, J., Linder, M., Nakari-Setälä, T., Penttilä, M., Tjerneld, F. and Sivars, U. 2002. A novel two-step extraction method with detergent/polymer systems for primary recovery of the fusion protein endoglucanase I-hydrophobin I. Biochim. Biophys. Acta 1569, pp. 139–150.

Colton, R.J., Engel, A., Frommer, J.E., Gaub, H.E., Gewirth, A.A., Guckenberger, R., Rabe, R., Heckl, W.M. and Parkinson, B. (Eds.). 1998. Procedures in scanning probe microscopies. John Wiley & Sons, Chichester, UK. 639 p.

Dammer, U., Hegner, M., Anselmetti, D., Wagner, P., Dreier, M., Huber, W. and Güntherodt, H.-J. 1996. Specific antibody / antigen interactions measured by force microscopy. Biophys. J., pp. 2437–2441.

de Vocht, M.L., Reviakine, I., Ulrich, W.P., Bergsma-Schutter, W., Wösten, H.A., Vogel, H., Brisson, A., Wessels, J.G. and Robillard, G.T. 2002. Self-assembly of the hydrophobin SC3 proceeds via two structural intermediates. Protein Sci. 11, pp. 1199–1205.

Debye, P. and Hückel, E. 1923. Zur Theorie der Elektrolyte. I. Gefrierpunktserniedrigung und verwandte Erscheinungen. Physikal. Z. 24, pp. 185–206.

Derjaguin, B.V. 1934. Untersuchungen über die Reibung und Adhäsion, IV: Theorie des Anhaftens kleiner Teilchen. Kolloid Z. 69, pp. 155–164.

Derjaguin, B.V. and Landau, L. 1941. Theory of the stability of strongly charged lyophobic sols and of the adhesion of strongly charged particles in solution of electrolytes. Acta Physicochim. URSS 14, pp. 633–662.

Drake, B., Prater, C.B., Weisenhorn, A.L., Gould, S.A., Albrecht, T.R., Quate, C.F., Cannell, D.S., Hansma, H.G. and Hansma, P.K. 1989. Imaging crystals, polymers and processes in water with atomic force microscope. Science 243, pp. 1586–1589.

Ducker, W.A., Senden, T.J. and Pashley, R.M. 1991. Direct measurement of colloidal forces using an atomic force microscope. Nature 353, pp. 239–241.

Dufrêne, Y.F. 2001. Application of atomic force microscopy to microbial surfaces: from reconstituted cell surface layers to living cells. Micron 32, pp. 153–165.

Dufrêne, Y.F. 2004. Using nanotechniques to explore microbial surfaces. Nat. Rev. Microbiol. 2, pp. 451–460.

Dufrêne, Y.F. and Lee, G.U. 2000. Advances in the characterization of supported lipid films with the atomic force microscope. Biochim. Biophys. Acta 1509, pp. 14–41.

Dufrêne, Y.F., Barger, W.R., Green, J.-B.D. and Lee, G.U. 1997. Nanometer-scale surface properties of mixed phospholipid monolayers and bilayers. Langmuir 13, pp. 4779–4784.

Duvshani-Eshet, M., Baruch, L., Kesselman, E., Shimoni, E. and Machluf, M. 2006. Therapeutic ultrasound-mediated DNA to cell and nucleus: bioeffects revealed by confocal and atomic force microscopy. Gene Ther. 13, pp. 163–172.

Ebner, A., Kienberger, F., Huber, C., Kamruzzahan, A.S., Pastushenko, V.P., Tang, J., Kada, G., Gruber, H.J., Sleytr, U.B., Sára, M. and Hinterdorfer, P. 2006. Atomic-force-microscopy imaging and molecular-recognition-force microscopy of recrystallized heterotetramers comprising an S-layer-streptavidin fusion protein. Chembiochem. 7, pp. 588–591.

Ebner, A., Kienberger, F., Kada, G., Stroh, C.M., Geretschläger, M., Kamruzzahan, A.S.M., Wildling, L., Johnson, W.T., Ashcroft, B., Nelson, J., Lindsay, S.M., Gruber, H.J. and Hinterdorfer, P. 2005. Localization of single avidin-biotin interactions using simultaneous topography and molecular recognition imaging. ChemPhysChem 6, pp. 897–900.

Egger, M., Ohnesorge, F., Weisenhorn, A.L., Heyn, S.P., Drake, B., Prater, C.B., Gould, S.A.C., Hansma, P.K. and Gaub, H.E. 1990. Wet lipid-protein membranes imaged at submolecular resolution by atomic force microscopy. J. Struct. Biol. 103, pp. 89–94.

Engel, A. and Müller, D.J. 2000. Observing single biomolecules at work with the atomic force microscope. Nat. Struct. Biol. 7, pp. 715–718.

Eriksson, J.C., Ljunggren, S. and Claesson, P.M. 1989. A phenomenological theory of long-range hydrophobic attraction forces based on a square-gradient variational approach. J. Chem. Soc. Faraday Trans. II 85, pp. 163–176.

Fan, H., Wang, X., Zhu, J., Robillard, G.T. and Mark, A.E. 2006. Molecular dynamics simulations of the hydrophobin SC3 at a hydrophobic/hydrophilic interface. Proteins 64, pp. 863–873.

Fardim, P., Gustafsson, J., von Schoultz, S., Peltonen, J. and Holmbom, B. 2005. Extractives on fiber surfaces investigated by XPS, ToF-SIMS and AFM. Colloids Surf. A 255, pp. 91–103.

Fido, R.J., Békés, F., Gras, P.W. and Tatham, A.S. 1997. Effects of α-, β-, γ- and ω-gliadins on the dough mixing properties of wheat flour. J. Cereal Sci. 26, pp. 271–277.

Field, J.M., Tatham, A.S., Baker, A.M. and Shewry, P.R. 1986. The structure of C hordein. FEBS Lett. 200, pp. 76–80.

Fleer, G.J., Cohen Stuart, M.A., Scheutjens, J.M.H.M., Cosgrove, T. and Vincent, B. 1993. Polymers at interfaces. 1. ed. Chapman & Hall, London, UK. 502 p.

Florin, E.L., Moy, V.T. and Gaub, H.E. 1994. Adhesion forces between individual ligand-receptor pairs. Science 264, pp. 415–417.

Fotiadis, D., Scheuring, S., Müller, S.A., Engel, A. and Müller, D.J. 2002. Imaging and manipulation of biological structures with the AFM. Micron 33, pp. 385–397.

Frisbie, D.C., Rozsnyai, L.F., Noy, A., Wrighton, M.S. and Lieber, C.M. 1994. Functional group imaging by chemical force microscopy. Science 265, pp. 2071–2074.

Fritz, J., Baller, M.K., Lang, H.P., Rothuizen, H., Vettiger, P., Meyer, E., Güntherodt, H.-J., Gerber, Ch. and Gimzewski, J.K. 2000. Translating biomolecular recognition into nanomechanics. Science 288, pp. 316–318.

Fritz, J., Katopodis, A.G., Kolbinger, F. and Anselmetti, D. 1998. Force-mediated kinetics of single P-selectin/ligand complexes observed by atomic force microscopy. Proc. Natl. Acad. Sci. USA 95, pp. 12283–12288.

Fritz, M., Radmacher, M. and Gaub, H.E. 1994. Granula motion and membrane spreading during activation of human platelets imaged by atomic force microscopy. Biophys J. 66, pp. 1328–1334.

Furuta, T. and Gray, D.G. 1998. Direct force-distance measurements on wood-pulp fibres in aqueous media. J. Pulp Pap. Sci. 24, pp. 320–324.

Gaines, G.L., Jr. 1966. Insoluble monolayers at liquid-gas interfaces. Wiley-Interscience, New York. 400 p.

Glatter, O. and Kratky, O. 1982. Small Angle X-ray Scattering. Academic Press, London. 515 p.

Goesaert, H., Brijs, K., Veraverbeke, W.S., Courtin, C.M., Gebruers, K. and Delcour, J.A. 2005. Wheat flour constituents: how they impact bread quality, and how to impact their functionality. Trends Food Sci. Technol. 16, pp. 12–30.

Goldsbury, C., Kistler, J., Aebi, U., Arvinte, T. and Cooper, G.J.S. 1999. Watching amyloid fibrils grow by time-lapse atomic force microscopy. J. Mol. Biol. 285, pp. 33–39.

Gosal, W.S., Myers, S.L., Radford, S.E. and Thomson, N.H. 2006. Amyloid under the atomic force microscope. Protein Pept. Lett. 13, pp. 261–270.

Gouy, M.G. 1910. Constitution of the electric charge at the surface of an electrolyte. J. Phys. 9, pp. 457–467.

Grandbois, M., Dettmann, W., Benoit, M. and Gaub, H.E. 2000. Affinity imaging of red blood cells using an atomic force microscope. J. Histochem. Cytochem. 48, pp. 719–24.

Griffiths-Jones, S.R., Maynard, A.J. and Searle, M.S. 1999. Dissecting the stability of a β-hairpin peptide that folds in water: NMR and molecular dynamics analysis of the β-turn and β-strand contributions to folding. J. Mol. Biol. 292, pp. 1051–1069.

Gunning, P.A., Mackie, A.R., Gunning, A.P., Woodward, N.C., Wilde, P.J. and Morris, V.J. 2004. Effect of surfactant type on surfactant-protein interactions at the air-water interface. Biomacromolecules 5, pp. 984–991.

Guo, L., Wang, R., Xu, H. and Liang, J. 2005. Why can the carbon nanotube tips increase resolution and quality of image in biological systems? Physica E 27, pp. 240–244.

Gustafsson, J. 2004. Surface characterization of chemical and mechanical pulp fibres by AFM and XPS. Ph.D. Thesis. Turku: Åbo Akademi University. 90 p.

Gustafsson, J., Ciovica, L. and Peltonen, J. 2003a. The ultrastructure of pine kraft pulps studied by atomic force microscopy (AFM) and X-ray photoelectron spectroscopy (XPS). Polymer 44, pp. 661–670.

Gustafsson, J., Lehto, J.H., Tienvieri, T., Ciovica, L. and Peltonen, J. 2003b. Surface characteristics of thermomechanical pulps; the influence of defibration temperature and refining. Colloids Surf. A: Physicochem. Eng. Aspects 225, pp. 95–104.

Györvary, E., Albers, W.M. and Peltonen, J. 1999. Miscibility in binary monolayers of phospholipids and linker lipid. Langmuir 15, pp. 2516–2524.

Györvary, E.S., Stein, O., Pum, D. and Sleytr, U.B. 2003. Self-assembly and recrystallization of bacterial S-layer proteins at silicon supports imaged in real time by atomic force microscopy. J. Microsc. 212, pp. 300–306.

Hafner, J.H., Cheung, C.L. and Lieber, C.M. 1999. Growth of nanotubes for probe microscopy tips. Nature 398, pp. 761–762.

Hakanpää, J. 2006. Structural studies of *Trichoderma reesei* hydrophobins HFBI and HFBII – the molecular basis for the function of fungal amphiphiles. Ph.D. Thesis. Joensuu: University of Joensuu. 42 p.

Hakanpää, J., Szilvay, G., Kaljunen, H., Maksimainen, M., Linder, M. and Rouvinen, J. 2006. Two crystal structures of *Trichoderma reesei* hydrophobin HFBI – The structure of a protein amphiphile with and without detergent interaction. Protein Sci. 15, pp. 2129–2140.

Hamaker, H.C. 1937. The London-van der Waals attraction between spherical particles. Physica 4, pp. 1058–1072.

Han, W., Mou, J., Sheng, J., Yang, J. and Shao, Z. 1995. Cryo atomic force microscopy: A new approach for biological imaging at high resolution. Biochemistry 34, pp. 8215–8220.

Hanley, S.J. and Gray, D.G. 1994. Atomic force microscope images of black spruce wood sections and pulp fibres. Holzforschung 48, pp. 29–34.

Hanley, S.J., Giason, J., Revol, J.-F. and Gray, D.G. 1992. Atomic force microscopy of cellulose microfibrils: comparison with transmission electron microscopy. Polymer 33, pp. 4639–4642.

Hansma, H.G. 2001. Surface biology of DNA by atomic force microscopy. Annu. Rev. Phys. Chem. 52, pp. 71–92.

Haugland, R.P. 1999. Handbook of fluorescent probes and research chemicals. 7. ed, on CD-ROM, Molecular probes. http://probes.invitrogen.com.

Heiner, A.P., Sugiyama, J. and Teleman, O. 1995. Crystalline cellulose I_α and I_β studied by molecular dynamics simulation. Carbohydr. Res. 273, 207–223.

Hektor, H.J. and Scholtmeijer, K. 2005. Hydrophobins: proteins with potential. Curr. Opin. Biotechnol.16, pp. 434–439.

Henderson, E. 1994. Imaging of living cells by atomic force microscopy. Prog. Surf. Sci. 46, pp. 39–60.

Henderson, E., Haydon, P.G. and Sakaguchi, D.S. 1992. Actin filament dynamics in living glial cells imaged by atomic force microscopy. Science 257, pp. 1944–1946.

Henriksson, Å. and Gatenholm, P. 2001. Controlled assembly of glucuronoxylans onto cellulose fibres. Holzforschung 55, pp. 494–502.

Hiemenz, P.C. and Rajagopalan, R. 1997. Principles of colloid and surface chemistry. 3. ed. Dekker, New York. 650 p.

Hinterdorfer, P. and Dufrêne, Y.F. 2006. Detection and localization of single molecular recognition events using atomic force microscopy. Nat. Methods 3, pp. 347–355.

Hinterdorfer, P., Baumgartner, W., Gruber, H.J., Schilcher, K. and Schindler, H. 1996. Detection and localization of individual antibody-antigen recognition events by atomic force microscopy. Proc. Natl. Acad. Sci. USA 93, pp. 3477–3481.

Hoh, J.H. and Hansma, P.K. 1992. Atomic force microscopy for high-resolution imaging in cell biology. Trends Cell Biol. 2, pp. 208–213.

Holmberg, M., Berg, J., Stemme, S., Ödberg, L., Rasmusson, J. and Claesson, P.M. 1997. Surface force studies of Langmuir-Blodgett cellulose films. J. Colloid Interface Sci. 186, pp. 369–381.

Hon, D. 1994. Cellulose: a random walk along its historical path. Cellulose 1, pp. 1–25.

Horton, M., Charras, G.T. and Lehenkari, P. 2002. Analysis of ligand-receptor interactions in cells by atomic force microscopy. J. Recept. Signal Transduct. Res. 22, pp. 169–190.

Hourigan, C.S. 2006. The molecular basis of coeliac disease. Clin. Exp. Med. 6, pp. 53–59.

Howland, R. and Benatar, L. 1993–1996. A practical guide to scanning probe microscopy. Park Scientific Instruments. 74 p.

Hugel, T. and Seitz, M. 2001. The study of molecular interactions by AFM force spectroscopy. Macromol. Rapid Commun. 22, pp. 989–1016.

Hutter, J.L. and Bechhoefer, J. 1993. Calibration of atomic-force microscope tips. Rev. Sci. Instrum. 64, pp. 1868–1873.

Häberle, W., Hörber, J.K.H., Ohnesorge, F., Smith, D.P.E. and Binnig, G. 1992. In situ investigations of single living cells infected by viruses. Ultramicroscopy 42–44, pp. 1161–1167.

Hörber, J.K.H. and Miles, M. 2003. Scanning probe evolution in biology. Science 302, pp. 1002–1005.

Höök, F. 1997. Development of a novel QCM technique for protein adsorption studies. Ph.D. Thesis. Göteborg, Chalmers University of Technology and Göteborg University. 60 p.

Ihalainen, P. 2004. Protein immobilization onto biofunctionalised Langmuir-Schaefer binary monolayers chemisorbed on gold. Ph.D. Thesis. Åbo: Åbo Akademi University. 53 p.

Israelachvili, J.N. 1992. Intermolecular and surface forces. 2. ed. Academic Press, London. 450 p.

Jandt, K. 2001. Atomic force microscopy of biomaterials surfaces and interfaces. Surf. Sci. 491, pp. 303–332.

Jönsson, B., Lindman, B., Holmberg, K. and Kronberg, B. 1998. Surfactants and polymers in aqueous solution. Wiley & Sons, Chichester, UK. 438 p.

Kaasgaard, T., Leidy, C., Crowe, J.H., Mouritsen, O.G. and Jørgensen, K. 2003. Temperature-controlled structure and kinetics of ripple phases in one- and two-component supported lipid bilayers. Biophys. J. 85, pp. 350–360.

Kada, G., Blayney, L., Jeyakumar, L.H., Kienberger, F., Pastushenko, V.Ph., Fleischer, S., Schindler, H., Lai, F.A. and Hinterdorfer. P. 2001. Recognition force microscopy/spectroscopy of ion channels: applications to the skeletal muscle Ca^{2+} release channel (RYR1). Ultramicroscopy 86, pp. 129–137.

Kasarda, D.D. 1980. Structure and properties of α-gliadins. Ann. Technol. Agric. 29, pp. 151–173.

Kasarda, D.D., Autran, J.-C., Lew, E.J.-L., Nimmo, C.C. and Shewry, P.R. 1983. N-terminal amino acid sequences of ω-gliadins: implications for the evolution of prolamin genes. Biochim. Biophys. Acta 747, pp. 138–150.

Kasas, S., Thomson, N.H., Smith, B.L., Hansma, H.G., Zhu, X., Guthold, M., Bustamante, C., Kool, E.T., Kashlev, M. and Hansma, P.K. 1997. *Escherichia coli* RNA polymerase activity observed using atomic force microscopy. Biochemistry 36, pp. 461–468.

Kienberger, F., Ebner, A., Gruber, H.J. and Hinterdorfer, P. 2006. Molecular recognition imaging and force spectroscopy of single molecules. Acc. Chem. Res. 39, pp. 29–36.

Kienberger, F., Kada, G., Mueller, H. and Hinterdorfer P. 2005. Single molecule studies of antibody-antigen interaction strength versus intra-molecular antigen stability. J. Mol. Biol. 347, pp. 597–606.

Kisko, K., Szilvay, G.R., Vuorimaa, E., Lemmetyinen, H., Linder, M.B., Torkkkeli, M. and Serimaa, R. 2007. Self-assembly of hydrophobin proteins HFBI and HFBII on air/water interface. Manuscript in preparation.

Kisko, K., Torkkeli, M., Vuorimaa, E., Lemmetyinen, H., Seeck, O.H., Linder, M. and Serimaa, R. 2005. Langmuir–Blodgett films of hydrophobins HFBI and HFBII. Surf. Sci. 584, pp. 35–40.

Klein, J. 1988. Surface forces with adsorbed and grafted polymers. In: Molecular conformation and dynamics of macromolecules in condensed systems (Studies in polymer science, Vol. 2). Elsevier, Amsterdam. 382 p.

Koljonen, K., Österberg, M., Johansson, L.-S. and Stenius, P. 2003. Surface chemistry and morphology of different mechanical pulps determined by ESCA and AFM. Colloids Surf. A. 228, 143–158.

Kontturi, E., Tammelin, T. and Österberg, M. 2006. Cellulose-model films and the fundamental approach. Chem. Soc. Rev. 35, pp. 1287–1304.

Kostiainen, M.A., Szilvay, G.R., Smith, D.K., Linder, M.B. and Ikkala, O. 2006. Multivalent dendrons for high-affinity adhesion of proteins to DNA. Angew. Chem. Int. Ed. 45, pp. 3538–3542.

Kroon-Batenburg, L.M.J., Leeflang, B.R., van Kuik, J.A. and Kroon, J. 2002. Interaction of mannan and xylan with cellulose microfibrils: An X-ray, NMR, and modeling study. 223rd ACS National Meeting, American Chemical Society, Washington, D.C.

Kuutti, L., Peltonen, J., Myllärinen, P., Teleman, O. and Forssell, P. 1998. AFM in studies of thermoplastic starches during ageing. Carbohydr. Polym. 37, pp. 7–12.

Kuutti, L., Peltonen, J., Pere, J. and Teleman, O. 1995. Identification and surface structure of crystalline cellulose studied by atomic force microscopy. J. Microsc. 178, pp. 1–6.

Langmuir, I. 1920. The mechanism of the surface phenomena of flotation. Trans. Faraday Soc. 15, pp. 62–75.

Langmuir, I. and Schaefer, V.J. 1938. Activities of urease and pepsin monolayers. J. Am. Chem. Soc. 60, pp. 1351–1360.

Leckband, D. 2000. Measuring the forces that control protein interactions. Annu. Rev. Biophys. Biomol. Struct. 29, pp. 1–26.

Lee, G.U., Chris, L.A. and Colton, R.J. 1994a. Direct measurements of the forces between complementary strands of DNA. Science 266, pp. 771–773.

Lee, G.U., Kidwell, D.A. and Colton, R.J. 1994b. Sensing discrete streptavidin-biotin interactions with atomic force microscopy. Langmuir 10, pp. 354–357.

Lehenkari, P.P., Charras, G.T., Nykänen, A. and Horton, M.A. 2000. Adapting atomic force microscopy for cell biology. Ultramicroscopy 82, pp. 289–295.

Lehenkari, P.P. and Horton, M.A. 1999. Single integrin molecule adhesion forces in intact cells measured by atomic force microscopy. Biochem. Biophys. Res. Commun. 259, pp. 645–650.

Lehn, J.-M. and Ball, P. 2000. Supramolecular chemistry. In: The new chemistry. Hall, N. (Ed.), Cambridge University Press, Cambridge, UK. Pp. 300–351.

Lekka, M., Laidler, P., Łabędź, M., Kulik, A.J., Lekki, J., Zając, W. and Stachura, Z. 2006. Specific detection of glycans on a plasma membrane of living cells with atomic force microscopy. Chem. Biol. 13, pp. 505–512.

Leporatti, S., Sczech, R., Riegler, H., Bruzzano, S., Storsberg, J., Loth, F., Jaeger, W., Laschewsky, A., Eichhorn, S. and Donath, E. 2005. Interaction forces between cellulose microspheres and ultrathin cellulose films monitored by

colloidal probe microscopy – effect of wet strength agents. J. Colloid Interface Sci. 281, pp. 101–111.

Li, H., Oberhauser, A.F., Fowler, S.B., Clarke, J. and Fernandez, J.M. 2000. Atomic force microscopy reveals the mechanical design of a modular protein. Proc. Natl. Acad. Sci. USA 97, pp. 6527–6531.

Li, W., Dobraszczyk, B.J. and Wilde, P.J. 2004. Surface properties and locations of gluten proteins and lipids revealed using confocal scanning laser microscopy in bread dough. J. Cereal Sci. 39, pp. 403–411.

Lifshitz, E.M. 1956. The theory of molecular attractive forces between solids. Sov. Phys. JETP 2, pp. 73–83.

Linder, M., Qiao, M., Laumen, F., Selber, K., Hyytiä, T., Nakari-Setälä, T. and Penttilä, M. 2004. Efficient purification of recombinant proteins using hydrophobins as tags in surfactant-based two-phase systems. Biochemistry 43, pp. 11873–11882.

Linder, M., Selber, K., Nakari-Setälä, T., Qiao, M., Kula, M.-R. and Penttilä, M. 2001. The hydrophobins HFBI and HFBII from *Trichoderma reesei* showing efficient interactions with nonionic surfactants in aqueous two-phase systems. Biomacromolecules 2, pp. 511–517.

Linder, M., Szilvay, G., Nakari-Setälä, T. and Penttilä, M. 2005. Hydrophobins: the protein-amphiphiles of filamentous fungi. FEMS Microbiol. Rev. 29, pp. 877–896.

Linder, M., Szilvay, G., Nakari-Setälä, T., Söderlund, H. and Penttilä, M. 2002. Surface adhesion of fusion proteins containing the hydrophobins HFBI and HFBII from *Trichoderma reesei*. Protein Sci. 11, pp. 2257–2266.

Lindsay, S.M., Nagahara, L.A., Thundat, T., Knipping, U., Rill, R.L., Drake, B., Prater, C.B., Weisenhorn, A.L., Gould, S.A. and Hansma, P.K. 1989. STM and AFM images of nucleosome DNA under water. J. Biomol. Struct. Dyn. 7, pp. 279–287.

Litvinov, R.I., Shuman, H., Bennett, J.S. and Weisel, J.W. 2002. Binding strength and activation state of single fibrinogen-integrin pairs on living cells. Proc. Natl. Acad. Sci. USA 99, pp. 7426–7431.

Liu, W., Christian, G.K., Zhang, Z. and Fryer, P.J. 2006. Direct measurement of the force required to disrupt and remove fouling deposits of whey protein concentrate. Int. Dairy J. 16, pp. 164–172.

Lum, K., Chandler, D. and Weeks, J.D. 1999. Hydrophobicity at small and large length scales. J. Phys. Chem. B 103, pp. 4570–4577.

Lushnikov, A.Y., Potaman, V.N., Oussatcheva, E.A., Sinden, R.R. and Lyubchenko, Y.L. 2006. DNA strand arrangement within the SfiI-DNA complex: atomic force microscopy analysis. Biochemistry 45, pp. 152–158.

Lyubchenko, Y.L. 2004. DNA structure and dynamics: an atomic force microscopy study. Cell Biochem. Biophys. 41, pp. 75–98.

Marčelja, S. and Radić, N. 1976. Repulsion of interfaces due to boundary water. Chem. Phys. Lett. 42, pp. 129–130.

Marčelja, S., Israelachvili, J.N. and Wennerström, H. 1997. Hydration in electrical double layers. Nature 385, pp. 689–690.

Marchessault, R.H., Settineri, W. and Winter, W. 1967. Crystallization of xylan in the presence of cellulose. Tappi 50, pp. 55–59.

Matzke, R., Jacobson, K. and Radmacher, M. 2001. Direct, high-resolution measurement of furrow stiffening during division of adherent cells. Nat. Cell Biol. 3, pp. 607–610.

Maximova, N., Österberg, M., Koljonen, K. and Stenius, P. 2001. Lignin adsorption on cellulose fibre surfaces: Effect on surface chemistry, surface morphology and paper strength. Cellulose 8, pp. 113–125.

McKendry, R., Theoclitou, M.-E., Rayment, T. and Abell, C. 1998. Chiral discrimination by chemical force microscopy. Nature 391, pp. 566–568.

Meyer, E.E., Rosenberg, K.J. and Israelachvili, J. 2006. Recent progress in understanding hydrophobic interactions. Proc. Natl. Acad. Sci. USA 103, pp. 15739–15746.

Mills, E.N., Huang, L., Noel, T.R., Gunning, A.P. and Morris, V.J. 2001. Formation of thermally induced aggregates of the soya globulin β-conglycinin. Biochim. Biophys. Acta 1547, pp. 339–350.

Moll, D., Huber, C., Schlegel, B., Pum, D., Sleytr, U.B. and Sára, M. 2002. S-layer-streptavidin fusion proteins as template for nanopatterned molecular arrays. Proc. Natl. Acad. Sci. USA 99, pp. 14646–14651.

Mora, F., Ruel, K., Comtat, J. and Joseleau, J.-P. 1986. Aspect of native and redeposited xylans at the surface of cellulose microfibrils. Holzforschung 40, pp. 85–91.

Morris, V.J., Gunning, A.P., Kirby, A.R., Round, A., Waldron, K, and Ng, A. 1997. Atomic force microscopy of plant cell walls, plant cell wall polysaccharides and gels. Int. J. Biol. Macromol. 21, pp. 61–66.

Mou, J., Czajkowsky, D.M., Sheng, S., Ho, R. and Shao, Z. 1996. High resolution surface structure of *E. coli* GroES oligomer by atomic force microscopy. FEBS Lett. 381, pp. 161–164.

Moy, V.T., Florin, E.-L. and Gaub, H.E. 1994. Intermolecular forces and energies between ligands and receptors. Science 266, pp. 257–259.

Müller, D.J., Baumeister, W. and Engel, A. 1996. Conformational change of the hexagonally packed intermediate layer of *Deinococcus radiodurans* monitored by atomic force microscopy. J. Bacteriol. 178, pp. 3025–3030.

Müller, D.J., Baumeister, W. and Engel, A. 1999. Controlled unzipping of a bacterial surface layer with atomic force microscopy. Proc. Natl. Acad. Sci. USA 96, pp. 13170–13174.

Müller, D.J. and Engel, A. 1999. Voltage and pH-induced channel closure of porin OmpF visualized by atomic force microscopy. J. Mol. Biol. 285, pp. 1347–1351.

Müller, D.J., Engel, A., Matthey, U., Meier, T., Dimroth, P. and Suda, K. 2003. Observing membrane protein diffusion at subnanometer resolution. J. Mol. Biol. 327, pp. 925–930.

Müller, D.J., Kessler, M., Oesterhelt, F., Möller, C., Oesterhelt, D. and Gaub, H. 2002. Stability of bacteriorhodopsin α-helices and loops analyzed by single-molecule force spectroscopy. Biophys. J. 83, pp. 3578–3588.

Müller, D.J., Schabert, F.A., Büldt, G. and Engel, A. 1995. Imaging purple membranes in aqueous solutions at sub-nanometer resolution by atomic force microscopy. Biophys J. 68, pp. 1681–1686.

Müller, S. and Wieser, H. 1995. The location of disulphide bonds in α-type gliadins. J. Cereal Sci. 22, pp. 21–27.

Nakari-Setälä, T. 1995. Highly expressed *Trichoderma reesei* genes. Cloning, characterization and use in protein production on glucose-containing media. Ph.D. Thesis. VTT, Espoo: VTT Publications 254. 94 p. ISBN 951-38-4792-6.

Nakari-Setälä, T., Aro, N., Ilmen, M., Munoz, G., Kalkkinen, N. and Penttilä, M. 1997. Differential expression of the vegetative and spore-bound hydrophobins of *Trichoderma reesei*. Cloning and characterization of the *hfb2* gene. Eur. J Biochem. 248, pp. 415–423.

Neuman, R.D. Berg, J.M. and Claesson, P.M. 1993. Direct measurement of surface forces in papermaking and paper coating systems. Nordic Pulp Paper Res. J. 8, pp. 96–104.

Niemi, H., Paulapuro, H. and Mahlberg, R. 2002. Review: Application of scanning probe microscopy to wood, fibre and paper research. Paperi ja Puu – Paper and Timber 84, pp. 389–406.

Ninham, B.W. and Parsegian, V.A. 1971. Electrostatic potential between surfaces bearing ionizable groups in ionic equilibrium with physiologic saline solution. J. Theor. Biol. 31, pp. 405–428.

Notley, S.M., Eriksson, M., Wågberg, L., Beck, S. and Gray, D.G. 2006. Surface forces measurements of spin-coated cellulose thin films with different crystallinity. Langmuir 22, pp. 3154–3160.

Oberhauser, A.F., Marszalek, P.E., Erickson, H.P. and Fernandez, J.M. 1998. The molecular elasticity of the extracellular matrix protein tenascin. Nature 393, pp. 181–185.

Oberleithner, H., Giebisch, G. and Geibel, J. 1993. Imaging the lamellipodium of migrating epithelial cells in vivo by atomic force microscopy. Pflugers Arch. 425, pp. 506–510.

Oesterhelt, F., Oesterhelt, D., Pfeiffer, M., Engel, A., Gaub, H.J. and Müller, D.J. 2000. Unfolding pathways of individual bacteriorhodopsins. Science 288, pp. 143–146.

Ohlsson, P.-Å., Tjärnhage, T., Herbai, E., Löfås, S. and Puu, G. 1995. Liposome and proteoliposome fusion onto solid substrates, studied using atomic force microscopy, quartz crystal microbalance and surface plasmon resonance. Biological activities of incorporated components. Bioelectrochem. Bioenerg. 38, pp. 137–148.

Osada, T., Itoh, A. and Ikai, A. 2003. Mapping of the receptor-associated protein (RAP) binding proteins on living fibroblast cells using an atomic force microscope. Ultramicroscopy 97, pp. 353–357.

Paige, M.F., Lin, A.C. and Goh, M.C. 2002. Real-time enzymatic biodegradation of collagen fibrils monitored by atomic force microscopy. Int. Biodeter. Biodegr. 50, pp. 1–10.

Park, J.W. and Lee, G.U. 2006. Properties of mixed lipid monolayers assembled on hydrophobic surfaces through vesicle adsorption. Langmuir 22, pp. 5057–5063.

Parker, J.L., Claesson, P.M. and Attard, P. 1994. Bubbles, cavities, and the long-ranged attraction between hydrophobic surfaces. J. Phys. Chem. 98, pp. 8468–8480.

Peltonen, J., Järn, M., Areva, S., Linden, M. and Rosenholm, J.B. 2004. Topographical parameters for specifying a three-dimensional surface. Langmuir 20, pp. 9428–9431.

Raab, A., Han, W., Badt, D., Smith-Gill, S.J., Lindsay, S.M., Schindler, H. and Hinterdorfer, P. 1999. Antibody recognition imaging by force microscopy. Nature Biotech. 17, pp. 901–905.

Rabinovich, Ya.I., Derjaguin, B.V. and Churaev, N.V. 1982. Direct measurements of long-range surface forces in gas and liquid media. Adv. Colloid Interface Sci. 16, pp. 63–78.

Radmacher, M., Cleveland, J.P., Fritz, M., Hansma, H.G. and Hansma, P.K. 1994a. Mapping interaction forces with the atomic force microscope. Biophys. J. 66, pp. 2159–2165.

Radmacher, M., Fritz, M., Hansma, H.G. and Hansma, P.K. 1994b. Direct observation of enzyme activity with the atomic force microscope. Science 265, pp. 1577–1579.

Raiteri, R., Grattarola, M., Butt, H.-J. and Skládal, P. 2001. Micromechanical cantilever-based biosensors. Sens. Actuators B 79, pp. 115–126.

Reviakine, I., Bergsma-Schutter, W. and Brisson, A. 1998. Growth of protein 2-D crystals on supported planar lipid bilayers imaged *in situ* by AFM. J. Struct. Biol. 121, pp. 356–361.

Richards, F.M. 1977. Areas, volumes, packing and protein structure. Ann. Rev. Biophys. Bioeng. 6, pp. 151–176.

Ridout, M.J., Gunning, A.P., Parker, M.L., Wilson, R.H. and Morris, V.J. 2002. Using AFM to image the internal structure of starch granules. Carbohydr. Polym. 50, pp. 123–132.

Rief, M., Gautel, M., Oesterhelt, F., Fernandez, J.M. and Gaub, H.E. 1997a. Reversible unfolding of individual titin immunoglobulin domains of AFM. Science 276, pp. 1109–1112.

Rief, M., Oesterhelt, F., Heymann, B. and Gaub, H.E. 1997b. Single molecule force spectroscopy on polysaccharides by atomic force microscopy. Science 275, pp. 1295–1297.

Rief, M., Pascual, J., Saraste, M. and Gaub, H.E. 1999. Single molecule force spectroscopy of spectrin repeats: low unfolding forces in helix bundles. J. Mol. Biol. 286, pp. 553–561.

Roberts, G.G. (Ed.). 1990. Langmuir-Blodgett films. Plenum Press, New York. 444 p.

Rodahl, M., Höök, F., Krozer, A., Brzezinski, P. and Kasemo, B. 1995. Quartz crystal microbalance setup for frequency and Q-factor measurements in gaseous and liquid environments. Rev. Sci. Instrum. 66, pp. 3924–3930.

Rousseau, D. 2006. On the porous mesostructure of milk chocolate viewed with atomic force microscopy. LWT Food Sci. Technol. 39, pp. 852–860.

Rutland, M.W., Carambassis, A., Willing, G.A. and Neuman, R.D. 1997. Surface force measurements between cellulose surfaces using scanning probe microscopy. Colloids Surfaces A: Physicochem. Eng. Aspects 123–124, pp. 369–374.

Sader, J.E., Chon, J.W.M. and Mulvaney, P. 1999. Calibration of rectangular atomic force microscope cantilevers. Rev. Sci. Instrum. 70, pp. 3967–3969.

Salmén, L. and Olsson, A.-M. 1998. Interaction between hemicelluloses, lignin and cellulose: structure-property relationships. J. Pulp Paper Sci. 24, pp. 99–102.

Salmi, J., Österberg, M. and Laine. J. 2006. The effect of cationic polyelectrolyte complexes on the interactions between cellulose surfaces. Colloids Surf. A, Physicochem. Eng. Aspects, in press.

Salmi, J., Österberg, M., Stenius, P. and Laine, J. 2007. Surface forces between cellulose surfaces in cationic polyelectrolyte solutions: The effect of polymer molecular weight and charge density. Nord. Pulp Paper Res. J., in press.

Santos, N.C. and Castanho, M.A. 2004. An overview of the biophysical applications of atomic force microscopy. Biophys. Chem. 107, pp. 133–149.

Sarlin, T., Nakari-Setälä, T., Linder, M., Penttilä, M. and Haikara, A. 2005. Fungal hydrophobins as predictors of the gushing activity of malt. J. Inst. Brew. 111, pp. 105–111.

Schabert, F.A., Henn, C. and Engel, A. 1995. Native *Escherichia coli* OmpF porin surfaces probed by atomic force microscopy. Science 268, pp. 92–94.

Scheuring, S. 2000. Atomic force and electron microscopic analysis of membrane channels and transporters. Ph.D. Thesis. Basel: University of Basel. 115 p.

Scheuring, S., Lévy, D. and Rigaud, J.-L. 2005. Watching the components of photosynthetic bacterial membranes and their in situ organisation by atomic force microscopy. Biochim. Biophys. Acta. 1712, pp. 109–127.

Scheuring, S., Müller, D.J., Ringler, P., Heymann, J.B and Engel, A. 1999. Imaging streptavidin 2D crystals on biotinylated lipid monolayers at high resolution with the atomic force microscope. J. Microsc. 193, pp. 28–35.

Scheuring, S., Ringler, P., Borgnia, M., Stahlberg, H., Müller, D.J., Agre, P. and Engel, A. 1999. High resolution AFM topographs of the *Escherichia coli* water channel aquaporin Z. EMBO J. 18, pp. 4981–4987.

Scheuring, S., Seguin, J., Marco, S., Lévy, D., Robert, B. and Rigaud, J.-L. 2003. Nanodissection and high-resolution imaging of the *Rhodopseudomonas viridis* photosynthetic core complex in native membranes by AFM. Proc. Natl. Acad. Sci. USA. 100, pp. 1690–1693.

Schoenenberger, C.-A. and Hoh, J.H. 1994. Slow cellular dynamics in MDCK and R5 cells monitored by time-lapse atomic force microscopy. Biophys. J. 67, pp. 929–936.

Scholtmeijer, K., Janssen, M.I., Gerssen, B., de Vocht, M.L., van Leeuwen, B.M., van Kooten, T.G., Wösten, H.A. and Wessels, J.G. 2002. Surface modifications created by using engineered hydrophobins. Appl. Environ. Microbiol. 6, pp. 1367–1373.

Schönberg, C., Oksanen, T., Suurnäkki, A., Kettunen, H. and Buchert, J. 2001. The importance of xylan for the strength properties of spruce kraft pulp fibres. Holzforschung 55, pp. 639–644.

Schwesinger, F., Ros, R., Strunz, T., Anselmetti, D., Güntherodt, H.-J., Honegger, A., Jermutus, L., Tiefenauer, L. and Plückthun, A. 2000. Unbinding forces of single antibody-antigen complexes correlate with their thermal dissociation rates. Proc. Natl. Acad. Sci. USA 97, 9972–9977.

Seelert, H., Poetsch, A., Dencher, N.A., Engel, A., Stahlberg, H. and Müller, D.J. 2000. Proton-powered turbine of a plant motor. Nature 405, pp. 418–419.

Sheng, S. and Shao, Z. 2002. Cryo-atomic force microscopy. Methods Cell Biol. 68, pp. 243–256.

Shewry, P.R. and Tatham, A.S. 1997. Disulphide bonds in wheat gluten proteins. J. Cereal Sci. 25, 207–227.

Shewry, P.R., Miles, M.J. and Tatham, A.S. 1994. The prolamin storage proteins of wheat and related cereals. Prog. Biophys. Molec. Biol. 61, pp. 37–59.

Shewry, P.R., Miles, M.J., Thomson, N.H. and Tatham, A.S. 1997. Scanning probe microscopies – applications in cereal science. Cereal Chem. 74, pp. 193–199.

Simola, J., Malkavaara, P., Alén, R. and Peltonen, J. 2000. Scanning probe microscopy of pine and birch kraft pulp fibres. Polymer 41, pp. 2121–2126.

Simola-Gustafsson, J., Hortling, B. and Peltonen, J. 2001. Scanning probe microscopy and enhanced data analysis on lignin and elemental-chlorine-free or oxygen-delignified pine kraft pulp. Colloid Polym. Sci. 279, pp. 223–231.

Singh, H. and MacRitchie, F. 2004. Changes in proteins induced by heating gluten dispersions at high temperature. J. Cereal Sci. 39, pp. 297–301.

Sjöström, E. 1993. Wood chemistry: fundamentals and applications. 2. ed. Academic Press, San Diego, CA. 293 p.

Solletti, J.M., Botreau, M., Sommer, F., Minh Duc, T. and Celio, M.R. 1996. Characterization of mixed miscible and nonmiscible phospholipid Langmuir–Blodgett films by atomic force microscopy. J. Vac. Sci. Technol. B 14, pp. 1492–1497.

Søndergaard, I., Jensen, K. and Krath, B.N. 1994. Classification of wheat varieties by isoelectric focusing patterns of gliadins and neural network. Electrophoresis 15, pp. 584–588.

SPIP, The Scanning probe image processor. 1998–2006. User's and reference guide, version 4.2. Image Metrology. 325 p.

Steltenkamp, S., Müller, M.M., Deserno, M., Hennesthal, C., Steinem, C. and Janshoff, A. 2006. Mechanical properties of pore-spanning lipid bilayers probed by atomic force microscopy. Biophys. J. 91, pp. 217–226.

Stillinger, F.H. 1973. Structure in aqueous solutions of nonpolar solutes from the standpoint of scaled-particle theory. J. Solution Chem. 2, pp. 141–158.

Sugiyama, J., Vuong, R. and Chanzy, H. 1991. Electron diffraction study on the two crystalline phases occurring in native cellulose from an algal cell wall. Macromolecules 24, pp. 4168–4175.

Szilvay, G.R., Nakari-Setälä, T. and Linder, M.B. 2006. Behavior of *Trichoderma reesei* hydrophobins in solution: interactions, dynamics, and multimer formation. Biochemistry 45, pp. 8590–8598.

Talbot, N.J. 1997. Fungal biology: Growing into the air. Curr. Biol. 7, pp. R78–R81.

Talbot, N.J. 1999. Fungal biology. Coming up for air and sporulation. Nature 398, pp. 295–296.

Tamayo, J. and Miles, M. 2002. Scanning probe microscopy for chromosomal research. Arch. Histol. Cytol. 65, pp. 369–376.

Tatham, A.S., Drake, A.F. and Shewry, P.R. 1989. Conformational studies of a synthetic peptide corresponding to the repeat motif of a C hordein. Biochem. J. 259, pp. 471–476.

Tatham, A.S., Miflin, B.J. and Shewry, P.R. 1985. The beta-turn conformation in wheat gluten proteins: Relationship to gluten elasticity. Cereal Chem. 62, pp. 405–412.

Tatham, A.S. and Shewry, P.R. 1985. The conformation of wheat gluten proteins. The secondary structures and thermal stabilities of α-, β-, γ- and ω-gliadins. J. Cereal Sci. 3, pp. 103–113.

Tatham, A.S. and Shewry, P.R. 1995. The S-poor prolamins of wheat, barley and rye. J. Cereal Sci. 22, pp. 1–16.

Tatham, A.S. and Shewry, P.R. 2000. Elastomeric proteins: biological roles, structures and mechanisms. Trends Biochem. Sci. 25, pp. 567–571.

Tatham, A.S., Shewry, P.R. and Belton, P.S. 1990. Structural studies of cereal prolamins, including wheat gluten. In: Advances in cereal science and technology. Volume X, Amer. Assn. of Cereal Chemists. Pp. 1–78.

Teleman, A., Larsson, P.T. and Iversen, T. 2001. On the accessibility and structure of xylan in birch kraft pulp. Cellulose 8, pp. 209–215.

Thompson, M.T., Berg, M.C., Tobias, I.S., Lichter, J.A., Rubner, M.F. and Van Vliet, K.J. 2006. Biochemical functionalization of polymeric cell substrata can alter mechanical compliance. Biomacromolecules 7, pp. 1990–1995.

Thomson, N.H., Kasas, S., Riederer, B.M., Catsicas, S., Dietler, G., Kulik, A.J. and Forró, L. 2003. Large fluctuations in the disassembly rate of microtubules revealed by atomic force microscopy. Ultramicroscopy 97, pp. 239–247.

Thomson, N.H., Miles, M.J., Ring, S.G., Shewry, P.R. and Tatham, A.S. 1994. Real-time imaging of enzymatic degradation of starch granules by atomic force microscopy. J. Vac. Sci. Technol. B 12, pp. 1565–1568.

Torii, A., Sasaki, M., Hane, K. and Okuma, S. 1996. A method for determining the spring constant of cantilevers for scanning probe microscopy. Meas. Sci. Technol. 7, pp. 179–184.

Torkkeli, M., Serimaa, R., Ikkala, O. and Linder, M. 2002. Aggregation and self-assembly of hydrophobins from *Trichoderma reesei*: low-resolution structural models. Biophys. J. 83, pp. 2240–2247.

Tromas, C., Rojo, J., de la Fuente, J.M., Barrientos, A.G., García, R. and Penadés, S. 2001. Adhesion forces between LewisX determinant antigens as measured by atomic force microscopy. Angew. Chem. Int. Ed. 40, 3052–3055.

Tucker, S.L. and Talbot, N.J. 2001. Surface attachment and pre-penetration stage development by plant pathogenic fungi. Annu. Rev. Phytopathol. 39, pp. 385–417.

Urisu, T., Rahman, M., Uno, H., Tero, R. and Nonogaki, Y. 2005. Formation of high-resistance supported lipid bilayer on the surface of a silicon substrate with microelectrodes. Nanomedicine 1, pp. 317–322.

van Lonkhuijsen, H.J., Hamer, R.J. and Schreuder, C. 1992. Influence of specific gliadins on the breadmaking quality of wheat. Cereal Chem. 69, pp. 174–177.

Vansteenkiste, S.O., Davies, M.C., Roberts, C.J., Tendler, S.J.B. and Williams, P. 1998. Scanning probe microscopy of biomedical interfaces. Prog. Surf. Sci. 57, pp. 95–136.

Verwey, E.J.W. and Overbeek, J.Th.G. 1948. Theory of stability of lyophobic colloids. Elsevier, Amsterdam. 205 p.

Viitala, T., Vikholm, I. and Peltonen, J. 2000. Protein immobilization to a partially cross-linked organic monolayer. Langmuir 16, pp. 4953–4961.

Vikholm, I., Györvary, E. and Peltonen, J. 1996. Incorporation of lipid-tagged single-chain antibodies into lipid monolayers and the interaction with antigen. Langmuir 12, pp. 3276–3281.

Vikholm, I. and Peltonen, J. 1996. Layer formation of a lipid-tagged single-chain antibody and the interaction with antigen. Thin Solid Films 284–285, pp. 924–926.

Vikholm, I., Peltonen, J. and Teleman, O. 1995. Atomic force microscope of lipid layers spread from vesicle suspensions. Biochim. Biophys. Acta 1233, pp. 111–117.

Wallqvist, A., Covell, D.G. and Thirumalai, D. 1998. Hydrophobic interactions in aqueous urea solutions with implications for the mechanism of protein denaturation. J. Am. Chem. Soc. 120, pp. 427–428.

Wang, X., Graveland-Bikker, J.F., de Kruif, C.G. and Robillard, G.T. 2004. Oligomerization of hydrophobin SC3 in solution: from soluble state to self-assembly. Protein Sci. 13, pp. 810–821.

Wannerberger, L., Nylander, T., Eliasson A.-C., Tatham, A.S., Fido, R.J., Miles, M.J. and McMaster, T.J. 1997. Interaction between α-gliadin layers. J. Cereal Sci. 26, 1–13.

Weegels, P.L., Marseille, J.P., Bosveld, P. and Hamer, R.J. 1994. Large-scale separation of gliadins and their bread-making quality. J. Cereal Sci. 20, pp. 253–264.

Weisel, J.W., Shuman, H. and Litvinov, R.I. 2003. Protein-protein unbinding induced by force: single-molecule studies. Curr. Opin. Struct. Biol. 13, pp. 227–235.

Weisenhorn, A.L. Egger, M., Ohnesorge, F., Gould, S.A.C., Heyn, S.-P., Hansma, H.G., Sinsheimer, R.L., Gaub, H.E. and Hansma, P.K. 1991. Molecular-resolution images of Langmuir-Blodgett films and DNA by atomic force microscopy. Langmuir 7, pp. 8–12.

Weisenhorn, A.L., Gaub, H.E., Hansma, H.G., Sinsheimer, R.L., Kelderman, G.L. and Hansma, P.K. 1990. Imaging single-stranded DNA, antigen-antibody

reaction and polymerized Langmuir-Blodgett films with an atomic force microscope. Scanning Microsc. 4, pp. 511–516.

Weisenhorn, A.L., Hansma, P.K., Albrecht, T.R. and Quate, C.F. 1989. Forces in atomic force microscopy in air and water. Appl. Phys. Lett. 54, pp. 2651–2653.

Wellner, N., Belton, P.S. and Tatham, A.S. 1996. Fourier transform IR spectroscopic study of hydration-induced structure changes in the solid state of ω-gliadins. Biochem. J. 319, 741–747.

Wessels, J., De Vries, O., Asgeirsdottir, S.A. and Schuren, F. 1991. Hydrophobin genes involved in formation of aerial hyphae and fruit bodies in *Schizophyllum*. Plant Cell 3, pp. 793–799.

Wessels, J.G.H. 1994. Developmental regulation of fungal cell wall formation. Annu. Rev. Phytopathol. 32, pp. 413–437.

Wessels, J.G.H. 1996. Fungal hydrophobins: proteins that function at an interface. Trends Plant Sci. 1, pp. 9–15.

Wetzer, B., Pum, D. and Sleytr, U.B. 1997. S-Layer stabilized solid supported lipid bilayers. J. Struct. Biol. 119, pp. 123–128.

Whangbo, M.H., Bar, G. and Brandsch, R. 1998. Qualitative relationships describing height and phase images of tapping mode atomic force microscopy. An application to micro-contact-printed patterned self-assembled monolayers. Appl. Phys. A 66, pp. S1267–S1270.

Whiteford, J.R. and Spanu, P.D. 2002. Hydrophobins and the interactions between fungi and plants. Mol. Plant Pathol. 3, pp. 391–400.

Whitesides, G.M. and Boncheva, M. 2002. Beyond molecules: Self-assembly of mesoscopic and macroscopic components. Proc. Natl. Acad. Sci. USA 99, pp. 4769–4774.

Whitesides, G.M. and Grzybowski, B. 2002. Self-assembly in all scales. Science 295, pp. 2418–2421.

Wieser, H. 2007. Chemistry of gluten proteins. Food Microbiol. 24, pp. 115–119.

Willemsen, O.H., Snel, M.M.E., van der Werf, K.O., De Grooth, B.G., Greve, J., Hinterdorfer, P., Gruber, H.J., Schindler, H., van Kooyk, Y. and Figdor, C.G. 1998. Simultaneous height and adhesion imaging of antibody-antigen interactions by atomic force microscopy. Biophys. J. 75, pp. 2220–2228.

Withers, J.R. and Aston, D.E. 2006. Nanomechanical measurements with AFM in the elastic limit. Adv. Colloid Interface Sci. 120, pp. 57–67.

Woodward, N.C., Wilde, P.J., Mackie, A.R., Gunning, A.P., Gunning, P.A. and Morris, V.J. 2004. Effect of processing on the displacement of whey proteins: applying the orogenic model to a real system. J. Agric. Food Chem. 52, pp. 1287–1292.

Wösten, H., De Vries, O. and Wessels, J. 1993. Interfacial self-assembly of a fungal hydrophobin into a hydrophobic rodlet layer. Plant Cell 5, pp. 1567–1574.

Wösten, H.A. 2001. Hydrophobins: multipurpose proteins. Annu. Rev. Microbiol. 55, pp. 625–646.

Wösten, H.A. and de Vocht, M.L. 2000. Hydrophobins, the fungal coat unravelled. Biochim. Biophys. Acta. 1469, pp. 79–86.

Wösten, H.A., Schuren, F.H. and Wessels, J.G. 1994. Interfacial self-assembly of a hydrophobin into an amphipathic protein membrane mediates fungal attachment to hydrophobic surfaces. EMBO J. 13, pp. 5848–5854.

Wösten, H.A., van Wetter, M.A., Lugones, L.G., van der Mei, H.C., Busscher, H.J. and Wessels, J.G. 1999. How a fungus escapes the water to grow into the air. Curr. Biol. 9, pp. 85–88.

Ye, J.S., Ottova, A., Tien, H.T. and Sheu, F.S. 2003. Nanostructured platinum-lipid bilayer composite as biosensor. Bioelectrochemistry 59, pp. 65–72.

Yllner, S. and Enström, B. 1956. Adsorption of xylan on cellulose fibers during the sulfate cook. I. Svensk Papperstidn. 59, pp. 229–232.

Zasadzinski, J.A.N., Helm, C.A., Longo, M.L., Weisenhorn, A.L., Gould, S.A.C. and Hansma, P.K. 1991. Atomic force microscopy of hydrated phosphatidylethanolamine bilayers. Biophys. J. 59, pp. 755–760.

Zauscher, S. and Klingenberg, D.J. 2000. Normal forces between cellulose surfaces measured with colloidal probe microscopy. J. Colloid Interface Sci. 229, pp. 497–510.

Zhong, Q., Inniss, D., Kjoller, K. and Elings, V.B. 1993. Fractured polymer/silica fiber surface studied by tapping mode atomic force microscopy. Surf. Sci. 290, pp. L688–L692.

Zlatanova, J., Lindsay, S.M. and Leuba, S.H. 2000. Single molecule force spectroscopy in biology using the atomic force microscope. Prog. Biophys. Mol. Biol. 74, pp. 37–61.

Åkerholm, M. and Salmén, L. 2001. Interactions between wood polymers studied by dynamic FT-IR spectroscopy. Polymer 42, pp. 963–969.

Örnebro, J., Nylander, T. and Eliasson, A.-C. 2000. Interfacial behaviour of wheat proteins. J. Cereal Sci. 31, pp. 195–221.

Örnebro, J., Wahlgren, M., Eliasson A.-C., Fido, R.J. and Tatham, A.S. 1999. Adsorption of α-, β-, γ- and ω-gliadins onto hydrophobic surfaces. J. Cereal Sci. 30, pp. 105–114.

Österberg, M. 2000a. On the interactions in cellulose systems: Surface forces and adsorption. Ph.D. Thesis. Stockholm: Royal Institute of Technology. 63 p.

Österberg, M. and Claesson, P.M. 2000. Interactions between cellulose surfaces: effect of solution pH. J. Adhesion Sci. Technol. 14, pp. 603–618.

Österberg, M., Laine, J., Stenius, P., Kumpulainen, A. and Claesson, P.M. 2001. Forces between xylan-coated surfaces: Effect of polymer charge density and background electrolyte. J. Colloid Interface Sci. 242, pp. 59–66.

Österberg, M., Schmidt, U. and Jääskeläinen. A.-S. 2006. Combining confocal Raman spectroscopy and atomic force microscopy to study wood extractives on cellulose surfaces. Colloids Surf. A, Physicochem. Eng. Aspects 291, pp. 197–201.

Appendix A: Experimental details of the cellulose-xylan work (section 3.1.2)

Materials

The cellulose used in cellulose-xylan interaction measurements with varying electrolyte (NaCl) concentrations were the same cellulose beads by Kanebo Co. (Japan) as those described in Publication I and section 2.1.1. The xylan was also the same commercial birch xylan supplied by Roth used in Publication I and also described in section 2.1.1. The reference solution was 1 mM NaCl, pH 10, and varying NaCl concentrations in 100 mg/ml xylan, pH 10 were 1, 10 and 100 mM. NaCl, HCl, and NaOH were all of analytical grade.

Sample preparation

Glueing of cellulose beads to cantilevers and glass supports was performed as described in Publication I. Cantilevers were calibrated by the thermal method (Hutter and Bechhoefer, 1993) prior to the glueing step. The cantilevers and sample supports with cellulose beads were freshly made and kept dry in a desiccator before use. Xylan was dissolved in alkali (NaOH), and diluted to the desired concentration (100 mg/ml) with certain electrolyte concentrations (1, 10 and 100 mM NaCl) at pH 10. New samples and solutions were prepared prior to force measurements.

Force measurements

The force measurements were performed by the colloidal probe technique (Ducker *et al*., 1991) using a NanoScope III Multimode AFM (Digital Instruments /Veeco, CA) equipped with a fluid cell and a scanner E (vertical engagement), using an O-ring. Based on the phenomena observed in previous measurement series, cellulose surfaces were allowed to equilibriate and to swell in water overnight and in reference solution (1 mM NaCl, pH 10) for 2 hours before force measurements. Cellulose-cellulose interaction forces were then measured in the reference solution and in xylan solutions (100 mg/ml) with varying NaCl concentrations (1, 10 and 100 mM). All measurements were performed at pH 10 in order to keep the xylan soluble. After changing the

solution in the measurement chamber, the system was allowed to stabilize for 3 hours before further measurements. Different loading forces were used (the sensitivity value from the constant compliance of force curves with higher loading force) and the time gap between consecutive force curves was 5 min. The force curves were obtained from slightly different areas still staying in the central area of the cellulose beads.

Data analysis

The data analysis included conversion of the raw data in NanoScopeIII format into ASCII by Scanning Probe Image Processor (SPIP, Image Metrology, Denmark) and further handling in Excel. The handling of the force curves was carried out as described in Publication I.

References

Ducker, W.A., Senden, T.J. and Pashley, R.M. 1991. Direct measurement of colloidal forces using an atomic force microscope. Nature 353, pp. 239–241.

Hutter, J.L. and Bechhoefer, J. 1993. Calibration of atomic-force microscope tips. Rev. Sci. Instrum. 64, pp. 1868–1873.

Appendices I–V of this publication are not included in the electronic version. Please order the printed version to get the complete publication (http://www.vtt.fi/inf/pdf/)

Series title, number and
report code of publication

VTT Publications 637
VTT-PUBS-637

Author(s)
Paananen, Arja

Title

On the interactions and interfacial behaviour of biopolymers
An AFM study

Abstract

Surface forces and interactions are a key issue in colloid and surface science, including biopolymer systems. Covalent and ionic bonds determine the structure and composition of materials, but the weaker non-covalent interactions define their functions. This thesis deals with the surface forces and interactions occurring between biopolymer surfaces and affecting the self-assembly and interfacial behaviour of biopolymers. The research was aimed at deepening the understanding of molecular interactions and the nature and strength of surface forces in the studied biopolymer systems. The main research tool was atomic force microscopy (AFM). This technique allows imaging of the sample topography in either gas or liquid environments at high resolution. Data on intra- and intermolecular interactions can also be obtained. Interesting phenomena revealed by AFM were supported and confirmed by other relevant surface analytical techniques.

The nanomechanical force measurements focused on interactions relevant in papermaking, i.e. between cellulose and xylan, and food technology, i.e. between gliadins (wheat gluten proteins). In the cellulose-xylan interaction work the colloidal probe technique was exploited by attaching cellulose beads to the tip and to the sample surface. The interaction between these beads was measured in different xylan solutions. The main result of the cellulosic systems provided a new perspective on the role of xylan in papermaking. It has been reported previously that the adsorption of xylan increases paper strength and that this is due to formation of hydrogen bonds. Our results indicate that the increase in paper strength cannot originate from such bonds in wet paper, but must be due to effects of xylan on fibre bonds during drying of paper.

The viscous and elastic properties of gliadins and glutenins facilitate the production of bread, pasta and many other food products from wheat flour. Gliadin proteins (α- and ω-gliadins) were attached to both the tip and the sample surfaces, and the interaction forces between monomeric gliadins (α-α, ω-ω, and α-ω) were measured. On the basis of the nanomechanical force measurements, different roles of different types of gliadins were proposed: whereas ω-gliadins still have a compact structure and are responsible for the viscous flow, α-gliadins have already started to participate in forming the network in dough. This may provide a new viewpoint in understanding the interfacial properties of gliadins in relation to baking.

The studies of interfacial behaviour of biopolymers focused on hydrophobins, which are very surface active proteins. Hydrophobins are amphiphilic proteins which self-assemble due to the interplay of various surface forces and interactions in solution and at interfaces. Films of Class II hydrophobins, HFBI and HFBII, at the air-water interface were transferred to solid supports and imaged by AFM. The interfacial films of hydrophobins were imaged at nanometer resolution. The results showed that both HFBI and HFBII form organised structures at the air-water interface. Moreover, the nanostructured films formed spontaneously. The HFBI films were imaged and the organised pattern was seen both on the hydrophobic and the hydrophilic side. The dimensions were similar to those of hydrophobin tetramers in solution obtained by small angle X-ray scattering. Protein engineering enabled assignment of a specific functionality to HFBI. The results confirmed the expected orientation of hydrophobins at the air-water interface, and indicated that the hydrophobin retained its capability to form organised films and the covalently attached molecule its functionality.

ISBN
978-951-38-7012-6 (soft back ed.)
978-951-38-7013-3 (URL: http://www.vtt.fi/publications/index.jsp)

Series title and ISSN	Project number
VTT Publications 1235-0621 (soft back ed.) 1455-0849 (URL: http://www.vtt.fi/publications/index.jsp)	16352

Date	Language	Pages
April 2007	English	106 p. + app. 66 p.

Keywords	Publisher
interactions, surface forces, atomic force microscopy, biopolymers, cellulose, hemicellulose, xylan, gluten proteins, gliadin, surface active protein, hydrophobin, HFBI, HFBII	VTT P.O. Box 1000, FI-02044 VTT, Finland Phone internat. +358 20 722 4404 Fax +358 20 722 4374

VTT PUBLICATIONS

619 Hienonen, Risto, Keskinen, Jari & Koivuluoma, Timo. Reliability of materials for the thermal management of electronics. 113 p. + app. 31 p.

620 Talja, Heli. Asiantuntijaorganisaatio muutoksessa. 2006. 250 s. + liitt. 37 s.

621 Kutila, Matti. Methods for Machine Vision Based Driver Monitoring Applications. 2006. 82 p. + app. 79 p.

622 Pesonen, Pekka. Innovaatiojohtaminen ja sen vaikutuksia metsäteollisuudessa. 2006. 110 s. + liitt. 15 s.

623 Hienonen, Risto & Lahtinen, Reima. Korroosio ja ilmastolliset vaikutukset elektroniikassa. 2007. 243 s. + liitt. 172 s.

624 Leviäkangas, Pekka. Private finance of transport infrastructure projects. Value and risk analysis of a Finnish shadow toll road project. 2007. 238 p. + app. 22 p.

625 Kynkäänniemi, Tanja. Product Roadmapping in Collaboration. 2007. 112 p. + app. 7 p.

626 Hienonen, Risto & Lahtinen, Reima. Corrosion and climatic effects in electronics. 2007. 242 p. + app. 173 p.

627 Reiman, Teemu. Assessing Organizational Culture in Complex Sociotechnical Systems. Methodological Evidence from Studies in Nuclear Power Plant Maintenance Organizations. 2007. 136 p. + app. 155 p.

628 Kolari, Kari. Damage mechanics model for brittle failure of transversely isotropic solids. Finite element implementation. 2007. 195 p. + app. 7 p.

629 Communications Technologies. VTT's Research Programme 2002–2006. Final Report. Ed. by Markku Sipilä. 2007. 354 p.

630 Solehmainen, Kimmo. Fabrication of microphotonic waveguide components on silicon. 2007. 68 p. + app. 35 p.

631 Törrö, Maaretta. Global intellectual capital brokering. Facilitating the emergence of innovations through network mediation. 106 p. + app. 2 p.

632 Lanne, Marinka. Yhteistyö yritysturvallisuuden hallinnassa. Tutkimus sisäisen yhteistyön tarpeesta ja roolista suurten organisaatioiden turvallisuustoiminnassa. 2007. 118 s. + liitt. 81 s.

633 Oedewald, Pia & Reiman, Teemu. Special characteristics of safety critical organizations. Work psychological perspective. 2007. 114 p. + app. 9 p.

634 Tammi, Kari. Active control of radial rotor vibrations. Identification, feedback, feedforward, and repetitive control methods. Espoo 2007. 151 p. + app. 5 p.

635 Intelligent Products and Systems. Technology theme – Final report. Ventä, Olli (ed.). 2007. 304 p.

636 Evesti, Antti. Quality-oriented software architecture development. 2007. 79 p.

637 Paananen, Arja. On the interactions and interfacial behaviour of biopolymers. An AFM study. 2007. 106 p. + app. 66 p.

638 Alakomi, Hanna-Leena. Weakening of the Gram-negative bacterial outer membrane. A tool for increasing microbiological safety. 2007. 95 p. + app. 37 p.

Julkaisu on saatavana	Publikationen distribueras av	This publication is available from
VTT PL 1000 02044 VTT Puh. 020 722 4404 Faksi 020 722 4374	VTT PB 1000 02044 VTT Tel. 020 722 4404 Fax 020 722 4374	VTT P.O. Box 1000 FI-02044 VTT, Finland Phone internat. + 358 20 722 4404 Fax + 358 20 722 4374

ISBN 978-951-38-7012-6 (soft back ed.) ISBN 978-951-38-7013-3 (URL: http://www.vtt.fi/publications/index.jsp)
ISSN 1235-0621 (soft back ed.) ISSN 1455-0849 (URL: http://www.vtt.fi/publications/index.jsp)